MODELLING TANNERY WASTEWATER TREATMENT TO EVALUATE ALTERNATIVE BIOPROCESSES CONFIGURATIONS

Dissertation

submitted to and approved by the

Department of Architecture, Civil Engineering and Environmental Sciences

University of Braunschweig – Institute of Technology

and the

Department of Civil and Environmental Engineering

University of Florence

in candidacy for the degree of a

Doktor-Ingenieur (Dr.-Ing.) /

Dottore di Ricerca in Civil and Environmental Engineering*)

by

Francesca Giaccherini

born August 17th, 1986

from Poggibonsi (Siena), Italy

Submitted on	02/09/2016
Oral examination on	10/11/2016
Professorial advisors	Prof. Claudio Lubello
	Prof. Thomas Dockhorn

2017

*) Either the German or the Italian form of the title may be used.

William Goode

"Spoon River Anthology" Edgar Lee Masters

TO all in the village I seemed, no doubt,

To go this way and that way, aimlessly.

But here by the river you can see at twilight

The soft-winged bats fly zig-zag here and there—

They must fly so to catch their food.

And if you have ever lost your way at night,

In the deep wood near Miller's Ford,

And dodged this way and now that,

Wherever the light of the Milky Way shone through,

Trying to find the path,

You should understand I sought the way

With earnest zeal, and all my wanderings

Were wanderings in the quest.

Table of contents

Introduction

Although not amongst the largest industrial segment worldwide, the leather tanning industry can be a dominant regional player in certain areas of the world (Lofrano et al., 2013). The production of leather requires large amounts of water for livestock, as well as for all the steps in hide-to-leather processing. The processing water may be associated with high organic load in terms of COD, organic nitrogen, sulphur, chemicals, high levels of suspended solids, and heavy metals (Mannucci et al., 2010).

The Italian tannery industry is represented by approximately 1400 tanneries, and it is situated in four main areas: Veneto, Lombardy, Tuscany, and Campania Regions. The Tuscan tannery district is the second largest in Europe and is divided into two different sectors where chrome and vegetable tanning processes are separately operated. It is located in the area surrounding Florence and Pisa. Within this territory, the Consorzio Cuoiodepur wastewater treatment plant (San Romano, San Miniato-PI) treats tannery wastewater from vegetable-based processes. From 1 kg of raw hide, the tanning process generates 0.7-0.6 kg of solid waste (fleshing) and 25-45 l of wastewater. Fleshing and tannery sludge are typically treated separately and sent to land application. Before final disposal, fleshing undergoes alkaline hydrolysis and biosolids are thermally dewatered. Since European regulations on application of biosolids to land is becoming increasingly stringent, it is important to evaluate alternative options. In recent years, research is aimed to explore solutions with less environmental impact such as the anaerobic digestion of tannery sludge and the co-digestion of sludge and the industrial solid waste.

The leather industry generates a considerable amount of wastes, however, the studies dealing with its potential valorisation are scarce (Bautista et al., 2015). The potential benefit of the anaerobic treatment of tannery wastewater and sludge relies on its high organic load and temperature and is confirmed by the increasing attention to the anaerobic treatment of this particular industrial wastewater (Daryapurkar et al., 2001, Lefebvre et al., 2004, Rajesh Banu and Kaliappan, 2007, Mannucci et al. 2010). However, acids, alkalis, chromium salts, tannins, solvents, sulphides, dyes, additives, and others compounds which are used in the

transformation of raw or semi-tanned hides into commercial goods, are not completely fixed to hides and leather and remain in the effluent (Lofrano et al. 2013). Hence, the presence of inhibiting compounds such as polyphenols, metals, and sulfide limited the application of anaerobic processes to tannery wastewater at full-scale (Munz et al., 2009; Roy et al., 2013). Even though several works on anaerobic digestion and co-digestion of tannery sludge and fleshing were published (Dhayalan et al., 2007; Di Bernardino et al., 2009; Thangamani et al., 2010; Zupancic et al., 2010; Sri Bala Kameswari et al., 2012), almost no information is available about the application of anaerobic processes on the sole vegetable tannery primary sludge or vegetable tannery primary sludge with fleshing.

One of the major limitations of applying anaerobic digestion to this type of tannery wastewater is that the sulphate reducing bacteria activity during the anaerobic digestion of tannery sludge causes high sulphide concentration in the produced biogas, making sulphide removal mandatory before methane utilization.

Moreover, the supernatant effluent from the anaerobic digestion is characterized by high ammonia concentration (up to 900 mg $N\text{-}NH_4$ l^{-1}); its nitrification in a side stream separated from the main treatment train allow the production of liquid streams with high nitrate and/or nitrite concentration that could be used as electron acceptor in autotrophic denitrification process (Munz et al., 2015). The advantages of anaerobic digestion are that the biological processes do not require the addition of chemicals, can remove hydrogen sulphide (H_2S) under varying operating conditions, and require only a few days for start-up. The use of alternative electron acceptors, instead of oxygen, would make the use of this technology more favorable for treating biogas produced from anaerobic digestion of tannery industrial sludge.

This study aimed at investigating an alternative treatment train comparing with the existing one to evaluate the technical feasibility of anaerobic digestion of vegetable tannery sludge and the co-digestion of sludge and fleshing. Moreover, the sulphide denitrification was tested to treat both the supernatant (after the digestion process) and the biogas. The process was investigated through both experimental activity and modelling activity. The experimental activity included batch and continuous reactors tests at different scales (bench,

laboratory and pilot scales). The modelling activity allowed, in addition to improving understanding of the processes, the evaluation of the alternative configurations.

The innovative contributions of this research are:

- Testing the anaerobic digestion of recalcitrant and potential inhibitory substrates, such as vegetable tannery sludge and fleshing;
- Upgrading the existing models to simulate high solids retention time wastewater treatment plants and sulphur metabolism.

The thesis is structured in 4 main Chapters and the Conclusions. The Future research is included at the end and the Appendix includes a presentation of the papers and conference proceedings submitted during the research activity. All the citations are listed alphabetically in the References. After this Introduction where the aim of the research and the goals reached are described, an explanation of the leather industry and the tanning process are described in the Chapter I. The second chapter includes a literature research on the existing model, activated sludge standard model (IWA-ASM) and the anaerobic digestion standard model (IWA-ADM1). Afterwards, the main part of the thesis is composed with the material and methods and the results and discussion of the research, Chapter III and IV, respectively. The Conclusions presents a critical summary of the results and the goals reached.

Chapter I: Leather tanning

Leather industry is a wide common worldwide and it can be a dominant regional player in certain areas of the world. (Lofrano et al, 2013). This manufacturing industry consists of several different processes, one of the most important activities being the tanning of the raw hides. Tanning processes are considered to be one of the most polluting industrial activities in the world (Mannucci et al. 2010). It involves the processing of raw materials (animal skin) in order to make it stronger for use in a variety of different products. The tanning process can be represented in three main phases: acquisition and pre-treatment of raw animal hides; treatment of the hides with a tanning agent; and drying and shining the hides before sending them to product manufacturers. The two main types of tanning are chrome tanning and vegetable tanning, with chrome tanning making up a large majority of the industry.

1.1. Leather tanning industry

Leather is originated from animals used in the food industry. The great part of the animals processed in the tanning industry are: lamb, goat, bovine, pork and mutton. However, only bovine, sheep and goat leathers are the most common worldwide.

Data sets on leather production were gathered from Un-Fao, 2013 repositories and reported in Table 1.

Table 1: Global leather productions, 2011. UN-FAO (2013).

Country	Bovine Leather Production (tonnes per year)	Sheep and Goat Leather Production (tonnes per year)
Latin American and Caribbean	$110\ 10^3$	16
Africa	$5\ 10^3$	49
Near East	$22\ 10^3$	98
Far East	$285\ 10^3$	225
North America	$21\ 10^3$	6
Europe	$71\ 10^3$	73
Rest of Europe	$0.4\ 10^3$	1
Area Former USSR	$38\ 10^3$	22
Oceania Developed	$3\ 10^3$	6
Developed Other	$6\ 10^3$	0.3
World	$562\ 10^3$	496

As shown in table 1, all over the world the bovine leather production is the most important with 562 10^3 t y^{-1} compared to 496 t y^{-1} of the sheep and goat one.

Figure 1 shows the bovine leather production trend from 1993 to 2011 in the World.

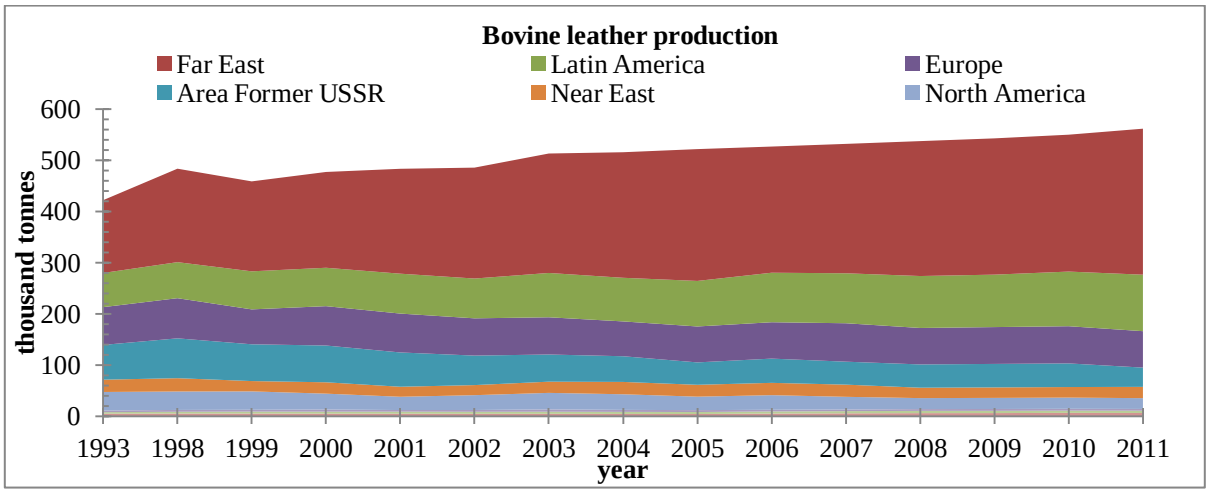

Figure 1: Bovine leather production trend from hide to leather stock from 1993 to 2011, UN-FAO (2013).

Globally it shows a positive trend due to the increasing production in the Far East and Latin America. A mild decrease is present in the other areas of the world only partially correlated with the last years economical crisis.

Figure 2 shows the livestock population in number of bovine animals and Figure 3 shows the global bovine leather production from raw hide to leather stock in tones per annum.

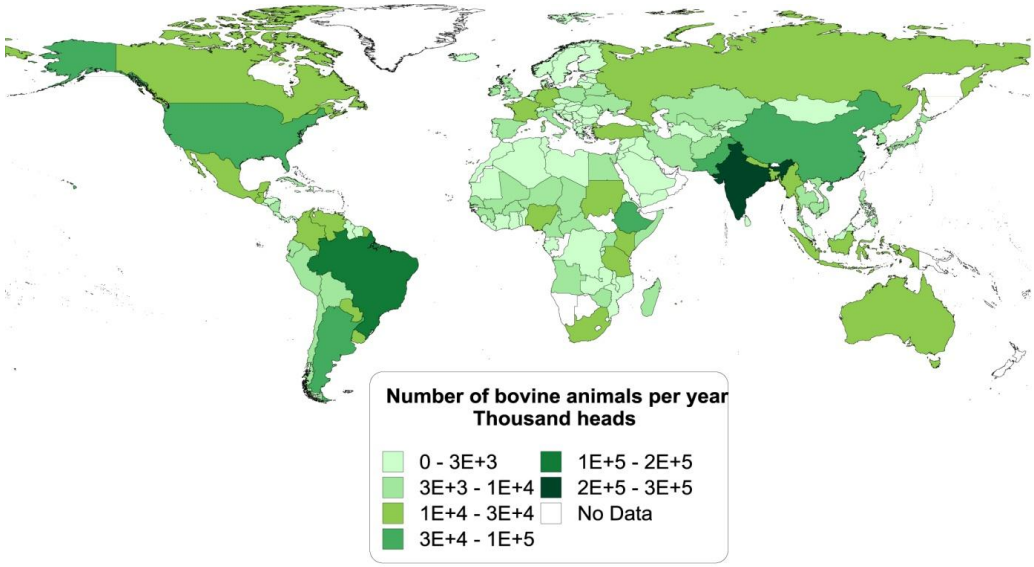

Figure 2: Global map of the livestock population in number of bovine animals, UN-FAO (2013).

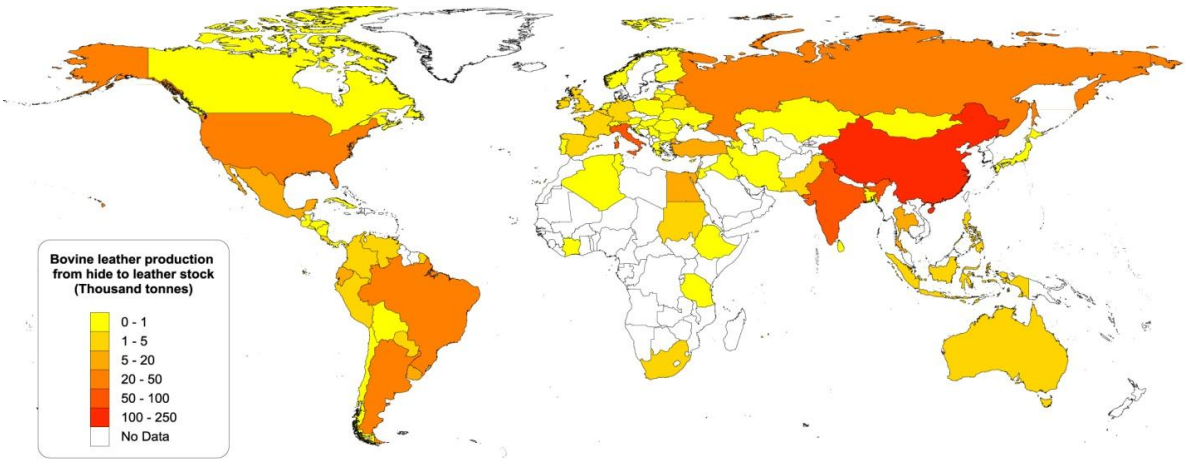

Figure 3: Global map of the bovine leather production (from hide to leather stock) in thousand tonnes per year, UN-FAO (2013).

As shown in figure 2 and figure 3 the main leather producers do not correspond to the main bovine breeders. The Public Republic of China is the most important producer, followed by India, Italy, Brazil, Russia, Argentina, United States and Turkey.

The average number of bovine animals is 1.63 10^9 heads, with an average of 1.4 tonnes per head it is possible to calculate an amount of 2.28 10^9 tonnes of animals. The amount of raw hide per year is 1.87 10^9 tonnes, that means the 82% of the bovine livestock becomes raw hide for the leather industry.

Figure 4 shows the bovine leather production per capita (kilograms per person).

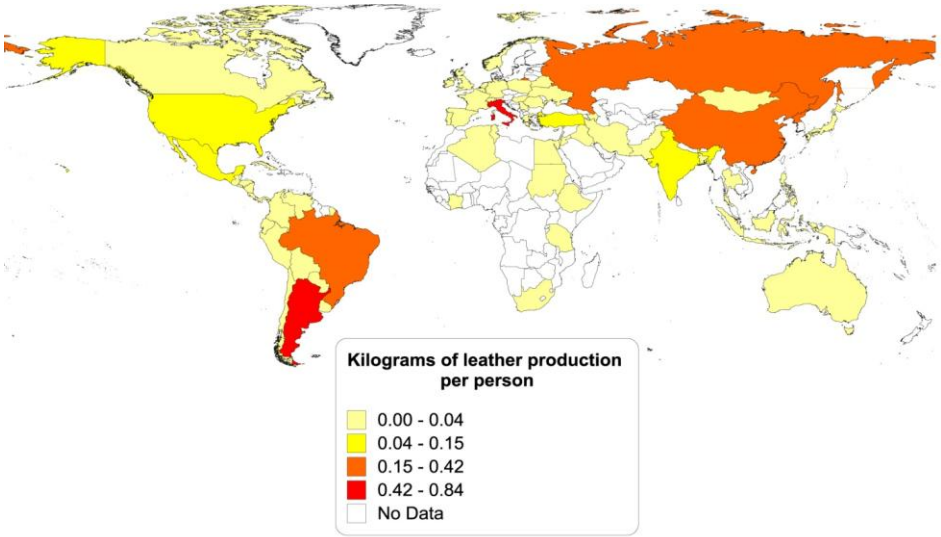

Figure 4: Map of the bovine leather production per capita for the 10 largest leather producers.

Figure 4 confirms the intensity of the Italian leather industry. Moreover, if we consider the Italian leather industry is located in 4 main districts (Lofrano et al., 2013), the production per capita can be evaluated to be 225 kg leather per person and 146 tonnes leather per km^2.

1.2. Leather processing

Leather processing allows to obtain a material stable, strong and durable on time. Tanning process is a complex combination of mechanical and chemical procedures. Figure 5 shows the tanning processes.

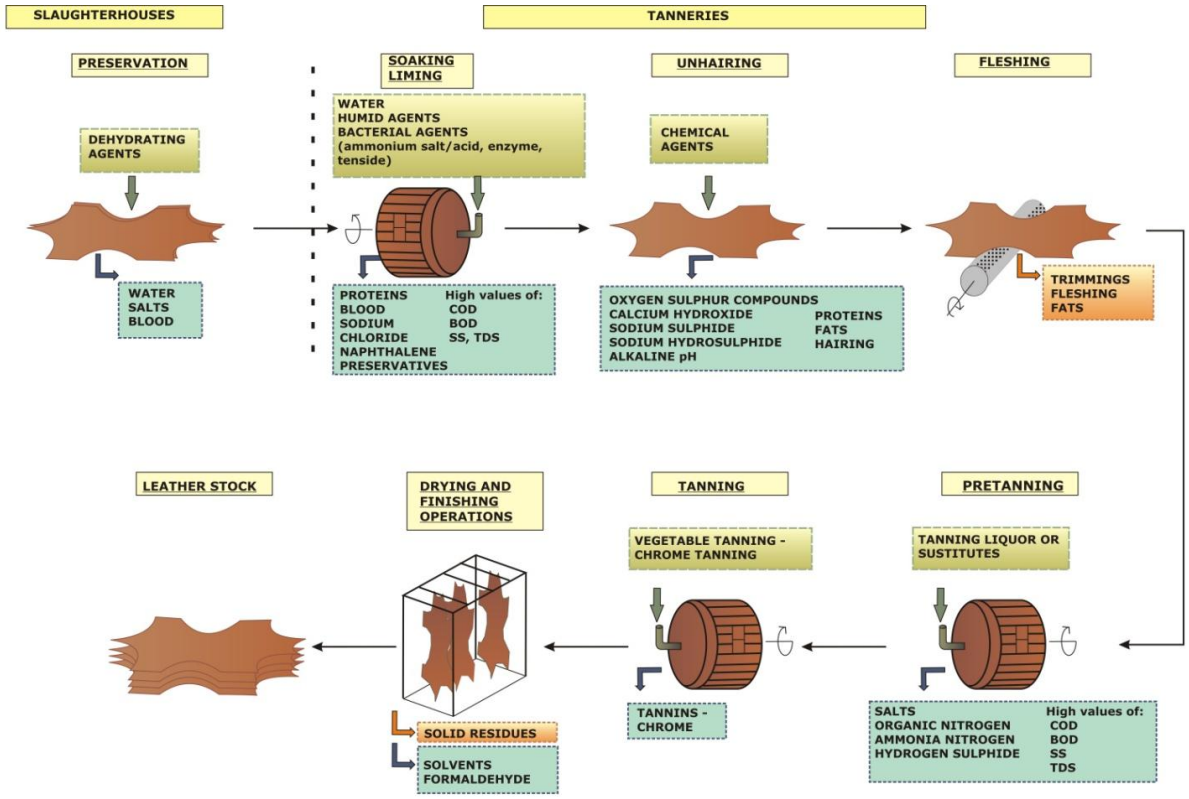

Figure 5: Tanning processes scheme.

As shown in figure 5 the first operation, preservation, is usually carried out in the slaughterhouse before the shipping of the raw material to the tanneries.

Six main operations in the process from raw hides to leather stock: soaking-liming; unhairing; fleshing; pre-tanning; tanning; drying and finishing operations.

1. Soaking and liming: through water, humid and bactericidal agents (such as ammonium salt, acids, enzyme and tenside), the raw hide regains their normal water contents. It is

within this stage that high volume of water used consequently results to high discharge of effluent with high pollutant load (Mwinyihija, 2010). The discharge is rich on: proteins, blood, sodium chloride, naphthalene, preservatives and characterized by high values of chemical oxygen demand COD, biochemical oxygen demand BOD, suspended solids SS, total dissolved solids TDS. It is estimated that for processing 1 ton of raw skins (weight of skins before soaking), the input in a typical input audit processing (kg) of lime is 100 with an output of 12.3, while Na_2S has an input of 35 with an output of 18.3 (Mwinyihija, 2010).

2. Unhairing: the process is done by chemical dissolution of the hair and epidermis with an alkaline medium of sulphide and lime. The wastewater is rich of oxygen sulphur components, calcium hydroxide, sodium sulphide, sodium hydrosulphide, alkaline pH, proteins, fats and hairing.
3. Fleshing and trimming: weak organic acids, digestive enzymes and inorganic acids, respectively, are used to remove lime, digest and remove the non-structural proteins and eventually bring the pH to a level that will enhance the tanning process (Cassano et al. 2001; Thanikaivelan et al. 2003).
4. Pre-tanning: this process commonly includes two sub-processes.
    a. Bating: the unhaired, fleshed and alkaline hides are neutralised (deliming) with acid ammonium salts and treated with enzymes, similar to those found in the digestive system, to remove hair remnants and to degrade proteins. During this process hair roots and pigments are removed. The hides become somewhat softer by this enzyme treatment.
    b. Pickling: this process increases the acidity of the hide to a pH of 3, enabling chromium tannins to enter the hide. Salts are added to prevent the hide from swelling. For preservation purposes, 0.03-2.00 weight percent of fungicides and bactericides are applied.
5. Tanning: this process can be done throughout the utilization of two different tanning agents, chrome tanning or vegetable tanning.
    a. Chrome tanning: after pickling, when the pH is low, chromium salts (Cr^{3+}) are added. To fixate the chromium, the pH is slowly increased through addition of a base. The process of chromium tanning is based on the cross-linkage of chromium ions with

free carboxyl groups in the collagen. It makes the hide resistant to bacteria and high temperature. The chromium-tanned hide contains about 2-3 dry weight percent of Cr^{3+}. Wetblue, i.e. the raw hide after the chrome-tanning process, has about 40 percent of dry matter.

b. Vegetable tanning: this process is usually accomplished in a series of vats (first the rocker-section vats in which the liquor is agitated and second the lay-away vats without agitation) with increasing concentrations of tanning liquor. Vegetable tannins are polyphenolic compounds of two types: hydrolysable tannins which are derivatives of pyrogallols and condensed tannins which are derivatives from catechol. Vegetable tanning probably results from hydrogen bonding of the tanning phenolic groups to the peptide bonds of the protein chains.
c. Finishing operations: Chromium tanned hides are often re-tanned during which process the desirable properties of more than one tanning agent are combined and treated with dye and fat to obtain the proper filling, smoothness and colour. Before actual drying is allowed to take place, the surplus water is removed to make the hides suitable for splitting and shaving. Splitting and shaving is done to obtain the desired thickness of the hide. The most common way of drying is vacuum drying. Cooling water used in this process is usually circulated and is not contaminated.
d. Crust: The crust that results after re-tanning and drying, is subjected to a number of finishing operations. The purpose of these operations is to make the hide softer and to mask small mistakes. The hide is treated with an organic solvent or water based dye and varnish. The finished end product has between 66 and 85 weight percent of dry matter.

1.2.1. Mass balance analysis

The first stages of the transformation process of hides into leather (beamhouse process) generate an important waste in the tanning industry, since a considerable fraction of solubilised proteins ends up in waste water with the corresponding increase in contamination parameters, especially when the process is carried out without hair recovery (Bautista et al., 2015).

The production of bovine raw hide has been estimated globally at about $6.43\ 10^6$ tonnes per year, after tanning processes the leather stock has been estimated at about $5.62\ 10^5$ tonnes

per year (Un-Fao, 2013). This means that only the 9% of the raw hide is used as leather and the 91% of the total mass is solid waste. According to Organization UNID (2000) from 1000 kg of wet salted hide with an average weight of 28 kg per hide, would give 255 kg of finished leather. This means that the 26% of the raw hide is used as leather, with a wastage of 75%.

According to Sykes and Corning (1987), each tonne of raw hide yields 200 kg of finished leather, $50m^3$ of contaminated wastewater with only 20% is transformed into useful material. As explained in the previous paragraph, the raw hide is treated with chemical agents water based to improve its quality and durability. Moreover, hairs and part of the skin layer are removed.

Depending on such factors as raw hide characteristics, technology and range of final products, the mass balance can vary widely. Table 2 shows the mass balance of each components in the typical average values, starting from wet salted raw hide.

Table 2: Leather tanning mass balance, Organization UNID, 2000.

Component		**Input kg**	**Output kg**
	Wet salted raw hide	1000	0
Liquid-based	Process water	16700	16000
	Tenside	3	3
	Sodium chloride NaCl	-	200
	Calcium hydroxide $Ca(OH)_2$	40	40
	Sodium sulphide Na_2S	25	25
	Ammonium salts	17	17
	Enzyme	3	3
Solid-based	Fleshing	-	300
	trimming	-	100
	Unusable pelt	-	800
	Finished product	-	300

The water consumption is generally reported in a range of 25-45 litre of water per kilograms of raw material (Buljian et al., 2000; Sundar et al., 2000; Mannucci et al., 2010; Lofrano et al., 2013). Moreover the Organization UNID, 2000 reports the water intensity of 0.13 m^3 m^{-2}

finished product, the density of the bovine leather is 1 kg m^{-2}, so the water intensity per finished product is evaluated around 130 l kg^{-1}.

Table 3 reports the chemicals mass balance on liquid based.

Table 3: Chemicals mass balance in leather processing,(Kral. & G. Clonfero, 2011).

Chemicals	Input	Retained	Wasted
	kg $tonnes^{-1}$ of wet-salted hide		
Chrome oxide Cr_2O_3	25	12	13
Organic tannins	25	20	5
Fat liquors	22	17	5
Dyestuffs	5	4	1
Acids, bases, salts	191	-	191
Tensides	3	-	3
Enzymes	5	-	5
Finishing Products	100	12	88

From the 20 to the more than 50% of each chemicals it is not retained by the treated material and wasted. These chemicals characterized tannery wastewater.

1.2.2. Solid waste and wastewater characterization

Tanning Industry is considered to be a major source of pollution and tannery waste- water in particular, is a potential environmental concern. Tanning industry wastes poses serious environ- mental impact on water (with its high oxygen demand, discolouration and toxic chemical constituents (Song et al. 2000), terrestrial and atmospheric systems. Tannery waste characteristically contains a complex mixture of both organic and inorganic pollutants (Mwinyihija, 2010).

Due to variations in raw material, process, chemicals, etc., solid waste and wastewater characterization can be different from district to district.

Table 4 shows the average composition of fleshing and trimmings.

Table 4: Composition of fleshing and trimmings, Organization UNID, 2000.

Component	Fleshing		Trimmings	
	kg	%	kg	%
Water	240	80	70	70
Collagen and proteins	24	8	18	18
Salts	24	8	9	9
Fats	12	4	3	3

As shown in table 4 the composition of fleshing and trimmings is wet based, plus a variety of organic matter and salt. Table 5 shows the physico-chemical characterization of the solid waste.

Table 5: Physico-chemical characterization of the tanning process solid waste.

Component	Unit	Fleshing		Trimmings
		Zupančič and Jemec, 2010	Vasudevan and Ravindran, 2007	Zupančič and Jemec, 2010
Total suspended solids	% TSS	63.5	33.3	48.7
Volatile suspended solids	% VSS	60.6	82.0	30.9
Total COD	mg g^{-1}	1600-1700	-	450-550
TOC	%	-	32.2	-
TKN	%	-	3.27	-
Phosphorus	%	-	0.26	-
Potassium	%	-	0.52	-
C:N ratio		-	8.5:1	-
pH		-	8.2	-

The organic matter is characterized by high values of chemical oxygen demand and a carbon to nitrogen ratio of almost 9 to 1.

Portavella (1994) found that 70% of COD from the beamhouse operations is due to the skins themselves and that only 30% comes from added chemical products. Although the values of the parameters may vary as a function of the type of raw material treated, there is no doubt that the beamhouse operations produced most contamination, much of which is due to the solubilised components (proteins) of hides or skins (Bautista et al., 2015).

Table 6 shows the chrome tanning effluents composition by process (Lofrano et al., 2013).

Table 7 shows the average of total pollution for chrome tanning (Kral and Clonfero, 2011).

Table 8 shows the vegetable tanning effluent composition (Mannucci et al., 2010).

Table 6: Chrome tanning effluents composition.

Parameter	Unit	Soaking		Unhairing liming		Bating deliming		Pickling		Chrome tanning		Re-tanning	
		Min	Max	Min	Max	Min	Max	Min	Max	Min	Max	Min	Max
pH		6	10	11.9	13	6	11	3.6	4	3.2	-	4	10
T	°C	10	30	10	25	20	35	-	-	-	-	20	60
BOD_5	mg l^{-1}	2000	5000	5000	20000	1000	4000	100		250	-	6000	15000
COD	mg l^{-1}	3000	31000	20000	58000	2500	7000	800	30000	400	3000	4365	75000
TSS	mg l^{-1}	2300	40000	6700	25000	2500	10000	29000	-	70000		-	-
TDS	mg l^{-1}	22000	33000	-	-	-	-	20000	-	67000		-	-
Cl^-	mg l^{-1}	15000	50000	3300	25000	2500	15000	8950	-	2000	30000	5000	10000
Sulphide	mg l^{-1}	0	700	2000	3300	25	250	-	-	-	-	-	-
Cr (III)	mg l^{-1}	-	-	-	-	-	-	-	-	4100	-	-	-
N_NH_3	mg l^{-1}	850	380	380		3800		670	-	-	-	-	-

Table 7: Average of the total pollution load for chrome tanning.

Parameter	Unit	Value
BOD5	mg O_2 l^{-1}	2000
COD	mg O_2 l^{-1}	4000
SS	mg l^{-1}	2000
Cr (III)	mg Cr l^{-1}	150
Sulphide	mg S l^{-1}	160
TKN	mg N l^{-1}	160
Cl^-	mg Cl l^{-1}	5000
Sulphate	mg SO_4^{2-} l^{-1}	1400
Oil and grease	mg l^{-1}	130
TDS	mg l^{-1}	10000
pH		6-9

Table 8: Vegetable tanning effluent composition.

Parameter	COD		TSS		pH		N org		NH_4		P	
Unit	mg l^{-1}		mg l^{-1}				mg l^{-1}		mg l^{-1}		mg l^{-1}	
Value	min	max	min	max	min	max	min	max	min	max	min	max
	900	19400	660	16144	7	8.5	360		102	400	8	40

Parameter	Sulphate		COD/SO_4^{2-}		Sulphide		Alkalinity		Tannins		Chloride		VFA	
Unit	mg l^{-1}				mg l^{-1}		mg $CaCO_3$ l^{-1}		mg l^{-1}		mg l^{-1}		mg l^{-1}	
Value	min	max	min	max	min	max	min	max	min	max	min	max	min	max
	180	6000	1	33.8	3	287	350	5000	600	2900	353	8400	63	486

As shown in tables 6, 7 and 8, a high range of variability characterizes the parameters, but the two types of tanning are characterized by basic pH and high value of total dissolved solids due to chlorides and sulphates. Moreover, vegetable wastewater is commonly characterized by the highest value of COD, nitrogen and recalcitrant compounds.

Several tannery effluent components contain nitrogen as part of their chemical structure, ammonia (from deliming materials) and the nitrogen contained in proteinaceous materials (from liming/unhairing operations). Combining intensive aerobic and anoxic biological treatment can break down the nitrogenous compounds. The oxygen demand is very high, thus leading to correspondingly high operational and energy costs. Calculations show that, with typical tannery effluent, some 40% of oxygen requirements are spent on removing the nitrogen component (Kral. and G. Clonfero, 2011).

The sulphide content in tannery effluent results from the use of sodium sulphide and sodium hydrosulphide and the breakdown of hair in the unhairing process. Under alkaline conditions, sulphides remain largely in solution. When the pH of the effluent drops below 9.5, hydrogen sulphide evolves from the effluent: the lower the pH, the higher the rate of evolution. Characterized by a smell of rotten eggs, a severe odour problem occurs (Kral. and G. Clonfero, 2011).

Two common types of salts are to be found in tannery effluent: sulphates and chlorides. Sulphates derives from the use of sulphuric acid or products with a high (sodium) sulphate content. Chloride is introduced into tannery effluents as sodium chloride usually on account of the large quantities of common salt used in hide and skin preservation or the pickling process.

1.3. Treatment of tannery effluent and solid waste

Multi-stage processes are required to reduce or remove organic matter, solids, nutrients, chromium and other pollutants before the water discharge or waste disposal. Therefore, the discharge is regulated by standards limits promulgated by relevant environmental authority. Table 9 shows limits for treated tannery effluents in France, Italy and India (Kral and Clonfero, 2011). Figure 6 shows a common treatment line.

Table 9: Discharge limits for treated tannery effluents in France, Italy and India.

Parameter	Unit	France		Italy		India	
		Surface	Sewer	Surface	Sewer	Surface	Sewer
pH		6.5-8.5	6.5-8.5	5.5-9.5	5.5-9.5	5.5-9.0	5.5-9.0
COD	mg l^{-1}	125	2000	160	500	250	-
BOD_5	mg l^{-1}	30	800	40	250	30	350
Suspended solids	mg l^{-1}	35	600	40-80	200	100	100
Ammonia nitrogen	mgN l^{-1}	-	-	15	30	50	50
TKN	mgN l^{-1}	-	-	-	-	100	-
Nitrate nitrogen	mgN l^{-1}	-	-	20	-	-	-
Sulphide	mgS l^{-1}	-	-	1	2	2	-
Hexavalent chromium	mgCr l^{-1}	0.1	0.1	0.2	0.2	0.10	2.0
Trivalent chromium	mgCr l^{-1}	1.5	1.5	-	4.0	-	-
Total chrome	mgCr l^{-1}	-	-	2.0	4.0	2	2
Chloride	mgCl^- l^{-1}	**	-	1200*	1200	-	-
Sulphate	mgS_SO_4^{2-} l^{-1}	**	-	1000*	1000	1000	1000
Aluminium	mgAl l^{-1}	-	-	1.0	2.0	-	-
Iron	mgFe l^{-1}	-	-	-	2.0	4.0-	-

* Special limits permitted by the regional authorities to certain wastewater treatment plant located close to the sea or if the effluent is mixed with municipal wastewater:

- At Santa Croce, Cuoiodepur and Fucecchio – chlorides ≤ 5000 mg l^{-1} and sulphates ≤ 1800 mg l^{-1};
- At Arzignano – chlorides ≤ 900 mg l^{-1} and sulphates ≤ 1800 mg l^{-1};
- At Solofra – chlorides ≤ 3500 mg l^{-1} and sulphates ≤ 1500 mg l^{-1};

** In France no discharge limits pertaining to chlorides, sulphates and TDS have been prescribed except in special case.

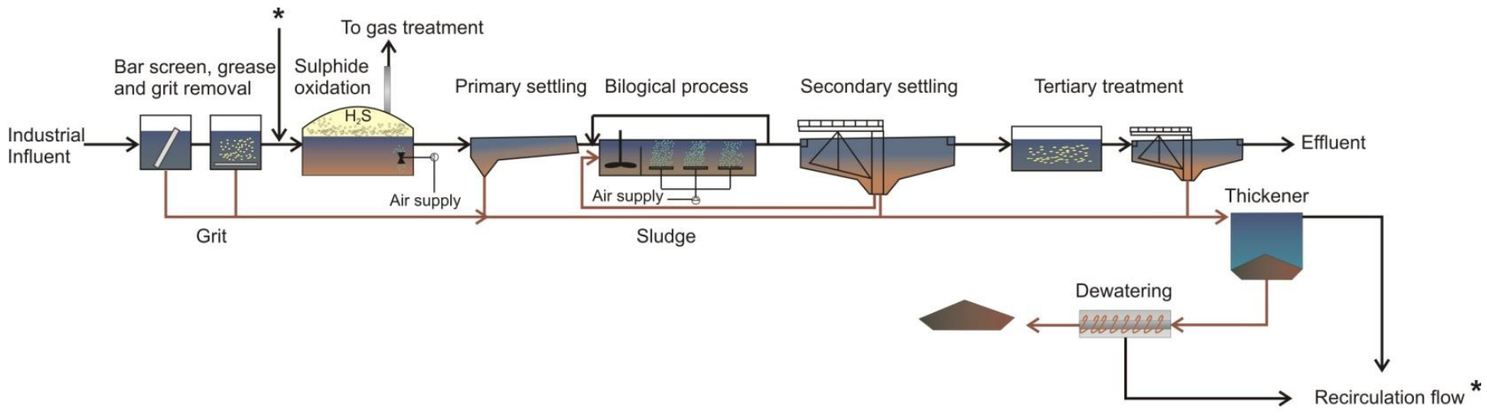

Figure 6: Tannery wastewater treatment process scheme.

As shown in table 9 different discharge limits are defined by Countries. Italy is generally characterized by the strongest limitations on the discharge of treated tannery effluents in surface body and sewer compared to France and India. However, special limits for chlorides and sulphates are defined by the regional authorities to certain wastewater treatment plant located close to the sea or if the effluent is mixed with municipal wastewater. In France no discharge limits pertaining to chlorides, sulphates and TDS have been prescribed except in special case.

To reach the limits a multistage process is required. As shown in Figure 6 the first step in the treatment is a preliminary treatment to remove large particles, sand, grit and grease. After that, the equalization tank is aerated for two main purposes: to keep all particulate matters in suspension and to oxidize sulphide. For odour control purposes, the reactor must be close and the gas collected and treated before the atmospheric discharging. The rest of the treatment does not differ from a common activated sludge process.

In certain cases, the quality of the final effluent does not meet the discharge limits, because of the recalcitrant COD, i.e., compounds that the micro-organisms present in the flock are unable to decompose. So, tertiary treatment are required usually more sophisticated and rather expensive treatments such as mineralization of organic compounds by oxidation with H_2O_2 in the presence of ferrous sulphate (Fenton process and its derivatives). Ozonation is sometimes included not so much to eliminate potentially harmful micro-organisms but to destroy part of the residual COD.

The sludge is commonly dewatered. Fleshing and tannery sludge are typically treated separately and sent to land application. In many cases, before final disposal, fleshing undergoes alkaline hydrolysis and biosolids are thermally dewatered.
Fleshing is an animal tissue waste obtained in the preparatory stages of leather processing in a tannery and the need of finding alternative solutions to manage and treat fleshing is increasingly eminent. The composition of fleshing varies widely. Fleshing represents the largest part of tannery industry waste, currently, in many districts, it undergoes alkaline hydrolysis to recover lipids and protein. However, this separation treatment requires costly and complex technologies and operation, usually affordable only for large tannery districts.

1.3.1. Anaerobic digestion of tannery sludge and solid waste

Due to its high methane potential 0.7–1.1 m^3 CH_4 kg^{-1} VS, FOG (fats, oils and greases) is a very interesting co-substrate for sewage sludge anaerobic co-digestion. Nonetheless, FOG dosing rate must be limited in order to avoid high concentration of LCFA (result of lipid degradation) in the digester, a potential inhibitor of the methanogenic activity. Moreover, FOG has been related with other operational problems like clogging in the liquid or gas systems, foaming and biomass flotation related to adsorption of lipids onto biomass (Mata-Alvarez et al., 2014).

The potential benefit of the anaerobic treatment of tannery wastewater and sludge relies on its high organic load and temperature and is confirmed by the increasing attention to the anaerobic treatment of this particular industrial wastewater (Daryapurkar et al., 2001; (Lefebvre et al., 2006; Banu et al., 2007; Mannucci et al., 2010). However, acids, alkalis, chromium salts, tannins, solvents, sulphides, dyes, additives, and others compounds which are used in the transformation of raw or semi-tanned hides into commercial goods, are not completely fixed by hides and leather and remain in the effluent (Lofrano et al., 2013). Hence, the presence of inhibiting compounds such as polyphenols, metals, and sulfide limited the application of anaerobic processes to tannery wastewater at full-scale (Vijayaraghavan and Murthy, 1997; Munz et al., 2007, 2008, 2009; Roy et al., 2011). However, anaerobic digestion is less efficient to degrade low molecular weight phenolic and polyphenolic compounds such as tannins and lipids. They exert inhibitory effects on various micro flora involved in the digestion process (Dhayalan et al., 2007) and thus tend to persist in the digesters and be released along with the digested effluents.

As also reported by Zupančič and Jemec, 2010, there are some older reports on anaerobic digestion of tannery waste (Cenni et al., 1982; Tunick et al., 1985; Lalitha et al., 1994; Urbaniak, 2006), and reports on hydrolysis of tannery waste (Raju et al., 1997) but few papers deal with the technology of anaerobic digestion of tannery waste. Moreover, even though in the last few years several works on anaerobic digestion and co-digestion of tannery sludge and fleshing have been published (Dhayalan et al., 2007; Berardino and Martinho, 2009; Thangamani et al., 2010; Zupančič and Jemec, 2010; Sri Bala Kameswari et

al., 2012), almost no information is available about the application of anaerobic processes on the sole vegetable tannery primary sludge or vegetable tannery primary sludge plus fleshing.

In a typical (complete) tannery process, fleshing production is about 25% of the sludge generated from wastewater treatment and represents a potential resource for bioenergy production (Bautista et al., 2015). The co-digestion of fleshing and tannery sludge is a potential solution to increase biogas yield of sole tannery sludge and, at the same time, mitigate the inhibitory effect of high ammonia and sulphide load deriving from fleshing hydrolysis; however, its feasibility still needs to be evaluated in real conditions and only few studies have been published.

Dhayalan et al. (2007) reported the results of treating, in batch conditions, untanned solids leather wastes, chrome and vegetable tanned samples and obtained higher performance from the digestion of vegetable tanning wastes than chrome tanning ones. In the same study, the effect of detanning pretreatment was also evaluated and results point at tanning agents as responsible for the low biodegradability of tannery wastes.

Berardino and Martinho, 2009 evaluated the co-digestion of sludge from tanneries' industrial wastewater treatment plant (WWTP) mixed with chromium free ("green") tanneries solid wastes at 20 days of hydraulic retention time (HRT) and at mesophilic temperature (35 ºC). The study confirmed that the sludge contains some compounds which are moderately inhibitory, requiring bacterial adaptation and appropriate mixtures of substrate during the start-up period. The addition of the "green" tannery wastes exerted a favorable effect on biodegradation and gas production, overcoming any inhibition phenomena.

Vasudevan et al., 2007 and Basak et al., 2014 addressed co-digestion of fleshing and secondary sludge, from tannery industry and domestic sewage, respectively, confirming process feasibility. Specifically, Vaseduvan et al., 2007 focused on acceleration of fleshing digestion process by mean of enzymatic pre-treatment, whose positive effect resulted in threefold higher biogas production for pre-treated samples compared to raw ones, with 64% of methane content.

Batch tests with fleshing and primary sludge from the tannery effluent treatment plant were performed by Thangamani et al., 2010. Anaerobic digestion was carried out under mesophilic conditions and batch reactors were operated at different initial volatile solid concentrations with a SRT of 8 weeks. The VSS removal efficiency resulted in 52, 44 and 41%, for initial VSS concentrations of 17.2, 21.2 and 26.7 g l^{-1} respectively. Methane content in the biogas varied between 71 and 77%. The work reported by Berardino and Martinho, 2009 showed that, at pilot-scale application, fleshing is a complex, difficult to manage and hard substrate, also due to its mechanical resistance to maceration and pumping. Moreover, as reported by Thangamani et al., 2010, the efficiency of anaerobic co-digestion of limed fleshing and primary sludge is dependent on the biodegradability of the types of fats and proteins present in the substrate.

Zupančič and Jemec, 2010, reported that the specific methane production potential at 55 °C is estimated to be 0.617 m^3 kg^{-1} of volatile suspended solids for tannery waste sludge, 0.377 m^3 kg^{-1} for tannery waste trimmings and 0.649 m^3 kg^{-1} for tannery waste fleshing.

1.4. Water footprint of leather tanning industry, carbon footprint and power demand of leather tanning wastewater processes

The production of leather requires high amounts of water for livestock, as well as for all the steps in hide-to-leather processing. The high complexity of the tannery wastewater matrix originates from a wide range of components such as: raw materials (skins) residues, excess dosage of reagents including a high concentration of proteins, lipids and salts (sulphide, sulphate and chloride), tanning agents such as natural and synthetic tannins (in the case of vegetal tanning), dyes and surfactants (Munz et al., 2008). Like all wastewater treatment, tannery wastewater is associated with direct and indirect emissions of greenhouse gases (Gori et al., 2011).

An expansion of the leather industry will cause more water consumption, therefore more wastewaters will be treated. The evaluation of the carbon footprint (CFP) and the power demand of the most common tannery wastewater treatment process was estimated for the 5 largest leather producing regions (Brazil, China, India, Italy and Russia). For the purpose of this research, we quantified only carbon and energy fluxes concerning the main treatment operations (Figure 7). Datasets on leather production from the Food and Agriculture

Organization were processed and wastewater flow rates calculated with assumptions based on previous studies (Buljian et al., 2000; Sundar et al., 2010; Mannucci et al., 2010 ; Lofrano et al., 2013).

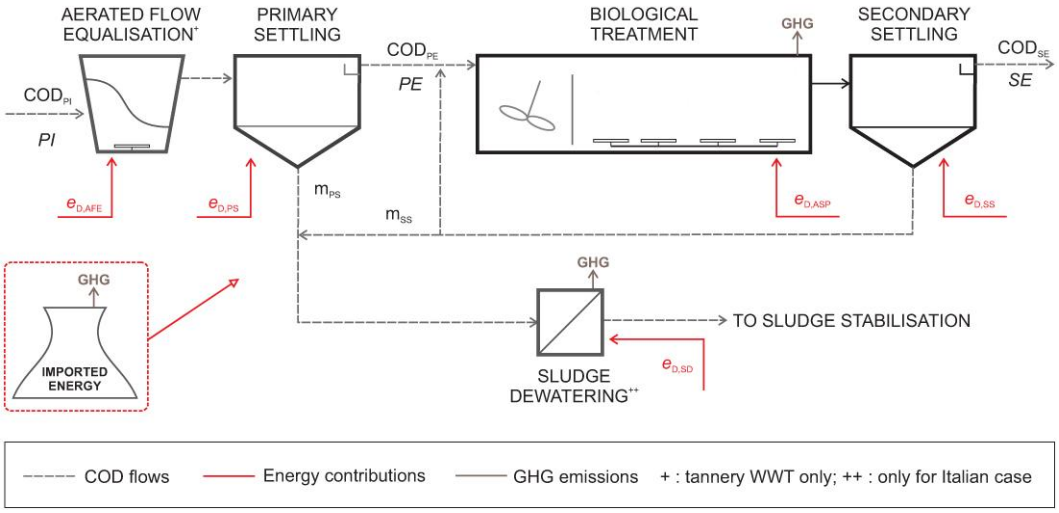

Figure 7: Typical wastewater treatment process employed for tannery wastewater treatment, layout and depiction of COD and energy flows.

The domain of this research is confined to the direct emissions from the process (also referred to as Scope I) and indirect emissions from imported energy (also referred to as Scope II). Hence, all the indirect emissions associated with chemicals, third party services, etc. (also referred to as Scope III) are not included to curb uncertainty. Therefore, we do not aim at performing a Life Cycle Assessment, nor we aim at substituting our carbon footprint model to it, but we intend to provide a quantitative tool with minimum uncertainty to compare process scenarios and there directly attributable emissions. The main carbon and energy fluxes in the treatment process included in the calculation are reported, summarized and defined in Figure 7 and Table 10.

Table 10: Summary of energy and carbon fluxes included in the energy demand and total carbon emission calculation of the tannery wastewater treatment.

Flux	Definition
Energy Demand	Aeration For Equalization^{+} ($ED_{,AFE}$) + Primary Settling ($ED_{,PS}$) + Activated Sludge Process ($ED_{,ASP}$) + Secondary Settling ($ED_{,SS}$) + Sludge Dewatering^{++} ($ED_{,SD}$)
Total carbon emitted	Aerobic Respiration (on site) + Energy Generation (off site) + NaOH production $^{,++}$ (off site)

$^{+}$ is evaluated only for industrial tannery treatment. $^{++}$ is evaluated only for the Italian case study.

As shown in Figure 7 and Table 10, the four components of the process energy demand considered were: aeration for equalization and biological oxidation; settling. The equalization tank is generally an aerated reactor for this specific industrial treatment with the main aims of: homogenization of the effluent; sulphide elimination, mostly catalytic oxidation (Kral and Buljian (2010). For that reason, the total energy requirement is characterized by the energy demand of the two aeration systems: aeration for the equalization and aeration for the biological oxidation process.

The energy demand for the equalization tank was evaluated by the simplified approximation reported from Kral and Buljian (2010): 2 kg of O_2 is needed to oxidize 1 kg S^{2-} to sulphate, whereas the oxygen transfer efficiency is approximately 1.5 kg O_2 kWh^{-1}. The energy consumption for the equalization tank was estimated at 1.33 kWh kg^{-1} S^{2-} oxidized. On the contrary, no oxidation phase is required for a municipal wastewater treatment plant.

The CFP has been evaluated using the method by Monteith et al (2005), including on-site and off-site emission for power generation.

The carbon dioxide equivalent emitted for energy generation was calculated for each country taking into account a specific factor ($kg_{CO2,eq}$ kWh^{-1}) depending on the source of the energy generation reported from energy information administration (epa 2015)

Off-site emissions for manufacturing of chemicals and others materials, as well as transportation, or other contributions (i.e., Scope III emission) were neglected. We made no distinction between the quantified emission and those for reporting, where applicable.

However, an additional evaluation was made for the Italian case study: the CFP and power demand for sludge dewatering.

Moreover, the emission due to caustic soda production (off-site, also referred to as Scope III) should be evaluated in the Italian tannery wastewater processes, because NaOH is commonly use in the chemical scrubbers to treat the gas stream, rich on H_2S to reach the standard quality for the gas effluent.

However, even though the caustic soda market in Italy is dominated by Solvay, its production is spread over the World in 52 countries and there is not specification where the product comes from. In table 2 is reported the sensitivity analysis of the emissions due to energy consumption for caustic soda production in Europe, considering an energy consumption for the production of 3.3 10^3 kWh per electrochemical unit ECU (Euro Chlor, 2010). The ECU is the combination of 1 tonne chlorine, 1.1 tonne caustic soda and 0.03 tonne hydrogen.

As shown in Table 11, in Europe the range of indirect emission for caustic soda produced is 2.8 10^3-7.4 10^3 $kg_{CO2,eq}$ $tonnes^{-1}$of NaOH. For this reason the evaluation of the Scope III emissions is difficult, because of the high range of $CO_{2,eq}$ emitted for caustic soda produced by Nation, moreover there is the uncertainty of the emissions due to the transportation of the product as a function of the distance.

In order to estimate the wastewater processed in the plant, it has been done a water intensity analysis. The water is related to the finished product because the all tanning process is considered, from hide to leather stock.

According to the mass balance in leather processing proposed in U.N.I.D.O., 2000, from 1 kg of raw material was obtained 0.3-0.4 kg of finish product, the water consumption is generally reported in a range of 25-45 liter of water per kilograms of raw material (Kral et al., 2000; Sundar et al., 2000; Mannucci et al., 2010; Lofrano et al., 2013).

Moreover the U.N.I.D.O. 2000 reports the water intensity of 0.13 m^3 m^{-2} finished product, the density of the bovine leather is 1 kg m^{-2}, so the water intensity per finished product is evaluated around 130 L kg^{-1}.

The average of water consumption for municipal use for Italy is estimated at 64 m^3 per capita (ISTAT, 2011).

Due to variations in raw material, process, chemicals, etc., wastewater characterization can be different from district to district. All assumed parameters and wastewater characteristics are summarized in Tables 12 and 13.

The wastewater characterization reported in Table 12 and the COD fractions reported in Table 13 were used to calculate the carbon emission and the energy demand of the biological treatment. The choice of COD fractions by Munz et al (2008) was dictated by the application to the Italian locality.

In Italy tannery industry utilized 6.7 10^4 m^3 of water per year. This Country count a population of around 59 million people and the municipal wastewater utilization was around 3.8 10^9 m^3 in 2011. Compared to other important industries, such as winery industry producing yearly more than 10 10^6 m^3 (Rosso and Bolzonella, 2009) and textile industry producing yearly 6.72 10^6 m^3 (Arpat, annuario dei dati ambientali 2016), the tannery process can be considered in the country one of the most water intensive.

Table 11: Sensitivity analysis of the indirect emission for caustic soda production in Europe.

Nation	$kg_{CO2,eq}$ $tonnes^{-1}$ NaOH	Nation	$kg_{CO2,eq}$ $tonnes^{-1}$ NaOH	Nation	$kg_{CO2,eq}$ $tonnes^{-1}$ NaOH	Nation	$kg_{CO2,eq}$ $tonnes^{-1}$ NaOH
Austria	3196	Danmark	4136	Italy	3966	Romania	5371
Belgium	5075	France	2536	Latvia	3704	Spain	3881
Bulgaria	4991	Germany	4328	Netherlands	6458	Ukraine	5715
Croatia	3401	Greece	4901	Poland	6711	United Kingdom	4575
Czech Republic	4686	Hungary	4260	Portugal	3280		

Table 12: Typical process characteristics assumed in the model. Industrial wastewater characterization UNIDO, 2011; Municipal wastewater characterization Metcalf & Eddy, 2003.

	Parameter	Unit	Industrial Wastewater	Municipal Wastewater
Wastewater Quality	$[BOD_5]_{PI}$	mg O_2 l^{-1}	2000	120
	$[BOD_5]_{SE}$	mg O_2 l^{-1}	25	
	$[COD]_{PI}$	mg O_2 l^{-1}	4000	300
	$[COD]_{SE}$	mg O_2 l^{-1}	125	
	[Suspended Solids] $_{PI}$	mg l^{-1}	2000	169
	$[Total\ nitrogen\ (TKN)]_{PI}$	mg N l^{-1}	650	50
	$[S^{2-}]_{PI}$	mg S l^{-1}	160	-
	$[SO_4^{2-}]_{PI}$	mg SO_4 l^{-1}	1400	-
Process characteristics	Mean cell retention time (MCRT)	d	20	20
	Wastewater temperature	°C	20	20
	Process-water oxygen transfer efficiency per unit depth (αSOTE/Z)	% m^{-1}	1.58	3.17

Table 13: COD fraction of Tannery wastewater, all value refers to % of total COD.

	Reference	S_S	S_I	X_S	X_I
Industrial Tannery Wastewater	Orhon and Ubay Cokgor (1997)	44.4	5.8	38.8	11
	Orhon et al. (1998)	47.5	9.5		11.5
	Orhon et al. (1999)	47.4	9.4	31.7	11.5
	Ganesh et al. (2006)	59.9	24.2	15.8	
	Karahan et al. (2008)	27.2	12.7	7.7	52.2
	Munz et al. (2008)	42	20	27	11
	Insel et al. (2009)	35	8	46	11
Municipal Wastewater	Metcalf & Eddy, 2003	22	5	50	24

Soluble biodegradable COD (S_S); Soluble non-biodegradable COD (S_I); Particulate biodegradable COD (X_S); Particulate non-biodegradable COD (X_I).

With the data analysis elaborated and showed previously, the energy demand of the 5 most important leather producers for the tannery wastewater treatment was evaluated (Figure 8).

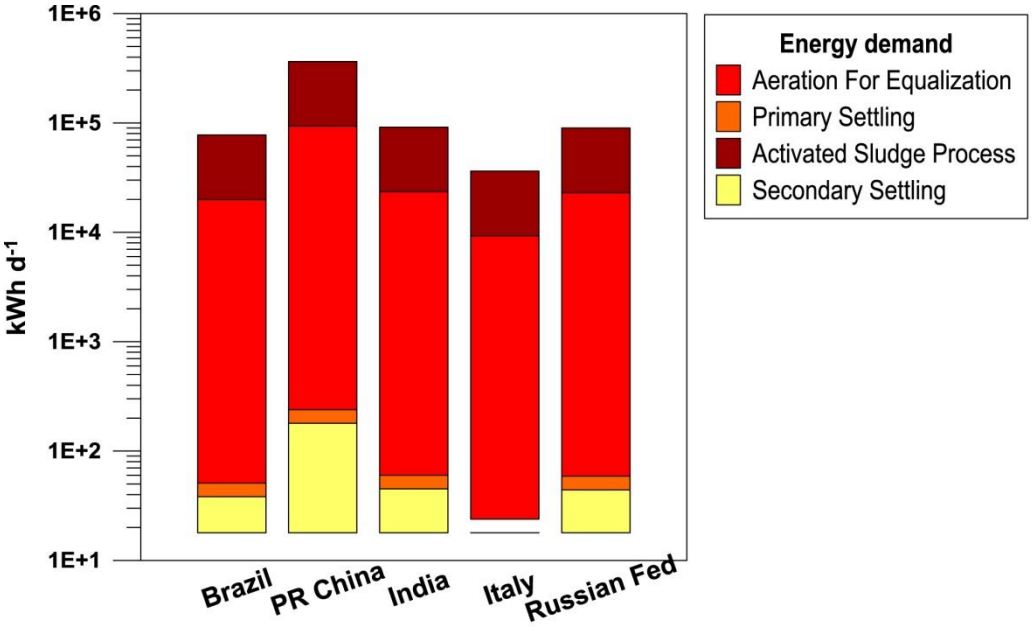

Figure 8: Energy demand of the tannery wastewater treatment of the most important producers.

As shown in Figure 8, the settling process requires less energy compared to the aeration process. Moreover, the activated sludge processes aeration tank requires more energy compared to equalization, and in fact it required almost three times more energy. The highest total power demand related to the highest producer (PR China) was estimated at 15 MW. The energy intensity of tannery wastewater treatment was evaluated at 3.6 kWh kg^{-1} bCOD removed (4.9 kWh m^{-3}).

Figure 9 shows the comparison of the energy demand between the tannery industry and municipal wastewater, refers to the Italian case study.

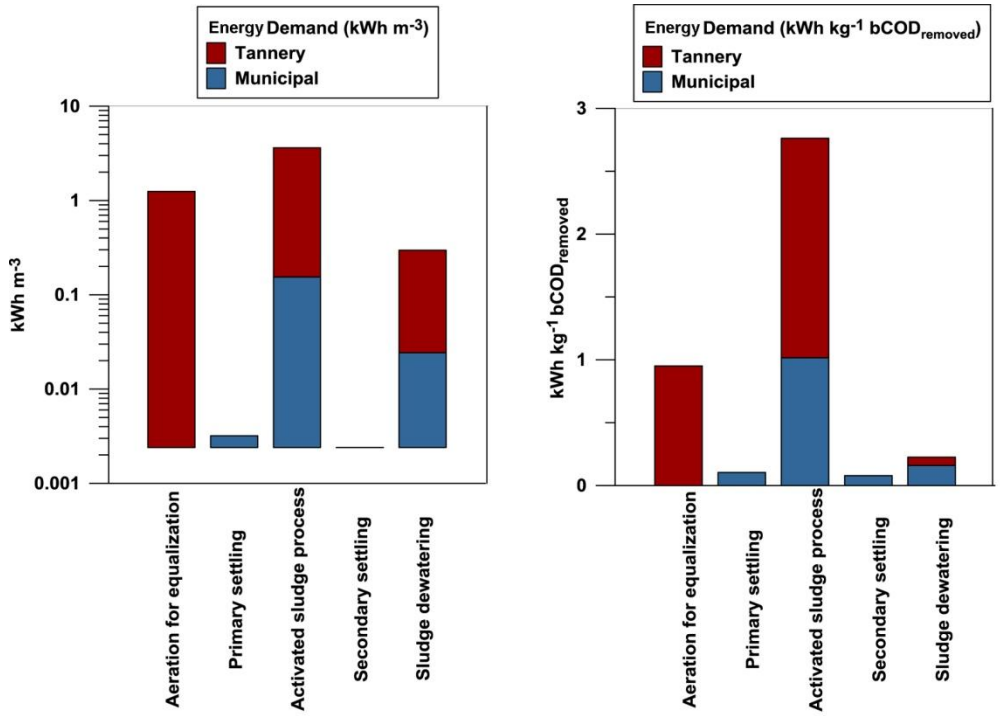

Figure 9: Comparison of the energy demand of the tannery and municipal wastewater treatment in Italy.

In Italy the power consumption of the municipal wastewater treatment was evaluated totally at 80 MW compared to 4 MW of the tannery industry. Moreover, the energy intensity is 1.4 kWh kg $bCOD_{removed}$ and 3.9 kWh kg $bCOD_{removed}$ for municipal and tannery wastewater treatment processes, respectively. In both cases, the energy demand is largely dominated by the aeration process (Rosso and Stenstrom 2008, Gori et al., 2013) at 1.0 and 3.7 kWh kg $bCOD_{removed}$ for municipal and tannery wastewater treatment, respectively.

Despite the power demand of the municipal and the tanning wastewater treatments in kWh m^{-3} are comparable, in terms of biodegradable COD removed the power demand of the tannery wastewater treatment was evaluated almost 3 times higher to the municipal wastewater treatment. This is due to the more complex substrate and recalcitrant compounds that characterize tannery wastewater.

Figure 10 shows the CFP for tannery wastewater treatment for the 5 largest producers.

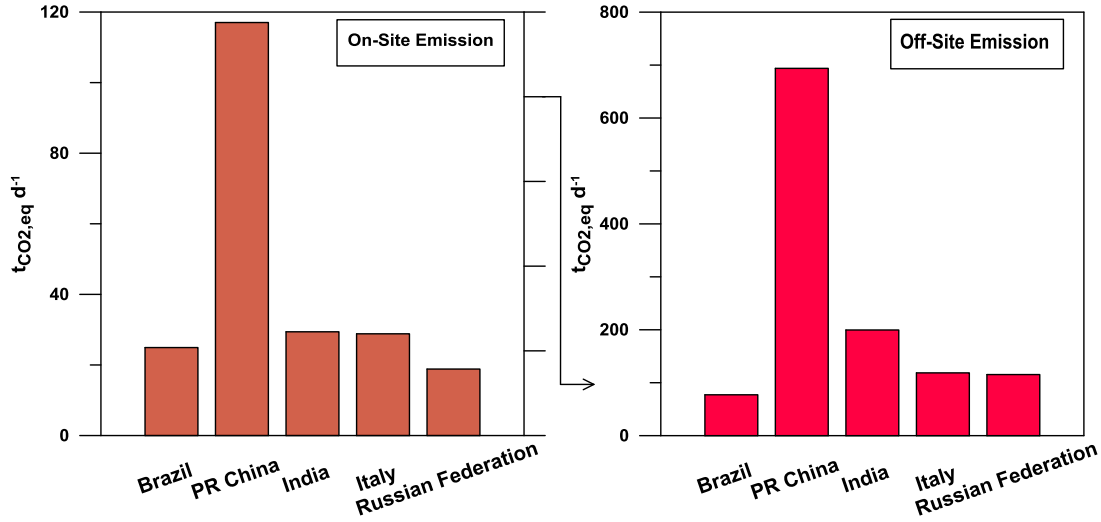

Figure 10: CFP of the tannery wastewater treatment of the 5 largest producers.

The off-site emission, due to energy generations dominates the carbon footprint analysis. The CFP of the tannery wastewater treatment amounts to 3.15 $kg_{CO2,eq}$ $kg^{-1}bCOD_{,removed}$ for the on-site emission, while the off-site emission is in the range 9.77–21.4 $kgCO_{2,eq}$ $kg^{-1}bCOD_{,removed}$. The country-specific carbon emission intensity for power generation is responsible for the wide range of off-site emission. As a term of reference, municipal wastewater treatment has a total CFP of approximately 2 $kg_{CO2,eq}$ $kg^{-1}bCOD_{,removed}$ (Gori et al, 2011). However, this does not necessarily reflect a high emission of the tannery wastewater process, since municipal wastewater is much more diluted, hence its emission per unit volume may be a more levelled comparison.

Figure 11 shows the comparison of the carbon footprint between the tannery industry and municipal wastewater, refers to the Italian case study.

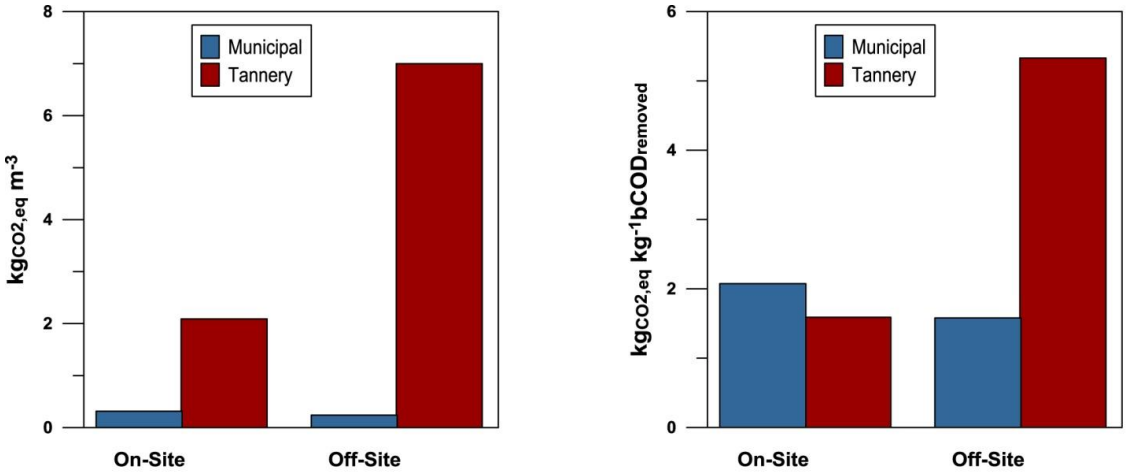

Figure 11: Comparison of the CFP of the tannery and municipal wastewater treatment in Italy.

The on-site emission of tannery and municipal are almost the same in terms of kg of $bCOD_{removed}$. On the contrary, tannery wastewater treatment requires more energy for this reason the off-site emission is almost 4 times higher compares to the municipal wastewater treatment. Our results shows that in Italy, the carbon footprint of tannery wastewater treatment is 11.17 kg CO_2,eq m^{-3} and therefore in the same range of the winery industry 9.86-17.1 kg CO_2,eq m^{-3} (Rosso and Bolzanella, 2009).

The emission due to leather production is evaluated in China at 73 kg CO_2,eq m^{-2} (Chen and Lee, 2014), hence, the industrial process emission is 103 10^9 kg CO_2,eq y^{-1}. Moreover, the on-site emission due to tannery wastewater treatment is evaluated globally in this study at 8.15 10^8 kg CO_2,eq y^{-1}. Therefore, it is possible to conclude the globally are emitted every year approximately 1.0 10^{11} kg CO_2,eq for leather production, from hide to leather stock, considering the industrial process and the emission due to wastewater treatment (on-site).

An efforts was made during this years to reduce the impact of the tannery processes, according to the report U.N.I.D.O. 2000, the challenge over the last decade was to reduce the waste of resources, only 53% of corium collagen and 15% of the chemicals purchased are retained in the finished leather.

To reduce emission for tannery wastewater treatment process, future investigations must be focused on the application of innovative technologies for the wastewater treatment, such as: biological scrubbers to control sulphur emissions; anaerobic sludge digestion to reduce biosolids disposal and reuse energy from biogas. Moreover the application of combined solid and liquid waste treatment from the same industrial process must be investigated, such as the co-digestion of waste sludge and solid waste from tanneries (Shanmugam and Horan, 2009; Thangamani et al., 2010; Zupančič and Jemec, 2010; Sri Bala Kameswari et al., 2010).
The carbon emission of the tannery wastewater treatment processes is estimated at 5.8 10^5 t $_{CO2,eq}$ y^{-1} and the power demand approximately at 30 MW. In Italy, leather tanning industry generates 5.8 10^4 t $_{CO2,eq}$ y^{-1} compared to 2.0 10^6 t $_{CO2,eq}$ y^{-1} of the municipal wastewater treatment.

Due to the high value of COD and the high level of recalcitrant compounds to be removed in the tannery wastewater, the research must be focused in processes with high COD removal and low emissions, such as the combination of the anammox process for

the sidestream and the anaerobic process to treat the sludge, as well as the implementation of biological processes for recalcitrant compounds with a low consumption such as fungal biomass.

Chapter II: Mathematical modelling of wastewater processes

Modelling activity can provide a better understanding of the processes, or can be used as a tool to improve certain plant phase, or test upgrade solutions. A model can be classified according to time variable and based on the amount of a prior information included. Figure 12 shows the model distinctions.

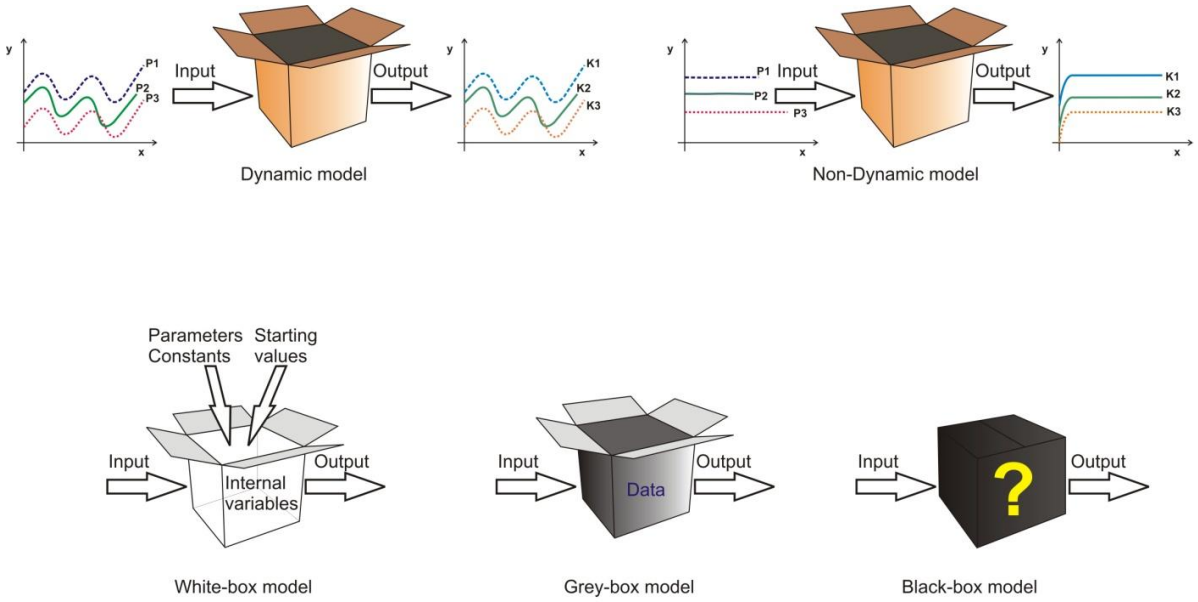

Figure 12: Model distinctions: dynamic and non-dynamic model; white, grey and black-box model.

The time classifications divided the model in the following categories:

- Dynamic model: time-dependent, the system is evaluated as time variable;
- Non-dynamic model: steady state, the system is in equilibrium and it is time-invariant.

The amount of a prior information included allows the distinction:

- White-box model: deductive and use the information to describe the biochemical reactions;
- Grey-box model: or mechanistically inspired models are those in which the parameters have a physical interpretation but are adjustable, for instance by a

parameter estimation procedure. This is often the result of an approximation or simplification of the described process;

- Black-box model: or data-driven models inductively link the input directly to the output without including any prior knowledge of the physical and chemical reactions occurring.

Activated sludge behaviour is now studied using complex models involving a large array of kinetic and stoichiometric coefficients (Avcioğlu et al., 2003). Activated Sludge Model No. 1 (ASM1) should be regarded as the pioneering effort in this respect, providing a giant improvement in the mechanistic understanding of carbon and nitrogen removal (Henze et al., 1987). It was soon modified for endogenous decay (Orhon et al. 1999). Recently, Activated Sludge Model No. 3 (ASM3) was proposed adopting endogenous decay and advocating biochemical storage as the primary mechanism of substrate utilization (Henze et al., 2000). Moreover, the IWA Anaerobic Digestion Modelling Task Group was established in 1997 at the 8th World Congress on Anaerobic Digestion (Sendai, Japan) with the goal of developing a generalised anaerobic digestion model, Anaerobic Digestion Model No. 1.

2.1 Activated sludge model

The first standardized activated sludge model was born in 1987 by a task group of the International Association on Water Quality (IAWQ, formerly IAWPRC). The first goal was to review existing models and the second goal was to reach a consensus concerning the simplest mathematical model having the capability of realistically predicting the performance of single-sludge systems carrying out carbon oxidation, nitrification and denitrification. The model was named Activated Sludge Model No. 1.

Although the model has been extended since then, for example to incorporate more fractions of COD to accommodate new experimental observations, to describe growth and population dynamics of floc forming and filamentous bacteria and to include new processes for describing enhanced biological phosphorus removal, the original model is probably still the most widely used for describing wastewater treatment processes all over the world. Due to its major impact on the WWT community it deserves some extra attention and it can still be considered as a ‘state-of-the-art’ model when biological phosphorus removal is not considered (Jeppsson and Olsson, 1996). The model is described in 8 reactions and 13 variables.

The ASM3 model (Gujer et al., 1999) was also developed for biological N removal WWTPs, with the same goals as ASM1. The major difference between the ASM1 and ASM3 models is that the latter recognises the importance of storage polymers in the heterotrophic activated sludge conversions. In the ASM3 model, it is assumed that all readily biodegradable substrate (S_S) is first taken up and stored into an internal cell component (X_{STO}) prior to growth. The heterotrophic biomass is thus modelled with an internal cell structure, similar to the phosphorus accumulating organisms (PAOs) in the biological phosphorus removal (bio-P) models. The internal component X_{STO} is subsequently used for biomass growth in the ASM3 model. Biomass growth directly on external substrate as described in ASM1 is not considered in ASM3. Figure 13 shows the models scheme.

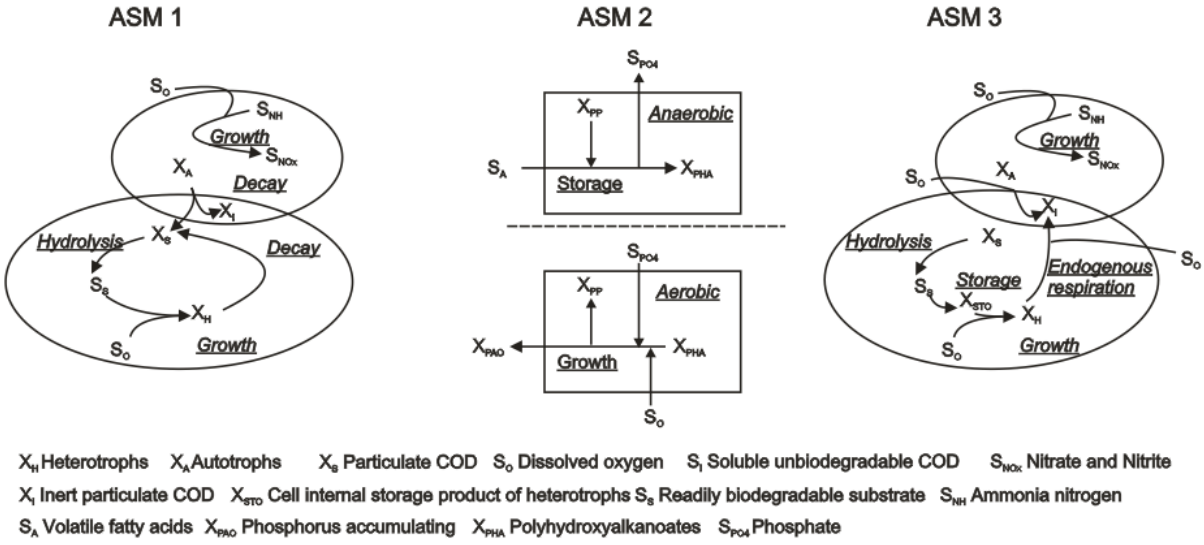

Figure 13: Substrate flows for autotrophic and heterotrophic biomass in the ASM1, ASM2 and ASM3 models.

The overview of models including bio-P will start with the ASM2 model, which extends the capabilities of ASM1 to the description of bio-P. Chemical P removal via precipitation was also included. The ASM2 publication mentions explicitly that this model allows description of bio-P processes, but does not yet include all observed phenomena. For example, the ASM2d model builds on the ASM2 model, adding the denitrifying activity of PAOs which should allow a better description of the dynamics of phosphate and nitrate (Gernaey et al., 2004).

Limitations

In ASM1, it is assumed that the pH is constant and near neutrality. Including alkalinity as one of the state variables in the model allows detection of possible pH problems. Nitrification is especially sensitive to inhibition by toxic components. In ASM1, the nitrification parameters are assumed to be constant. This means that any inhibitory effect of the wastewater on the nitrification kinetics is assumed to be included in the calibrated nitrification parameters. It is thus only possible to represent an "average inhibitory effect" of the wastewater. The standard models were developed to simulate municipal wastewater, thus reflects the influent characterization, difficult or almost impossible is the industrial wastewater influent simulation. The ASM series acknowledged that these models have been designed for domestic wastewater treatment at SRT≤30 days.

2.2 Anaerobic digestion model

The anaerobic digestion process allows the energetic valorisation of various types of biomass (including organic wastes) and reduce the disposal. Although the process has been known and implemented for many decades, it is not yet fully understood. This is mainly due to the complexity of the different (microbial and physicochemical) reactions involved. Further development is needed to optimise the process, including a more fundamental understanding of the underlying mechanisms, together with the availability of mathematical models for both simulation and control purposes (Lauwers et al., 2013).

The first anaerobic digestion models date back to the mid-sixties with the model proposed by Andrews and Pearson. The substrate of the digestion was assumed to consist of dissolved organic substances, which were converted to methane by microbial acidogenesis and acetoclastic methanogenesis. Further developments and integrations during these years until 1997, when the IWA developed a standard model to described the process, Anaerobic Digestion Model No. 1 (ADM1).

Figure 14 shows a scheme of a typical single-tank digester.

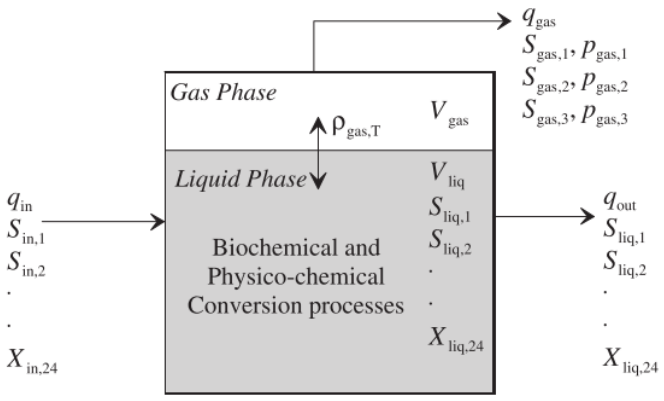

q= flow; V=volume; $S_{stream,i}$=concentration of liquid components; $X_{stream,i}$=concentration of particulate components; i is the component index.

Figure 14: Schematic representation of a typical single tank digester (Batstone et al., 2002).

The anaerobic digestion process is a complex system of reactions in sequential and parallel steps. The reactions can be divided into two main types:

- Biochemical reactions. These are normally catalysed by intra or extracellular enzymes and act on the pool of biologically available organic material. Disintegration of composites (such as dead biomass) to particulate constituents and the subsequent enzymatic hydrolysis of these to their soluble monomers are extracellular. Degradation of soluble materials are mediated by organisms intracellularly, resulting in biomass growth and subsequent decay.
- Physico-chemical reactions. These are not biologically mediated and encompass ion association/dissociation, and gas-liquid transfer.
- Precipitation.

The first two are included in the ADM1, while the precipitation is not represented. Figure 15 shows the model scheme including biochemical processes.

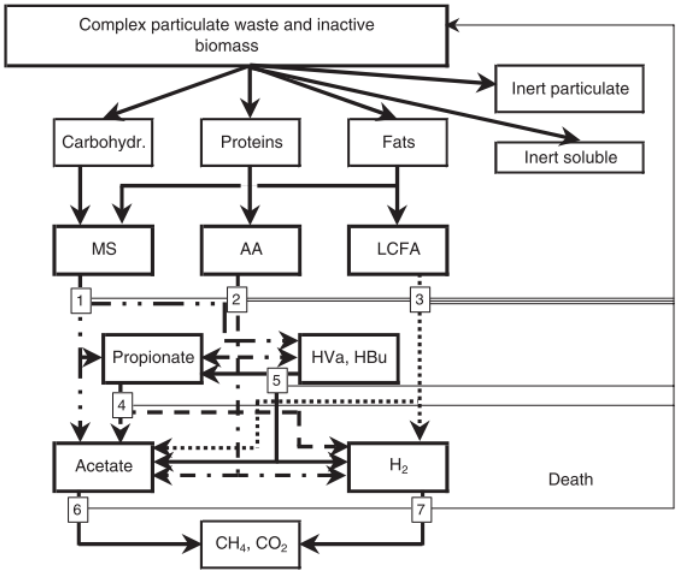

(1) acidogenesis from sugars, (2) acidogenesis from amino acids, (3) acetogenesis from LCFA, (4) acetogenesis from propionate, (5) acetogenesis from butyrate and valerate, (6) aceticlastic methanogenesis, and (7) hydrogenotrophic methanogenesis.

Figure 15: AMD1 as implemented including biochemical processes (Batstone et al., 2002).

As shown in figure 15, the model includes 3 biological cellular steps: acidogenesis or fermentation, acetogenesis, or anaerobic oxidation of both VFAs and LCFAs and methanogenesis, as well as an extracellular (partly non-biological) disintegration step and an extracellular hydrolysis step.

All bio-chemical extracellular steps were assumed to be first order, which is a simplification based on empiricism, reflecting the cumulative effect of a multi-step process (Eastman and Ferguson, 1981).

Two separate groups of acidogens degrade monosaccharide and amino acids to mixed organic acids, hydrogen and carbon dioxide. The organic acids are subsequently converted to acetate, hydrogen and carbon dioxide by acetogenic groups that utilise LCFA, butyrate and valerate (one group for the two substrates), and propionate. The hydrogen produced by these organisms is consumed by a hydrogen-utilising methanogenic group, and the acetate by an aceticlastic methanogenic group. Substrate uptake Monod-type kinetics (slightly different from ASM Monod growth kinetics) are used as the basis for all intracellular bio- chemical reactions. Biomass growth is implicit

in substrate uptake. Death of biomass is represented by first order kinetics, and dead biomass is maintained in the system as composite particulate material. Inhibition functions include pH (all groups), hydrogen (acetogenic groups) and free ammonia (aceticlastic methanogens). pH inhibition is implemented as one of two empirical equations, while hydrogen and free ammonia inhibition are represented by non-competitive functions. The other uptake-regulating functions are secondary Monod kinetics for inorganic nitrogen (ammonia and ammonium), to prevent growth when nitrogen is limited, and competitive uptake of butyrate and valerate by the single group that utilises these two organic acids (Batstone et al., 2002).

The physico-chemical reactions are: liquid-liquid like ion association/dissociation; liquid-gas exchanges like gas transfer; liquid–solid transformations like precipitation and solubilisation of ions. Only the first two reactions are included in the ADM1 because modelling precipitation is complicated, and because models that include precipitation reactions are recent (van Langerak et al., 1997, Batstone et al., 2002).

The original ADM1 structure has the advantage that it serves as a platform for further modification which leads to refinement of the model. Most modifications are dedicated to specific situations or substrates, e.g. the occurrence of high concentrations of cyanide or sodium, although some are generally applicable, such as a thermodynamic dependence of the stoichiometry (Lauwers et al., 2013).

Because the substrate definition differs between ASM and ADM1, a crucial element is the interfacing between the two models. Although the interface can be done following the scheme in 6 steps (Lauwers et al., 2013):

1) Negative COD (dissolved oxygen and nitrate) is subtracted from readily degradable matter, slowly degradable matter, heterotrophic biomass and autotrophic biomass;
2) S_S and organic nitrogen are allocated to amino acids, remaining S_S is allocated to monosaccharides;
3) X_S and particulate organic nitrogen is allocated to proteins with the remaining X_S converted to 70% lipids and carbohydrates;
4) The activated sludge biomass consisting of biodegradable and non-degradable components;
5) The degradable part is converted to proteins, using nitrogen in the sludge, with the remainder converted to lipids and carbohydrates. The inert ASM1 components

(biomass decay products X_P, inert soluble S_I, particulate X_I and the non-degradable biomass) are converted to the ADM1 inerts (S_I and X_I) taking nitrogen into account for the differences in nitrogen content, the remaining nitrogen is allocated to the inorganic nitrogen;

6) From S_{NO}, ammonia and the alkalinity, the inorganic carbon content and the cations and anions are calculated using the charge balance.

2.3 Sulphide denitrification model

The heterotrophic denitrification is the main process for nitrogen oxides removal from wastewater (Pan et al., 2013). Although autotrophic denitrification with sulphide as electron donor has been investigated by several researchers with the main applicative purpose of applying it in the treatment of liquid streams (Lu et al. 2009), sulphide removal through denitrification was recently tested on biogas and other gaseous streams (Kleerebezem and Mendez 2002). Autotrophic denitrification has drawn received increasing interests (An et al., 2010; Fajardo et al., 2012; Sierra-Alvarez et al., 2007; Soares, 2002; Vaiopoulou et al., 2005). In the process, sulphur compounds e.g., S^{2-}, S, $S_2O_3^{2-}$,$S_4O_6^{2-}$ and SO_3^{2-}, are used as energy source and electron donors to remove nitrite or nitrate (Chung et al., 2014; Qian et al., 2015a, 2015b; Sahinkaya et al., 2014).

Compared with heterotrophic denitrification, sulphide denitrification is an attractive alternative for treatment of organic carbon-deficient wastewaters, and eliminates the need for carbon sources (Fajardo et al., 2012). Furthermore, autotrophic denitrification process produces less excess sludge than heterotrophic denitrification (Shao et al., 2010), consequently it reduces the sludge treatment costs.

Biological processes, do not require the use of chemicals, can remove H_2S under varying operating conditions and require only a few days for biological process start-up (Wu et al. 2001; Namini et al. 2008). The use of alternative electron acceptors, instead of oxygen, would make the use of this technology more favourable for the treatment of the biogas produced from anaerobic digestion of tannery industrial sludge. The supernatant originated from the anaerobic digestion is characterized by high ammonia concentration (up to 900 mg $N\text{-}NH_4$ l^{-1}); its nitrification in a side stream separated from the main treatment train will allow the production of liquid streams with high nitrate and/or nitrite concentration that could be used as electron acceptor in autotrophic denitrification process (Munz et al., 2015). The process has been studied in the last decade (Beristain et

al., 2006; Kim et al., 2004; Sun and Nemati, 2012; van Hulle et al., 2010). However, there is a lack on the modelization of the process to better understand the biological pathways and/or validate the application in full scale plant.

Mora et al., 2014 a, b proposed a kinetic model describing the two-step denitrification ($NO_3^- \rightarrow NO_2^- \rightarrow N_2$) was calibrated and validated through the estimation of several kinetic parameters from the fitting of experimental respirometric profiles obtained using either nitrate or nitrite as electron acceptors for both acclimated and non-acclimated biomass.

Xu et al., 2016 propose a kinetic model for anaerobic digestion process with 4 processes and 5 components with 9 parameters to describe the sulphide biooxidation and nitrite removal process. In this model, 4 oxidation-reduction reactions using sulphide as electronic donor in the AD process are taken into account.

Both studies show matching results in terms of data-model simulation for nitrogen and sulphur components. However, the model describes only the kinetic activity of the process and not the full process.

2.4 Modelling software

In the software's family available to model a wastewater treatment plant three were chosen for the modelling phase in this study: Aquasim (Eawag, Switzerland); PetWin 4.1 (Envirosim, Canada) and SUMO (Dynamita, France).

Aquasim was developed to perform such analyses for technical and natural aquatic systems. It allows its users to define the spatial configuration of the system to be investigated as a set of compartments, which can be connected to each other by links. The available compartment types are mixed reactors, biofilm reactors (consisting of a biofilm and a bulk fluid phase), advective-diffusive reactors (plug flow reactors with or without dispersion), saturated soil columns (with sorption and pore volume exchange), river sections (describing water flow and substance transport and transformation in open channels) and lakes (describing stratification and substance transport and transformation in the water column of the lake and in adjacent sediment layers). Compartments can be connected by two types of links (lakes cannot be linked to other compartments). Advective links represent water flow and advective substance transport between compartments, including bifurcations and junctions. Diffusive links represent boundary layers or membranes, which can be penetrated selectively by certain substances. The user

of the program is free in specifying any set of state variables and transformation processes to be active within the compartments. For the model as defined by the user, the program is able to perform simulations, sensitivity analyses and parameter estimations using measured data. These features make the program a very useful research tool.

The limitations of this software are: a graphic interface is not available; full plant representations are possible, however to perform the simulations too much time is required.

PetWin software was born to model the petrochemical wastewater, so allows the inclusion of industrial component and sulphur compounds. The user can define and analyze behavior of complex treatment plant configurations with single or multiple petrochemical and other wastewater inputs. Most types of petroleum and petrochemical wastewater treatment systems can be configured in PetWin using the many process modules. The simulator includes:

- A range of activated sludge bioreactor modules – suspended growth reactors (diffused air or surface aeration), various SBRs, media reactors for Integrated fixed film activated sludge and MBBR systems, variable volume reactors.
- Anaerobic and aerobic digesters.
- Various settling tank modules – primary, ideal and 1-D model settlers.
- Different input elements – industrial influent (COD-based), other wastewater influent (COD- or BOD-based), user-defined (state variable concentrations), metal addition for chemical phosphorus precipitation (ferric or alum), methanol for denitrification.
- Other process modules – holding tanks, equalization tanks, dewatering units, flow splitters and combiners.

The PetWin model merges both activated sludge and anaerobic biological processes. Additionally, the model integrates pH and chemical phosphorus precipitation processes.

Complex treatment plant schemes can be configured by a graphical interface. The PetWin simulator suite presently includes two modules:

- A steady state module for analyzing systems based on constant influent loading and/or flow weighted averages of time-varying inputs. This unit is also very useful for mass balancing over complex plant configurations.
- An interactive dynamic simulator where the user can operate and manipulate the treatment system "on the fly".

The limitation of the software is that the model structure is fixed and it is barely impossible to change it.

SUMO is a powerful, open process source, multipurpose simulation environment developed for environmental models, particularly municipal and industrial wastewater treatment plant modelling. A wide range of plant configurations can be simulated in Sumo. Sumo models are written in an Excel based open process source code language called SumoSlang (Sumo Simulation Language, copyright Dynamita).
Sumo can simulate traditional biokinetic models dynamically or in steady-state, mixed equilibrium-kinetic models and direct algebraic models depending on the simulation mode. The simulator is supplied with internally researched and developed whole plant models as well as focus models (e.g. with focus on the fate of nitrogen and GHG). The seven most widely known published models are also included in the Sumo Museum for N and P removal. Sumo models can be run through several different interfaces.
The software merges both activated sludge and anaerobic biological processes. A variety of model options can be selected:

- The calculation of the gas phase concentrations;
- The integration of the pH;
- The chemical precipitations of some components.

Complex treatment plant schemes can be configured by a graphical interface. The models are written in an Excel based open process source code language called SumoSlang (Sumo Simulation Language, copyright Dynamita), so a customizable Excel front end can also be prepared from a template provided. Both, steady state and dynamic simulations can be performed.

The limitation of the software is the instability of the hardware, i.e. sometimes the software can crash in a middle of a simulation.

Tables 14 and 15 show the model components in the comparison between the softwares implementations (PetWin 4.1, SUMO) and the standard models (ASM 1, ASM 2d, ASM 3 and ADM 1).

Table 14: Model components in PetWin 4.1, SUMO, ASM 1, ASM 2d and ASM 3.

Description	PetWin 4.1	SUMO	ASM 1	ASM 2d	ASM 3
Ordinary heterotrophic organisms	x	x	x	x	x
Readily biodegradable complex COD (non-VFA)	x	x	x	x	x
VFAs	x	x			
Acetate	x	x		x	
Soluble inert COD	x	x	x	x	x
Slowly biodegradable particulate	x	x	x	x	x
Particulate inert COD	x	x	x	x	x
Colloidal unbiodegradable organics		x			
Colloidal biodegradable substrate		x			
Endogenous products	x	x	x		
Dissolved oxygen	x	x	x	x	x
Autotrophs: Ammonia oxidizing biomass	x	x	x	x	x
Autotrophs: Nitrite oxidizing biomass	x	x			
Particulate biodegradable organic nitrogen	x	x	x	x	x
Soluble biodegradable organic nitrogen	x	x	x	x	x
Colloidal biodegradable organic N		x			
Colloidal unbiodegradable organic N		x			
Soluble unbiodegradable organic N		x			
Particulate unbiodegradable organic N		x			
Ammonia N	x	x	x	x	x
Nitrate N	x	x	x	x	x
Nitrite N	x	x			
Dissolved Nitrogen	x	x	x	x	x
Polyphosphate accumulating organisms	x	x		x	
Stored PHA	x	x		x	x
PO4 (including metal complex)	x	x		x	
Releasable stored poly P	x	x		x	
Ferric hydroxide	x	x		x	
Ferric phosphate	x	x		x	
Sulphur oxidizing bacteria	x				
Sulphide	x				
Sulphate	x				
Industrial - Soluble biodegradable volatile COD, 3 different characterizations	x				

Description	PetWin 4.1	SUMO	ASM 1	ASM 2d	ASM 3
Soluble hydrocarbon COD	x				
Adsorbed hydrocarbon COD	x				
Methanol		x			
Anammox organisms		x			
Anoxic methanol utilizers		x			

Table 15: Model components of anaerobic digestion process in PetWin 4.1, SUMO and ADM1.

Description	PetWin	SUMO	ADM 1
Acetotrophic sulphur reducing bacteria	x		-
Propionate degrading sulphur reducing bacteria	x		-
Hydrogenotrophic sulphur reducing bacteria	x		-
Heterotrophic Growth through Fermentation	x	x	x
Propionic Acetogens	x		x
Acidoclastic methanogens	x	x	x
Hydrogenotrophic methanogens.		x	x

As shown in tables 14 and 15 the lack in the standard models is the sulphur compounds, for the case study. Moreover, to simulate a wastewater treatment plant with the anaerobic digestion an interface of the two models (ASM and ADM) is required. Almost all of the software that includes the anaerobic digestion process represented it with less processes and details compare to the complexity of the ADM.

Chapter III: Materials and methods

The research activity took place in the Tuscan tannery district. Within this territory the Consorzio Cuoiodepur wastewater treatment plant located in San Romano-Pisa, treats vegetable tannery wastewater. In the plant, the research activity took place in the CER2CO (Research Center for Tannery Wastewater) laboratory.

The anaerobic digestion and co-digestion tests have been conducted in the following different scales:

- Bench scale batch tests
- Laboratory scale tests
- Pilot scale tests.

Table 16 shows the operational conditions of the investigation.

Table 16: Operational conditions of the investigation, anaerobic digestion experimental tests.

Process		**Scale**	**Equipment**	**Substrate**
Anaerobic co-digestion	Batch tests	Bench	Oxitop ® bottles (1 l each)	VTPS+TIF
	Continuous tests	Pilot	3 reactors (130 l each)	VTPS+TIF
Anaerobic digestion	Batch tests	Bench	Oxitop ® bottles (1 l each)	VTPS+CDPS
	Continuous tests	Laboratory	2 reactors (4 l each)	VTPS+CDPS
		Pilot	1 reactor (5 m^3)	VTPS

Moreover, figure 16 shows the operational conditions (different SRT and substrate) tested for the continuous tests.

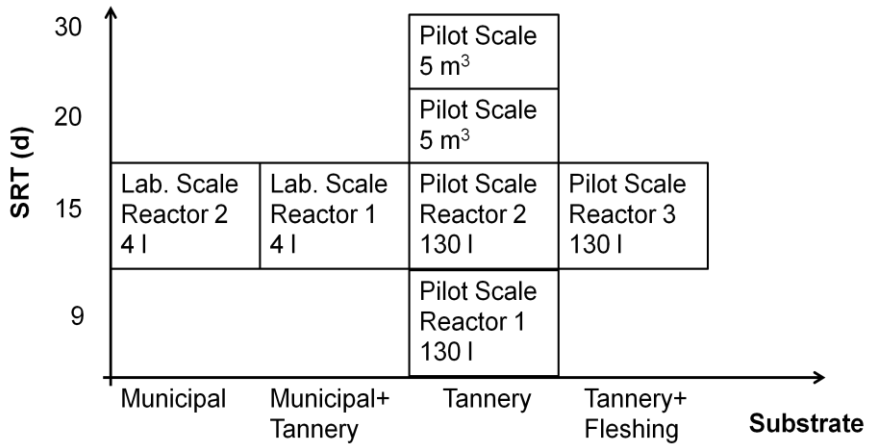

Figure 16: Operational conditions tested in the experimental phase.

This chapter will include the description of the materials and methods. All reactors, analytical procedures, experimental setup and the assumptions of the modelling phase will be presented. Moreover, it will include the presentation of the Tuscan tannery district, Cuoiodepur WWTP and S.G.S. plant.

3.1 Case study: Tuscan tannery district

The Italian tannery industry produces 9% of the global and 73% of the European bovine leather (Un-Fao, 2013). As show in figure 17 the leather industry in Italy is divided in four main poles within the regions: Lombardy, Veneto, Tuscany and Campania.

Figure 17: Italian leather industry, Lofrano et al., 2013.

The Tuscan tannery district is the second largest in Europe and its production consists for the 35% of the Italian leather production and it is concentrated in the area surrounding Florence and Pisa.

The peculiarity of the district is the division in two different sectors or sub-districts where chrome and vegetable tanning processes are separately operated.

Figure 18 shows the georeferencing of the district.

Figure 18: Tuscan tannery district georeferincing.

The district is in the following territories: Santa Croce Sull'arno (Pi), San Miniato (Pi), Fucecchio (Fi), Castelfranco Di Sotto (Pi), Santa Maria A Monte (Pi). As shown in figure 18 the Arno river divided the area and its reflect the divion of the sub-districts. On the North area of the Arno river chrome tanning is operated, while in the South part vegetable tanning is operated.

Within this territory 3 wastewater treatment plants are dedicated to process almost exclusively the wastewater from the tannery industry: Consorzio Aquarno, Depuratore di Santa Croce sull'Arno and Depuratore di Castel Franco di Sotto, Consorzio Cuoiodepur; while Consorzio S.G.S. is the plant dedicated for the solid waste treatment for the all district.

The two main wastewater treatment plants are managed by two consortiums (Consorzio Aquarno and Consorzio Cuoiodepur), separated for the type of process applied: chrome tanning, the former and tanning tannins, the latter.

Figure 19 shows the wastewater and solid waste plants treatment localization.

Figure 19: Tuscan tannery district, map georeferincing the wastewater treatment plants.

In the next paragraph the attention is focused on the vegetable wastewater treatment at Consorzio Cuoiodepur and the solid treatment at Consorzio S.G.S..

3.1.1. Consorzio Cuoiodepur S.p.A.

The Cuoiodepur WWTP (San Miniato, PI, Italy) treats vegetable tanning wastewater from the tanneries located in San Miniato and Monopoli Val d'Arno and the municipal wastewater of the area surrounding San Romano, San Donato, San Miniato Basso and Ponte a Egola.

The wastewater treatment plant is a chain of very complex treatment. It includes, high process units and non-common type treatments. This is due to the matrix treated, the high load in terms of suspended solids, biodegradable organic compounds and inhibiting, salinity, oxidized and reduced sulfur and nitrogen compounds. The main objectives of the plant operation is the removal of the organic load and nitrogen compounds from the water line and hydrogen sulfide from gaseous effluents.

Figure 20 shows the plant framing.

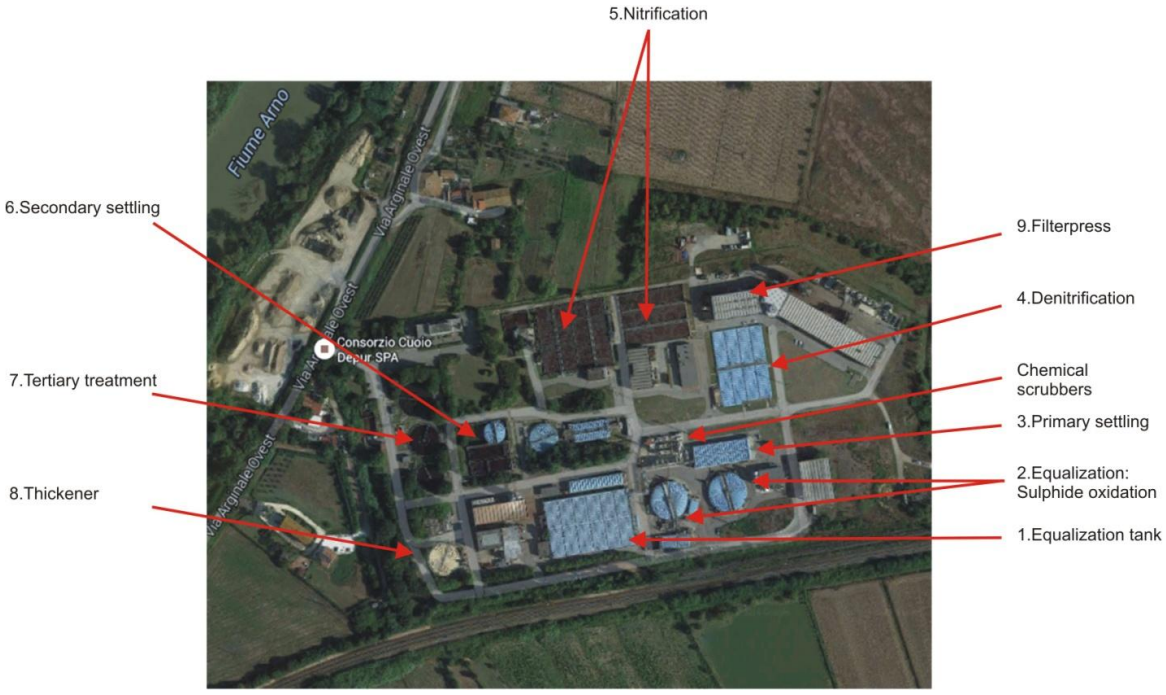

Figure 20: Cuoiodepur wastewater treatment plant scheme.

The industrial wastewater is subjected to fine screening (2 mm) to remove the big particles and trimmings from the beam-house operations (i.e. during the calcination phase). After that, the wastewater is subjected to grit oil removal in a cover tank for the detention of odorous emissions, which provides the collections of the H_2S desorbed from the sewage to the system centralized chemical scrubbers. One of the peculiarity of the plant is the cover reactors for the primary line: equalization, sulphide oxidation, primary settling and denitrification. That is necessary to avoid odors emissions due to the sulphide stripping to H_2S. Moreover, the gas phase collected in the cover reactors is treated in the chemical scrubbers.

Figure 21 shows the wastewater treatment plant configuration.

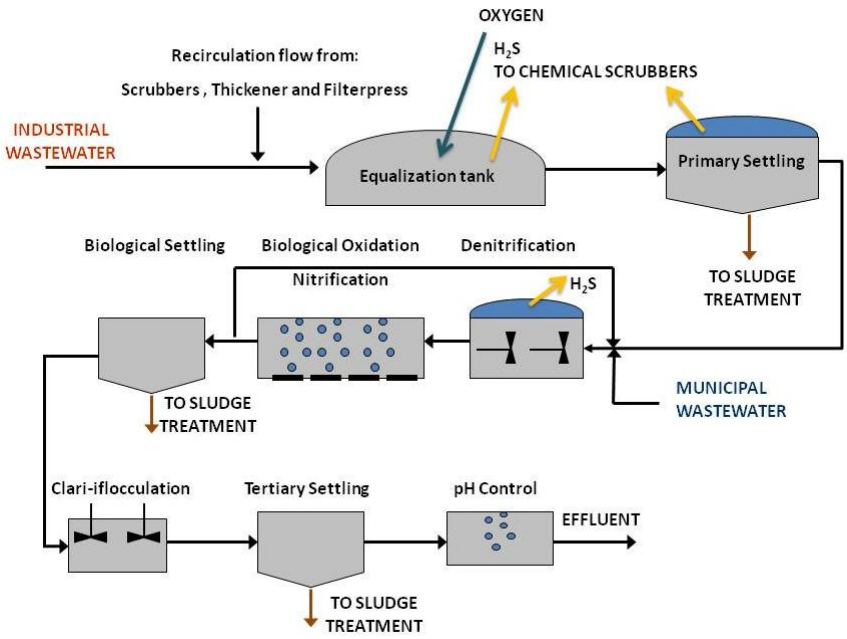

Figure 21: Cuouodepur wastewater plant scheme.

After the preliminary treatment, the sewage is collected to the equalization, two circular tanks of 3750 m^3 each. As shown in figure 21, here is collected also flow the recirculation flows as the supernatants of the chemical scrubbers, the supernatant of the thickener and the filtrate obtained with the filter presses of the sludge treatment processes. The equalization process involves two important functions: the equalization of the daily flow variation; the sulphide oxidation with pure oxygen. The oxygen is produced in the plant through a zeolite air adsorption process. The tank is covered and collects odor emissions to the scrubbers.

The primary settling has a total volume of 1260 m^3. Primary sludge is more than the 70% of the total sludge volume produced in the plant and are characterized by the 4% of dry matter. The primary effluent goes to biological treatment process after the mixing with the municipal wastewater influent.

The denitrification process is the first step of the biological treatment with a tank of 11000 m^3 of total volume. Cover reactor with submerged mixing to allows the mixing of the activated sludge. The biological oxidation-nitrification reactor volume is 26000 m^3 with an average air flow rate of 20.000 $Nm^3 h^{-1}$ provides by submerged fine bubbles. The

biological oxidation is characterized by an average hydraulic retention time of 50 hours, 2/3 of the total hydraulic retention time for the all biological process (72 hours=3 days). The temperature in the tank is in the range 20-23 °C (summertime 28-30°C, wintertime 18-20°C). The internal recirculation for the biological process is characterized by a flow rate of 7 times the total flow, while the rest of the flow goes the secondary settling.

The secondary settling is characterized by a pre-step of post-denitrification. All the sludge from the secondary settling (2% of dry matter) is the recirculation in the biological process.

Tertiary treatment includes the flocculation with ferrous chloride ($FeCl_2$) and polyelectrolytes at basic pH (10.5 - 11); basic conditions is provided by adding hydrated lime. The sludge obtained (4% of dry matter) goes to thickening, along with the primary sludge. Before the discharging the effluent goes to pH correction. The pH limits are defined by low at 6.5-8.5 for the discharge in the river. The limits are reach with a carbon dioxide dosage.

The sludge, after thermal drying and mixing with by-products of the industrial tannery process, is used to produce fertilizers.

Figure 22 shows the sludge treatment scheme.

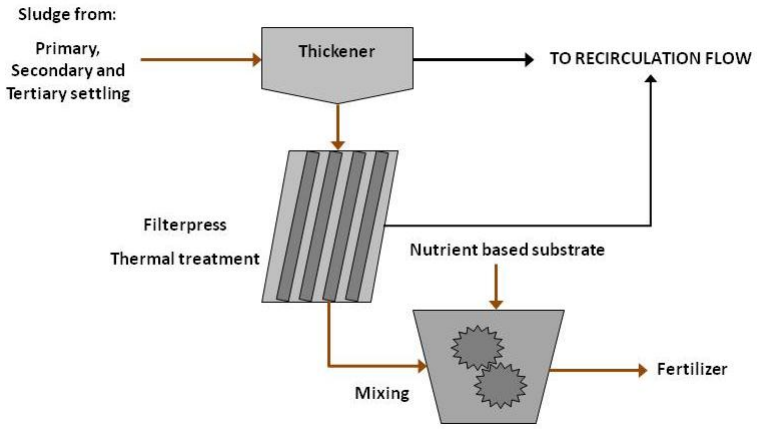

Figure 22: Cuoiodepur sludge treatment scheme.

As shown in figure 22 sludge treatment is made up of three processes: thickening, dewatering and mixing with nutrient based substrates. The thickener allows to mix the sludge and reach the 5-6% of dry matter (from 3-4%). The dewatering is done by thermal

treatment and adding polyelectrolyte, after the process the water content is less than 65% (from 95%).

The chemical scrubbers allows to reduce and remove odor emissions. Six wet based chemical scrubbers, total capacity of 70000 Nm^3 h^{-1}, treats the gas stream with a basic solution of caustic soda. This process afford the limit requirements: hydrogen sulphide ≤ 1.5 $mg^{-1}Nm^3$ (≤0.105 kg h^{-1}) and ammonia 5.0 $mg^{-1}Nm^3$ (≤0.350 kg h^{-1}).

Figure 23 shows the sampling points in the plant.

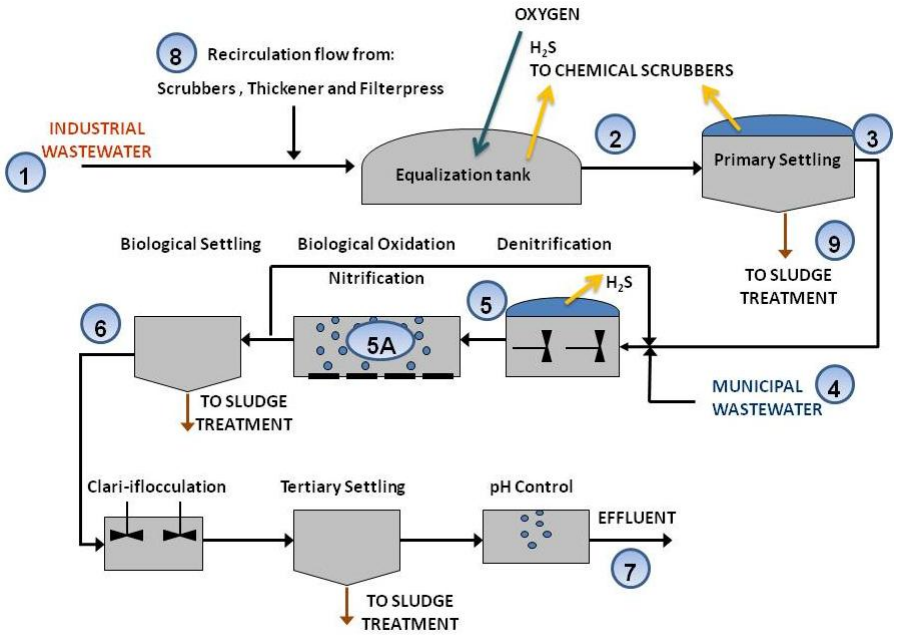

Figure 23: Scheme of sampling points in the Cuoiodepur plant.

In table 17 is shown the frequency and the parameters analyzed for each sampling point.

Table 17: Sampling analysis, parameters and frequency.

No.	Parameters	Frequency
1	Q, filtered COD, total COD, TSS,TN, NH_4^+, S^{2-}*, SO_4^{2-}, pH, chloride, total phosphorus, TOC	Daily, * occasionally
2	Q, TSS, pH	Daily
3	Q, total COD, TSS, NH_4^+, S^{2-}, pH	Daily
4	Q, total COD, TSS,TN, NH_4^+, pH, total phosphorus	Daily
5	Q, filtered COD, TSS, pH	Daily
5A	MLSS, MLVSS, DO, pH, T	Daily
6	Q, filtered COD, TSS,TN, NH_4^+, NO_3, NO_2, S^{2-}, SO_4^{2-}, pH, chloride, TOC	Daily
7	Q, filtered COD, TSS,TN, NH_4^+, NO_3, NO_2, S^{2-}, SO_4^{2-}, pH, chloride, TOC	Daily
8	Total COD, SO_4^{2-}, S^{2-}, pH	Occasionally
9	Total COD, filtered COD, TSS, VSS, TN, NH_4^+, SO_4^{2-}, S^{2-}, pH, metals	Weekly

The samples of the daily investigation is flow rate proportional, while the weekly and the occasionally samples were sampled and analyzed for specific investigations.

3.1.2. Consorzio S.G.S.

Consorzio S.G.S. is a private company with 230 joined tanneries, in order to collect and treat the secondary raw material (fleshing and trimming), extract fats and proteins to reuse in the market. The plants treats 200 tonnes per day of solid waste. Hairs and fleshing are treated separately because of their definition, for the Italian regulation the former is considered solid waste, while the latter is consider a by-product of the industries. Figure 24 shows the treatment scheme that is almost the same for fleshing, trimming and hairs.

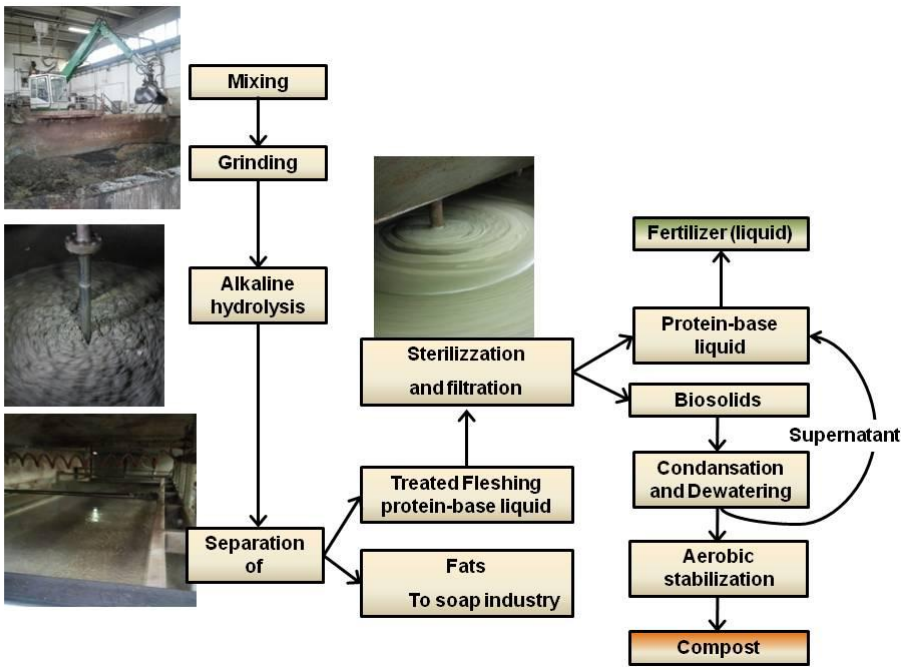

Figure 24: Fleshing, trimmings and hairs scheme treatment process.

As shown in figure 24, after the mixing and grinding of solids, an alkaline hydrolysis is carried out. Temperature, pH and process time is controller as a function of the free aminoacids in the mixture. This process allows the separation of fats and protein based liquid, the fats are recovered by soap industry. the thermal treatment of sterilization is done at 133°C for 20 minutes to reach the conditions regulated by law. The filtration allows the separation of the liquid phase protein based to the solid phase (biosolids and hydrated lime). The solid phase is then condensated and dewatered to remove the water content, these processes allow to reach the 97% of dry matter.

The whole process is done with the capture and controls of odor emissions, the gas stream reach on H_2S is treated by chemical scrubbers.

3.2 Anaerobic batch tests

The anaerobic batch tests were conducted with six Oxitop ® (WTW Ltd, Germany) that consists in a glass vessel or bottle. Each bottle has two lateral branches, a measuring pressure head and a magnetic stirrer. The lateral branches were used for the flux of the nitrogen gas to reduce the oxygen in the headspace and for the NaOH trap. The measuring pressure head tracks the pressure of the head space and the magnetic stirrer

provides the mixing of the liquid phase. The recorder provides the data collection. The Oxitop glass vessel working volume was 600 ml, filled with substrate and inoculum.

Figure 25 shows the equipment.

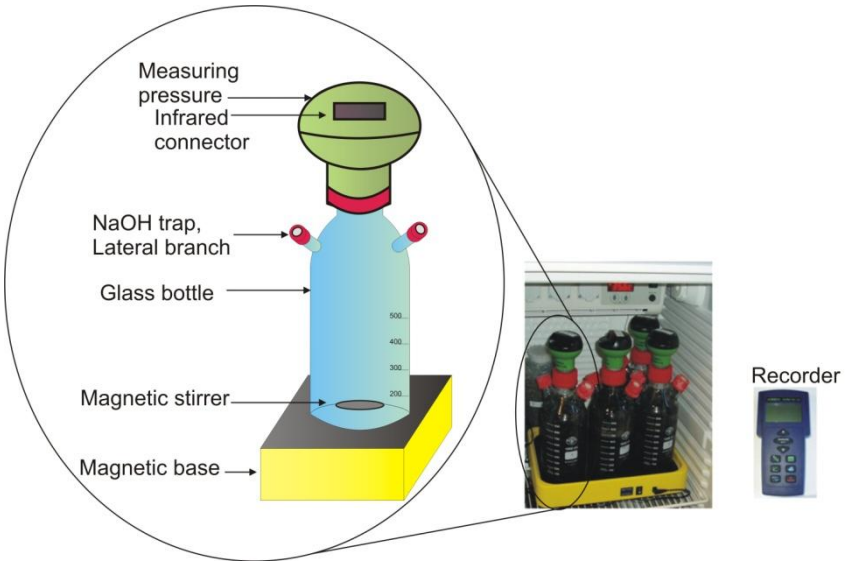

Figure 25: Anaerobic batch tests Oxitop ® (WTW Ltd, Germany) equipment.

In the co-digestion tests, before being used as substrate, fleshing was grounded using a meat-grinding machine. The inoculums-substrate (I/S) ratio was chosen as 1:1 because in previous study on co-digestion of tannery solid waste, for the I/S ratio of 1:1, maximum conversion rate of substrate was observed (Sri Bala Kameswari et al., 2012).

Each batch test were carried out in triplicate, in a closed temperature-controlled anaerobic digester. The temperature was maintained at 35 ± 0.5 °C for an HRT of 15 or 20 days (Pitk et al., 2012). The mixture was monitored at the beginning and at the end of each tests, according to IRSA-CNR methods (Italian Institute of Water Research-National Research Council): COD, TS and VS. Sulphates were evaluated through ionic chromatography (ICS1000, Dionex, U.S.A) while Sulphides were measured through colorimetric analysis using cuvette test (Hach-Lange, Germany).

Two sets of batch tests were conducted with an inoculums to substrate VS ratio of 1:1, using as substrate:

1. A mixture of VTPS:CDPS at different volumetric ratio (from 0:100 up to 100:0 in tests T1 to T6);

2. A mixture of VTPS: TIF at different mass ratio (1:2, 1:1, 2:1 in tests T7, T8 and T9, respectively). As inoculum, it was used anaerobic sludge from a pilot scale reactor fed with vegetable tannery sludge, operated in mesophilic conditions (35°C) and with 20 days of SRT.

The mass ratio of the substrate in the tests and the initial concentration in terms of volatile mass content of each tests is reported in table 18.

Table 18: Mass of fleshing (TIF), conventional domestic primary sludge (CDPS), vegetable tannery primary sludge (VTPS) and the initial VS concentration in the tests.

Test	**TIF** **g VS**	**CDPS** **g VS**	**VTPS** **g VS**	**Initial VS concentration** **g VS l^{-1}**
T1	-	3.3	0	16.1
T2	-	1.8	0.3	20.1
T3	-	2.0	2.1	17.6
T4	-	1.3	2.5	26.4
T5	-	0.5	1.3	20.1
T6	-	0	3.0	17.4
T7	3.4		1.7	16.9
T8	3.6		3.6	24.2
T9	1.6		3.2	15.9

One of the most important parameters for a batch assay design is the load of the solid substrate introduced into the digester (Raposo et al., 2012). Little and contradictory details about the influence of this parameter was found in the literature. Moreover, the influences of VS concentration is analyzed for the co-digestion of solid waste and sludge, while very few information are available for the digestion of sludge only.

Table 19 shows the comparison between volumetric and mass ratio of the two types of sludge in experiments T1-T6. Test T1 and T6 were used as controls for single substrate of VTPS and CDPS, respectively. Vegetable tannery primary sludge has a higher organic load compared to the common domestic primary sludge, which means higher mass ratio values result when volumetric ratios are converted.

The composition of the VTPS, CDPS, TIF used in the batch experiments, in terms of VS, COD and SO_4^{2-}, is reported in table 20.

Table 19: Volumetric and mass ratio of the substrates VTPS:CDPS in the tests.

Test	VTPS:CDPS Volumetric ratio	VTPS:CDPS Mass ratio g VS g^{-1}VS
T1	0:100	-
T2	20:80	0.18
T3	40:60	1.05
T4	60:40	1.92
T5	80:20	2.80
T6	100:0	-

Table 20: Characterization of fleshing (TIF), conventional domestic primary sludge (CDPS), vegetable tannery primary sludge (VTPS).

Test	TIF			CDPS			VTPS		
	VS	COD	SO_4^{2-}	VS	COD	SO_4^{2-}	VS	COD	SO_4^{2-}
	g l^{-1}			g l^{-1}			g l^{-1}		
T1	-	-	-	13.34	18.94	0.01	0	0	0
T2	-	-	-	15.00	30.94	0.02	15.72	34.40	0.15
T3	-	-	-	13.34	18.94	0.01	20.93	27.10	1.10
T4	-	-	-	13.00	18.46	0.01	16.67	34.40	1.00
T5	-	-	-	15.00	30.94	0.02	15.72	22.60	0.15
T6	-	-	-	0	0	0	12.20	37.36	1.50
T7	3.40	-	-	-	-	-	21.27	33.89	0.95
T8	3.60	-	-	-	-	-	19.30	37.36	0.09
T9	1.60	-	-	-	-	-	21.27		0.95

Cumulative biogas production, COD and VS removal were used as key parameters for the estimation of the anaerobic process efficiency. Oxitop® reactors are equipped with a pressure transducer for the measurement of the pressure variation in the headspace due to biogas production. The volume of the produced biogas was estimated in normal conditions from the measured pressure using Equation 1.

$$V_{biogas} = \frac{V_{hs} P_R}{T_R} \frac{T_N}{P_N} \quad \text{(Eq. 1)}$$

Where:

- V_{hs} is the volume of the headspace;

- P_R is the recorded pressure;
- P_N is pressure in normal conditions = 1 atm
- T_R is temperature inside reactor = 35°C = 308 K;
- T_N is temperature in normal conditions = 20°C = 293 K.

3.3 Continuous tests

The continuous tests were performed in two scales: laboratory and pilot scale. The laboratory scale includes two reactors of 4 liters each, while the pilot scale includes three reactors of 130 liters each and a 5 cubic meter reactor.

According to the mass balance of COD and sulphur compounds the estimation of the theoretical methane production and the estimation of the concentration of hydrogen sulphide in the biogas were done. The mass balances were done with the average values of the data after the start-up. The steady state was assumed when COD, VS and sulphate of the effluent resulted with variation of less than 10% for more than 7 time.

The mass balances of the reactors were evaluated according Equation 2 and Equation 3.

$$0 = COD_{in} - COD_{out} - COD_{SO_4^{2-}} - COD_{CH_4} - P_x \text{ (Eq.2)}$$

Where:

- COD_{in} is the COD influent in the reactor;
- COD_{out} is the COD in the effluent sludge;
- $COD_{SO_4^{2-}}$ is the COD due to sulphate reduction ($= \Delta SO_4 * 0.67\ gCOD\ g^{-1}SO_4$);
- COD_{CH_4} is the conversion factor from COD to methane ($0.35 \frac{NLCH_4}{gCOD}$);
- P_x is the COD used in anabolic metabolism, $P_x = \frac{Y*VSS}{(1+(k_d*SRT))} * 1.42$.

$$H_2S_{gas\ stream} = \frac{(\Delta S\_SO_4^{2-} - \Delta S\_S^{2-})}{PM\ (S)}\ [n\ mol\ d^{-1}] \text{ (Eq.3)}$$

Where:

- $H_2S(gas\ stream)$ is the estimation of the concentration of the hydrogen sulphide in the gas stream;
- $\Delta S\_SO_4^{2-}$ is the difference between sulphate influent and the sulphate in the effluent;

- ΔS_S^{2-} is the difference between sulphide influent and the sulphide in the effluent (liquid stream);
- $PM\ (S)$is the sulphur molecular weight.

Two inhibition factors (ammonia and sulphide) were evaluated. In the calculation of the inhibition factor of free ammonia the Equation 4 was used.

$$I_{NH^+_3} = \frac{1}{1+{[NH_3]}/{K_{I,NH3}}} \text{ (Eq.4)}$$

Where the inhibition constant is $K_{I,NH3} = 0.0018\ M$.

Moreover, the concentration of free ammonia was calculated according to Anthonisen et al., 1976:

$$N\_NH_3 = \frac{N\_NH_4^+ * 10^{pH}}{K_b/K_W + 10^{pH}};\ K_b/K_W = e^{(6344/273+T)} \text{ (Eq.4.a)}$$

An empirical equation was used for the inhibition factor of sulphide (Equation 5).

$$I_{H_2S} = 1 - \frac{[H_2S]}{K_{I,H2S}} \text{ (Eq.5)}$$

Where the inhibition constant is $K_{I,H2S} = 0.008\ M$.

Because little reliable information about H_2S inhibition kinetics is available, the inhibition factor as given in Eq. 5 can be considered a reasonable approximation (Fedorovich et al., 2003).

The inhibition factors are combined as in Equation 6:

$$I_{factors} = I_{H_2S} * I_{NH^+_3} \text{ (Eq.6)}$$

3.3.1. Laboratory scale tests

Two identical continuous-flow stirred-tank reactor constitute the experimental set-up. Both reactors have a double chamber allows the recirculation of the hot water to maintain the temperature required for the process. Temperature and pH were monitored.

Figure 26 shows the reactor layout.

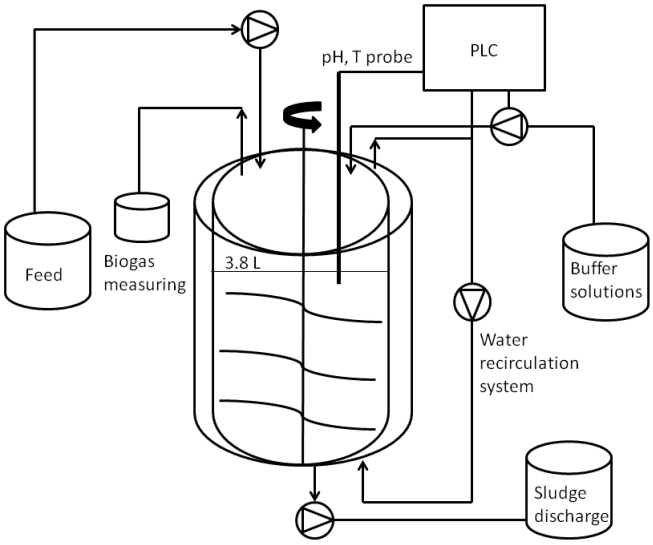

Figure 26: Laboratory scale tests, reactors layout.

Reactor 1 has been fed with a mixture of VTPS and CDPS, while Reactor R2 was fed with 100% of CDPS. Both reactors were inoculated with a mixture of anaerobic sludge from a municipal anaerobic digester (54%), anaerobic biomass acclimated to VTPS (15%), bovine manure (22%) and primary tannery sludge from Cuoiodepur WWTP (VTPS, 9%). Acclimated biomass to VTPS was obtained in batch condition after 100 days of operation. Continuous tests were operated at 35±0.5°C, pH was 7±0.02 and solids retention time (SRT) was controlled at 15 days. Feeding and effluent were monitored according to IRSA-CNR methods: COD, sulphates, TS and VS.

The scope of the test was the evaluation of a gradual adaptation of anaerobic biomass to VTPS through the feeding of a mixture of tannery and civil sludge with increasing fraction of industrial sludge. After the inoculum phase, the fraction of primary sludge in the feeding of R1 was increased stepwise to encourage the adaptation of the anaerobic biomass. Every phase lasted more than 45 days (3 times SRT) and the feeding have been changed once the steady state have been reached.

Operational conditions maintained in R1 during the experiment are reported in below:

- Phase 1: 10% of VTPS, from 0 to 69 day;
- Phase 2: 20% of VTPS, from 70 to 127 day;
- Phase 3: 30% of VTPS, from 128 to 251 day;
- Phase 4: 40% of VTPS, from 252 to 270 day.

3.3.2. Pilot scale tests

In the pilot scale tests different substrates and SRT were tested. The anaerobic digestion of tannery sludge only and the co-digestion with tannery sludge and solid waste (fleshing) were evaluated. Moreover, four SRT were tested: 9, 15, 20 and 30 days.

Figure 27 shows the conditions tested in the reactors.

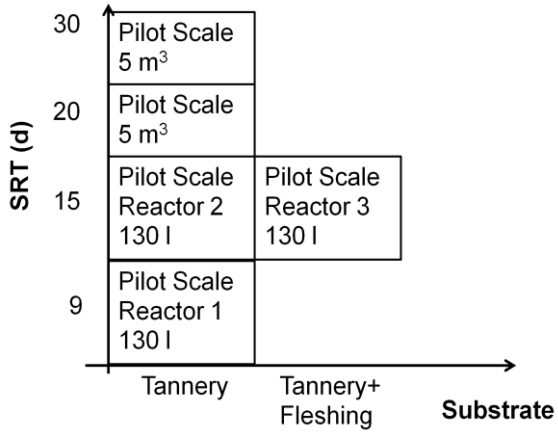

Figure 27: Operational conditions of the pilot scale reactors.

Figure 28 shows the layout and the operational conditions of the three 130 liters volume reactors.

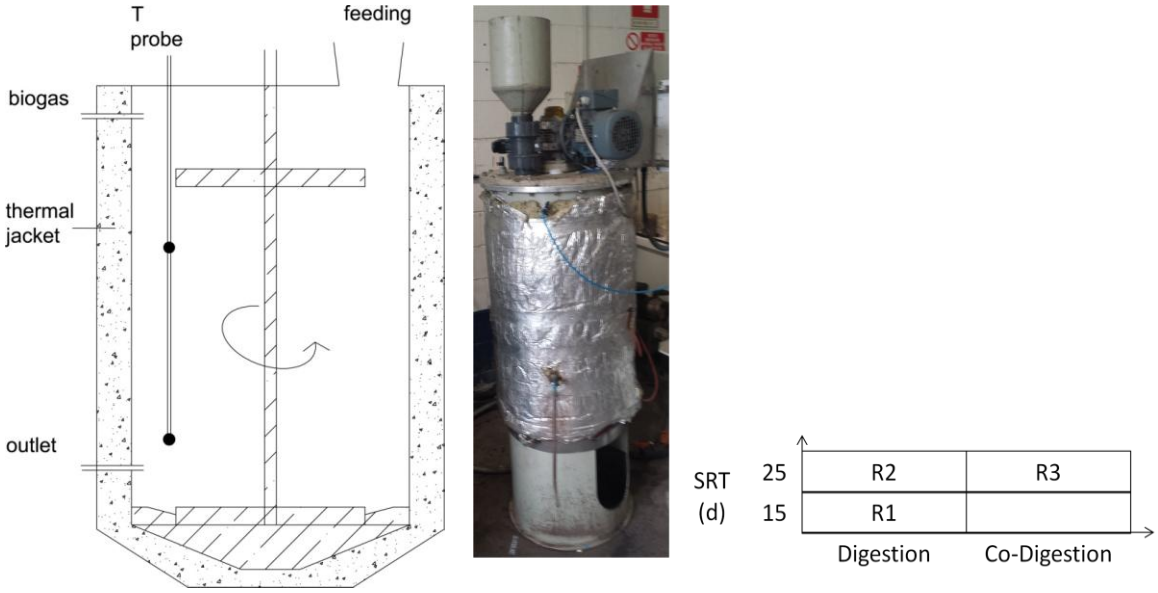

Figure 28: Pilot scale tests, reactors (130 l each) layout and operational conditions.

As shown in figure 28 a thermal jacket allows to maintain the temperature required during the process, controlled by a probe. A vertical shaft mix the liquid phase.

Three laboratory scale reactors were inoculated with anaerobic sludge from a tannery industrial anaerobic digestor (75%) and primary tannery sludge from Cuoiodepur WWTP (VTPS, 25%). Reactors were maintained at mesophilic conditions (35±0.5°C), pH was 7±0.02, with a retention time (SRT) of 25 d for approximately 1 year.

After the start-up phase (t=115 d) when reactors were fed only tannery sludge, the first reactor (R1) was kept as control (i.e., tannery sludge only and SRT of 15 days), while the second (R2) was fed with only tannery sludge and 25 days of SRT. The third reactor (R3) was fed with fleshing plus tannery sludge. Two sludge/fleshing mass ratios were evaluated, 8:1 (t=116-230 d) and 3:1 (t=231-302 d).

Feeding and effluent were changed twice a week and monitored according to IRSA-CNR methods: COD, Sulphates, TS and VS. Reactors were fed with only VTPS. VTPS was collected twice a week and directly used for reactors feeding, whereas TIF samples were delivered every two weeks and stored in at 4 °C.

Table 21 shows the mass and the COD to sulphate ratios tested.

Table 21: Operating conditions of the reactors (130 l each), SRT, temperature, mass and COD:SO_4^{2-} ratios.

Reactor	**SRT(d)**	**T (°C)**	**VTPS:TIF mass ratio**	**COD:SO_4^{2-}**	**days**	
Reactor 1	15	36±0.5	1:0	50±20	186	
Reactor 2	25	36±0.5	1:0	50±23	186	
Reactor 3	25	36±0.5	8:1	107±55	115	Label I
			3:1	147±51	71	Label II

COD and VS removal efficiency were used as parameters for the estimation of the anaerobic process efficiency. Sulphate reduction was included in mass balances by considering 0.67 g of COD removed per g of SO_4^{2-} reduced to sulphide (Barrera et al., 2014). The theoretical methane production (Nm^3 CH_4 kg^{-1} VS_{ad}) was calculated stoichiometrically from COD and VS reduction. Theoretical biogas production (m^3 biogas kg^{-1} VS_{ad}) was derived from the theoretical methane production through the observed average methane percentage.

Figure 29 shows the reactor layout, 5 cubic meter of volume.

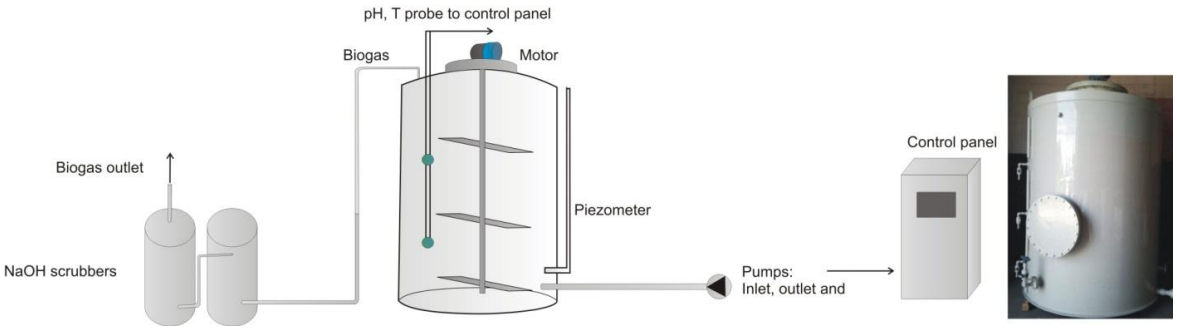

Figure 29: Pilot scale tests, reactor (5 m^3) layout.

An electric motor connected to a vertical shaft allows the mixing of the liquid phase. The biogas was collected by the headspace and treated in NaOH scrubbers to remove the carbon dioxide and the hydrogen sulphide before the flame combustion. A piezometric tube allows the liquid level control. The sludge was maintained at fixed temperature through the recirculation in the heat exchanger water-sludge. Two pumps allow the recirculation for heating, the sludge loaded and discharge. Temperature and pH were controlled and regulated at 2 levels by the probes through the control panel.

Pilot scale reactor was inoculated with a mixture of anaerobic sludge from a municipal anaerobic digester (67%), primary tannery sludge from Cuoiodepur WWTP (VTPS, 11%) and anaerobic sludge from a tannery industrial anaerobic digestor (22%). Reactor was maintained at mesophilic conditions (38±1.0°C) and the pH was controlled at 7±0.5. After the start-up phase (t=87 d) when reactor was fed with a mixture of tannery sludge and tap water (1:1 volume), reactor was fed with only tannery sludge.

The sludge retention time was set as SRT=20 d (0<t<104 d), followed by a second set point of SRT=30 d (105<t<155 d). Feeding and effluent were changed twice a week and monitored according to IRSA-CNR methods: COD, Sulphates, TS and VS.

3.4 Sulphide denitrification laboratory scale tests

The autotrophic denitrification process for the removal of both hydrogen sulphide (in the biogas) and nitrate (or nitrite) contained in the oxidized anaerobic digestion supernatant have been simulated using liquid and gaseous sulphide solutions. Two SBR (Sequential Batch Reactor) of 4 liters each, have been designed, built and monitored for the study of the process starting from liquid substrate solutions.

Figure 30 shows reactors layout.

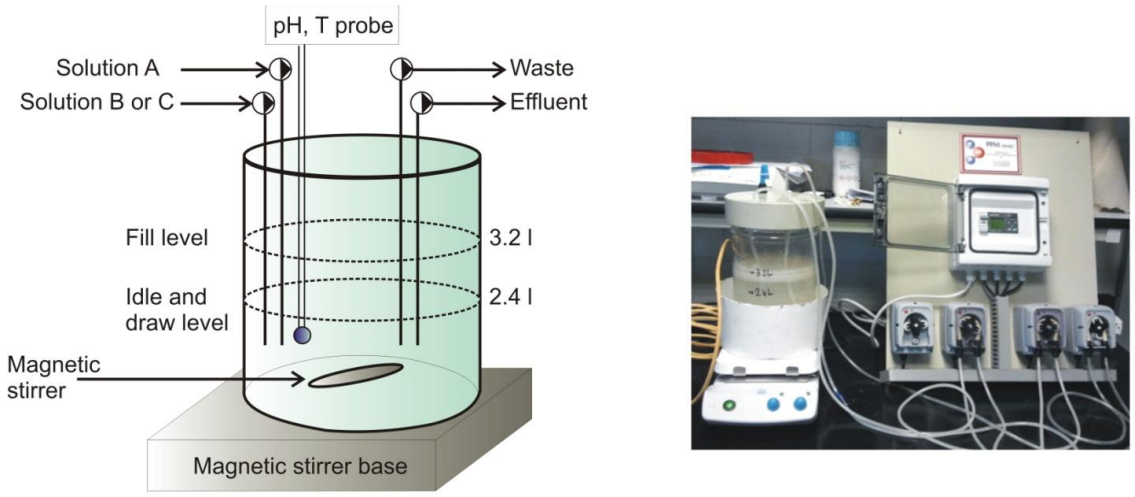

Figure 30: Sulphur denitrification test, reactor layout.

The pH have been monitored daily referring to the pH of the supernatant and was maintained lower than 8.8 units by dosing HCl solution. The temperature of the mixed liquor was not controlled and varies according to room temperature. SBR phases were controlled automatically through the use of a control panel that turns on and off in order to the protocol of all the actuators of the system (pumps and mixer). The flows have been set to obtain an hydraulic retention time (HRT) of 1 h while the solids retention time (SRT) depends on the solids concentration and was controlled through the mixed liquor waste flow.

Figure 31 shows the SRB phases.

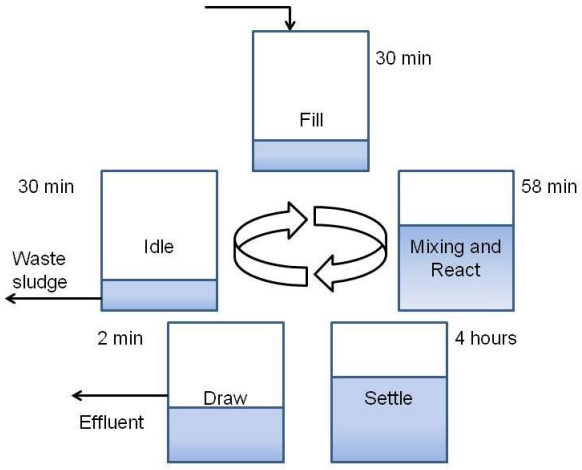

Figure 31: Sequential Batch Reactor phases.

Five phases were performed in cycle of 5 hours each: fill, mixing and reaction, settle, draw and idle.

Three different solutions (A, B and C) were used to feed the reactors. Solution A was used for both reactors. Solutions B and C were alternatively used depend on nitrate or nitrite denitrification process (Reactor 1 or Reactor 2, respectively).

Table 22 shows the solutions composition.

Table 22: Influents composition for the sulphur denitrification laboratory scale test.

Solution A (within 10 l of distilled water)		**Solution B (within 10 l of distilled water)**		**Solution C (within 10 l of distilled water)**	
	g		**g**		**g**
$NaHCO_3$	12.375	KNO_3	16.279	$NaNO_2$	9.583
Na_2S $3H_2O$	4.125	Na_2HPO_4 $2H_2O$	6.610	Na_2HPO_4 $2H_2O$	6.610
		KH_2PO_4	5.273	KH_2PO_4	5.273
HCl	Adjusting at pH 8	NH_4Cl	0.502	NH_4Cl	0.502
		$MgSO_4$ $7H_2O$	0.623	$MgSO_4$ $7H_2O$	0.623

Each solution was dosed at 400 ml per cycle, while the discharge was at 800 ml. Three phases were considered for Reactor 1 with 6 operational conditions shows in table 22, while table 23 shows operational conditions of Reactor 2.

During Label III the waste sludge was used as inoculums for Reactor 2. Table 24 shows operational condition of Reactor 2.

Table 23: Operational conditions, Reactor1.

	Time start	**Time end**	**Solution A**	**Solution B**	**SRT**	**S_{IN}**	**N-$NO_{3,IN}$**	**N/S**
	d	**d**	**mg S l^{-1}**	**mg N-NO_3 l^{-1}**	**d**	**mg d^{-1}**	**mg N-NO_3 d^{-1}**	**g S g^{-1} N-NO_3**
Label I	25	45	200	155	-	340	250	0.73
Label II	46	91	340	220	20	650	350	0.54
Label III	92	160	375	220	5	650	350	0.54

Table 24: Operational conditions, Reactor 2.

Time start	Time end	Solution A	Solution C	SRT	S_{IN}	$N\text{-}NO_{2,IN}$	N/S
d	d	mg S l^{-1}	mg $N\text{-}NO_2$ l^{-1}	d	mg d^{-1}	mg $N\text{-}NO_2$ d^{-1}	g S g^{-1} $N\text{-}NO_2$
26	72	214	205	14.5	342	328	0.95

To close the sulphur mass balance was evaluated an intermediate products elemental sulphur and thiosulphate following Equation 7 and Equation 8:

$$S\_S_0 = ({}_pCOD - \frac{VSS}{TSS}\frac{COD}{VSS}TSS_{out})\ \frac{gCOD}{gS_0} \text{ (Eq.7)}$$

Where:

- S_S_0 is the concentration of the elemental sulphur;
- $pCOD$ is the particulate COD in the reactor;
- $\frac{VSS}{TSS}$ is the volatile suspended solids to total suspended solids ratio;
- $\frac{COD}{VSS}$ is the COD to volatile suspended solids ratio(1.42 gO_2 g^{-1}VSS);
- TSS_{out} is the concentration of the total suspended solids in the effluent.

$$S\_S_2SO_3^{2-} = ({}_sCOD - NO_2^- \frac{gCOD}{gN\_NO_2^-}\frac{gCOD}{gS\_S_2SO_3^{2-}})\ \frac{MM\ S}{MM\ S_2SO_3^{2-}} \text{ (Eq.8)}$$

Where:

- $S\_S_2SO_3^{2-}$ is the concentration of thiosulphate;
- $sCOD$ is the soluble COD in the reactor;
- NO_2^- is the nitrite concentration;
- $\frac{gCOD}{gN\_NO_2^-}$ is the COD to nitrite ratio(1.14 gO_2 $g^{-1}N\_NO_2^-$);
- $\frac{gCOD}{gS\_S_2SO_3^{2-}}$ is the COD to thiosulphate ratio(1 gO_2 $g^{-1}S\_S_2SO_3^{2-}$);
- $MM\ S$ is the molecular mass of sulphur;
- $MM\ S_2SO_3^{2-}$ is the molecular mass of thiosulphate.

Equation 8 was evaluated following the hypothesis: $sCOD = COD_{Thiosulphate} + COD_{Nitrite}$.

3.5 Process modelling

Three softwares have been used to model the wastewater treatment plant: Aquasim (Eawag, Switzerland) PetWin 4.1 (Envirosim, Canada) and SUMO (Dynamita, Frances). In Aquasim was conducted the simulation of the batch tests through the standard model IWA-ADM1, while in PetWin 4.1 and SUMO were conducted the simulations of the full plant.

3.5.1. ADM1 modelling

A modified version of the IWA-ADM1 model is proposed to simulate the anaerobic digestion of tannery primary sludge and common domestic primary sludge batch tests, though Aquasim software. The modifications includes the introduction of 3 sulphate reducing biomasses: acetotrophic, proprionate-degrading and hydrogenotrophic sulphate reducing bacteria.

Starting from the modifications proposed by Fedorovich et al., 2003 and Barrera et al., 2015, all the processes added to the ADM1 are listed in Table 25.

Based on experimental observations, butyric acid can be neglected as organic matter for SRB in the model structure because the concentration of butyric acid was less than 5% of the total volatile fatty acids concentration. A dual term Monod type kinetics was used to describe the uptake rate of these substrates (Fedorovich et al., 2003, Barrera et al., 2015).

Table 26 shows the acid-base reactions for the sulphide and sulphate acid-base reactions.

Table 25: Biochemical rate coefficients and kinetic rate equation added to the ADM1 to model the sulphate reduction in the anaerobic digestion process.

Component→ Process↓	**S_{pro}**	**S_{ac}**	**S_{h2}**	**S_{so4}**	**S_{h2s}**	**S_{co2}**	**S_{IN}**	**X_C**	**X_{proSRB}**	**X_{acSRB}**	**X_{h2SRB}**	**Rate**
Uptake Pro-SRB	-1			$-(1-Y_{pSRB})*\frac{0.43}{64}$	$(1-Y_{pSRB})*\frac{0.43}{64}$	$-(C_{pro}-(1-Y_{pSRB})*0.57*C_{pro}-Y_{pSRB}*C_{biom})$	$-N_{biom}*Y_{pSRB}$		Y_{pSRB}			$km_{proSRB}*X_{proSRB}*\frac{S_{pro}}{(Ks_{pro}+S_{pro})}*\frac{S_{so4}}{(Ks_{so4}+S_{so4})}*I_{NH,lim}*I_{pH,pro,lim}*I_{H2,pro,lim}*I_{H2S,lim}$
Uptake Ac-SRB		-1		$-(1-Y_{aSRB})*\frac{1}{64}$	$(1-Y_{aSRB})*\frac{1}{64}$	$-(C_{ac}-Y_{aSRB}*C_{biom}-(1-Y_{aSRB})*C_{ch4})$	$-N_{biom}*Y_{aSRB}$			Y_{aSRB}		$km_{acSRB}*X_{acSRB}*\frac{S_{ac}}{(Ks_{ac}+S_{ac})}*\frac{S_{so4}}{(Ks_{so4}+S_{so4})}*I_{NH,lim}*I_{pH,ac,lim}*I_{H2S,lim}$
Uptake H2-SRB			-1	$-(1-Y_{h2SRB})*\frac{1}{64}$	$(1-Y_{h2SRB})*\frac{1}{64}$	$-(Y_{h2SRB}*C_{biom}-(1-Y_{h2SRB})*C_{ch4})$	$-N_{biom}*Y_{h2SRB}$				Y_{h2SRB}	$km_{h2SRB}*X_{h2SRB}*\frac{S_{h2}}{(Ks_{h2}+S_{h2})}*\frac{S_{so4}}{(Ks_{so4}+S_{so4})}*I_{NH,lim}*I_{pH,h2,lim}*I_{H2S,lim}$
Decay Pro-SRB							$N_{biom}-N_{Xc}$	1	-1			$X_{proSRB}*k_{dec,proSRB}$
Decay Ac-SRB							$N_{biom}-N_{Xc}$	1		-1		$X_{acSRB}*k_{dec,acSRB}$
Decay H2-SRB							$N_{biom}-N_{Xc}$	1			-1	$X_{h2SRB}*k_{dec,h2SRB}$
	Proprionate	**Acetate**	**Hydrogen gas**	**Sulphate**	**Sulphide**	**Carbon dioxide**	**Inorganic nitrogen**	**Composites**	**Proprionate degrading SRB**	**Acetotrophic SRB**	**Hydrogenotrophic SRB**	

Table 26: Rate coefficients and kinetic rate equation for acid-base reactions in the implementation added to ADM1 to model the sulfate reduction process in the anaerobic digestion.

Component→ Process↓	**S_{h2s}**	**$S_{hs,ion}$**	**S_{so4}**	**$S_{hso4,ion}$**	**Rate**
Acid-base H_2S	1	-1			$K_{A/B,h2s}(S_{hs,ion}(S_{H+}+K_{a,h2s})-K_{a,h2s}S_{h2s})$
Acid-base SO_4^{2-}			-1	1	$K_{A/B,so4}(S_{so4}S_{H+}-(K_{a,h2s}+S_{H+}))$

3.5.2. Full plant modelling

Two different plant configurations were simulated in PetWin 4.1, while three different plant configurations were simulated in SUMO. The first configuration simulated in both softwares (Configuration 1) represents the current plant scheme. Figure 32 A shows the Configuration 1 implemented in PetWin 4.1, while Figure 32 B shows the Configuration 1 implemented in SUMO.

The second configuration simulated in both softwares (Configuration 2) represents a possible future expansion to include anaerobic sludge stabilization. Starting from the current configuration scheme (Configuration I), the anaerobic digestion of the primary sludge was added. Moreover, to reduce the size of the digestor, a thickener was added in the sludge line after the primary settling (Configuration II). Figure 33 A shows the layout of Configuration 2 in PetWin 4.1 and Figure 33 B shows the layout of Configuration 2 in SUMO.

In the third configuration (Configuration III) implemented only in SUMO starting from Configuration II, after the dewatering of the sludge, a biological oxidation and a sulphide denitrification process were added. The biogas in the process was simulated as an influent, because of the impossibility of the direct connection from the digestor. Figure 34 shows the plant scheme of Configuration 3 with the nitrogen/sulphur fluxes in the new treatments line. Figure 35 shows Configuration 3 implemented in SUMO.

In all the configurations, four influents were considered: the industrial and the municipal wastewater flows and two extra influents to account for (i) the recirculation flow from the chemical scrubbers which treat the gas stream, mostly characterized by sulfates and (ii) the tertiary stream recirculation. In the real case tertiary treatments includes chemico-physical process (using $FeCl+Ca(OH)_2$) and pH correction. Two equalization tanks like in the plant configuration, one aerated while one is anoxic. In the equalization tank the air flow rate is estimated in the plant at 10 tonnes O_2 per day equal at 300 $Nm^3O_2\ hr^{-1}$. The biological treatment (denitrification/nitrification) are represented with anoxic reactors and aerobic reactors. The anoxic and aerobic processes are represented with more reactors for each process to simulate the non-complete mixing as in reality. During the monitoring phase was observed that part of the aerobic reactor was under anoxic conditions, to represent that in the model the 20% of the entire volume of the aerobic reactor was considered in anoxic conditions, named Aerobic 2.

A

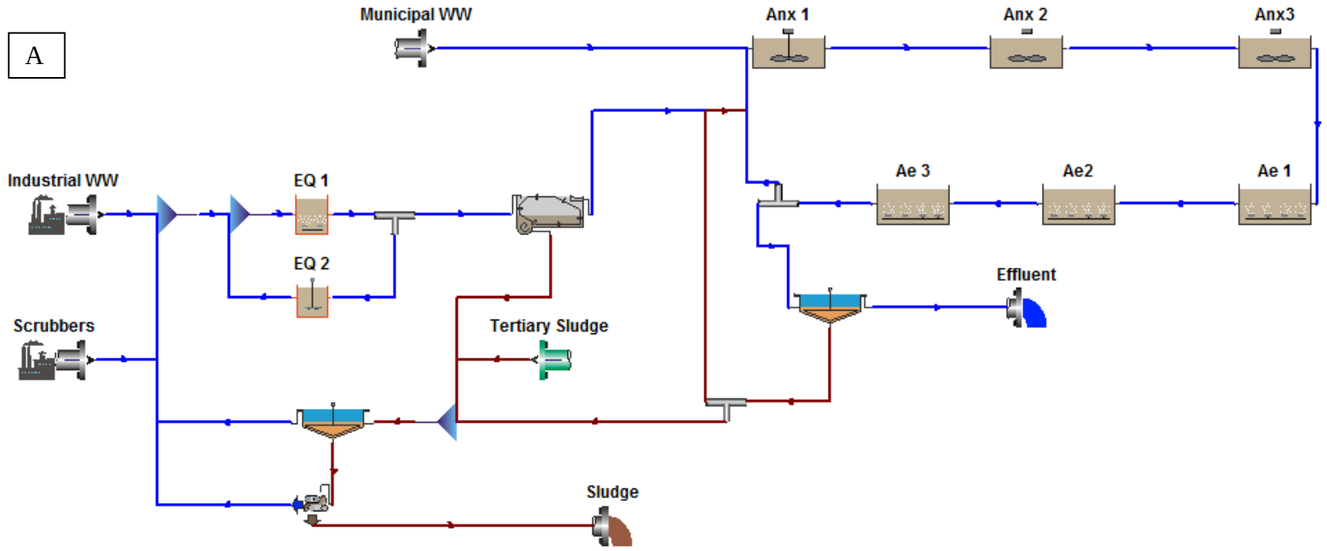

B

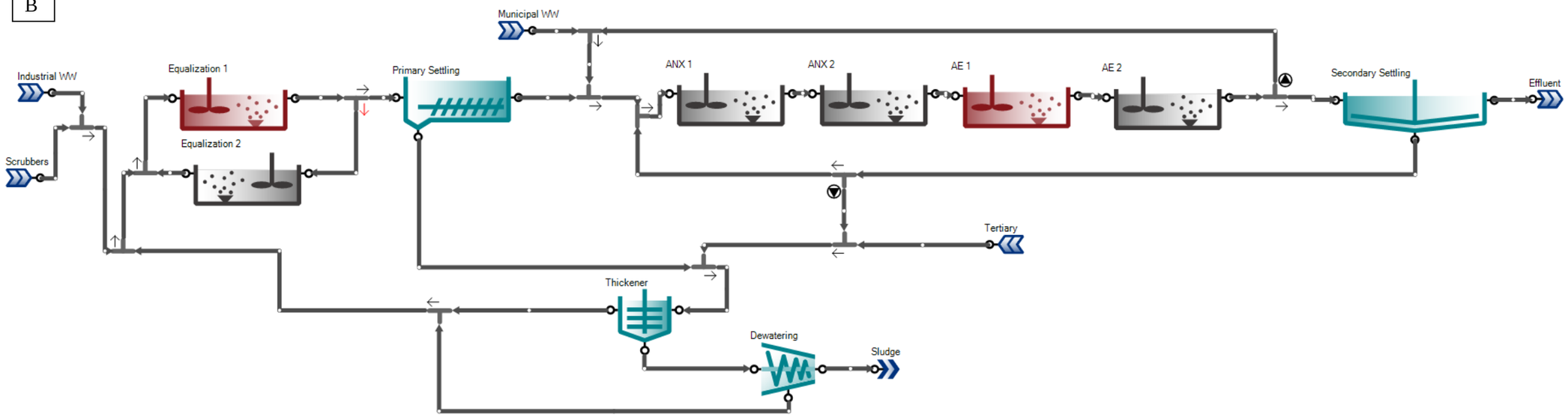

Figure 32: A) Model scheme Configuration I implemented in PetWin 4.1. **B)** Model scheme Configuration I implemented in SUMO.

A

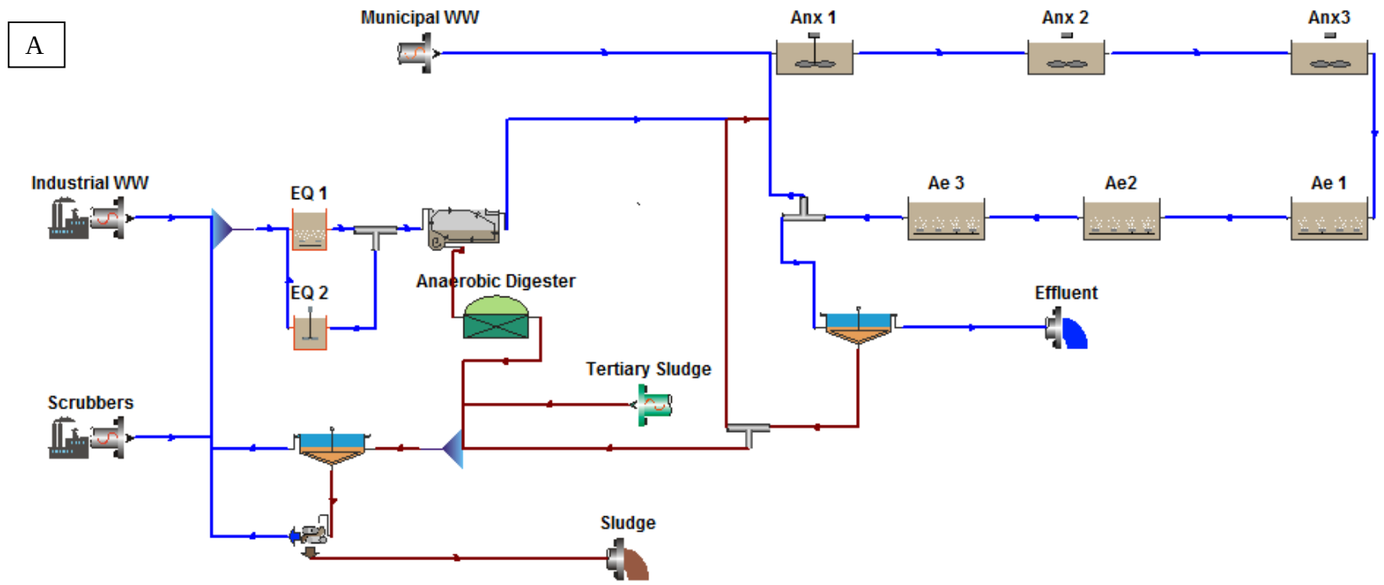

B

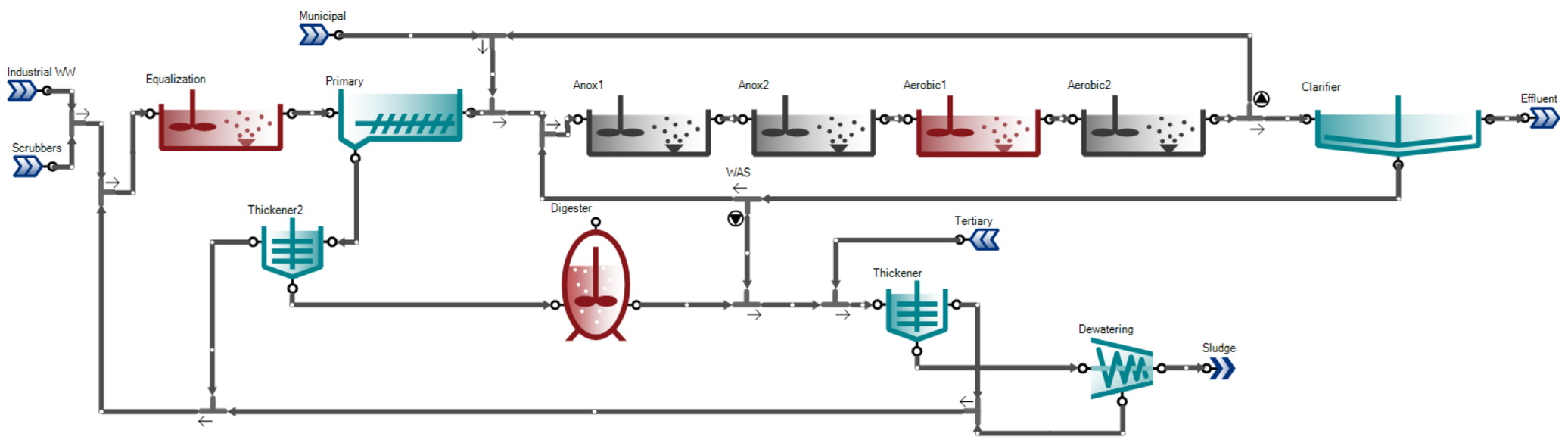

Figure 33: A) Model scheme Configuration II implemented in PetWin 4.1. **B)** Model scheme Configuration II implemented in SUMO.

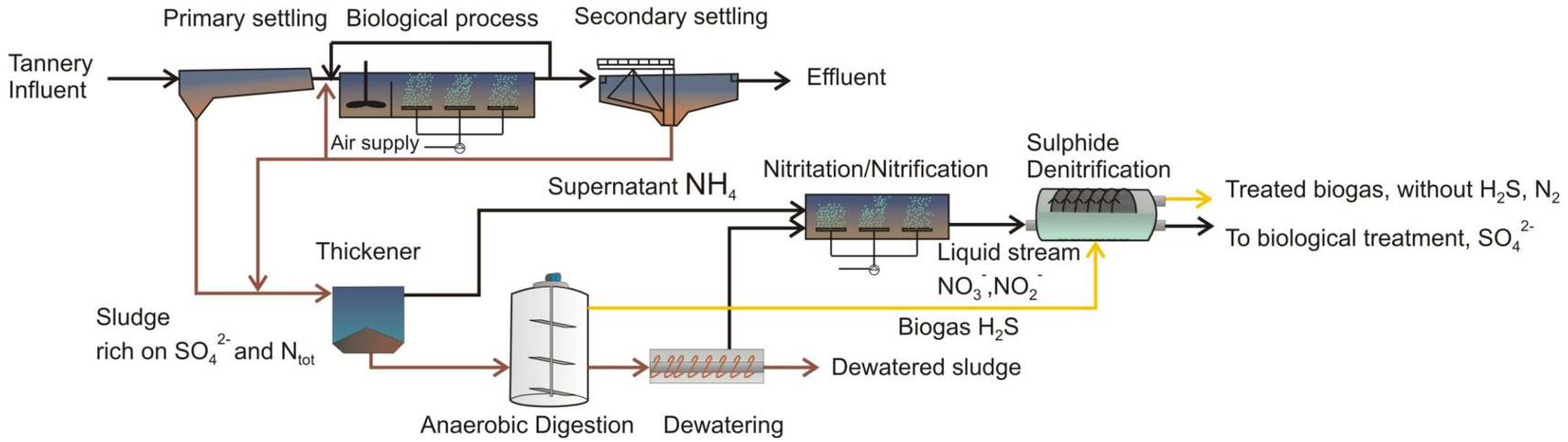

Figure 34: Plant scheme with anaerobic digestion and sulphide denitrification implemented in the model.

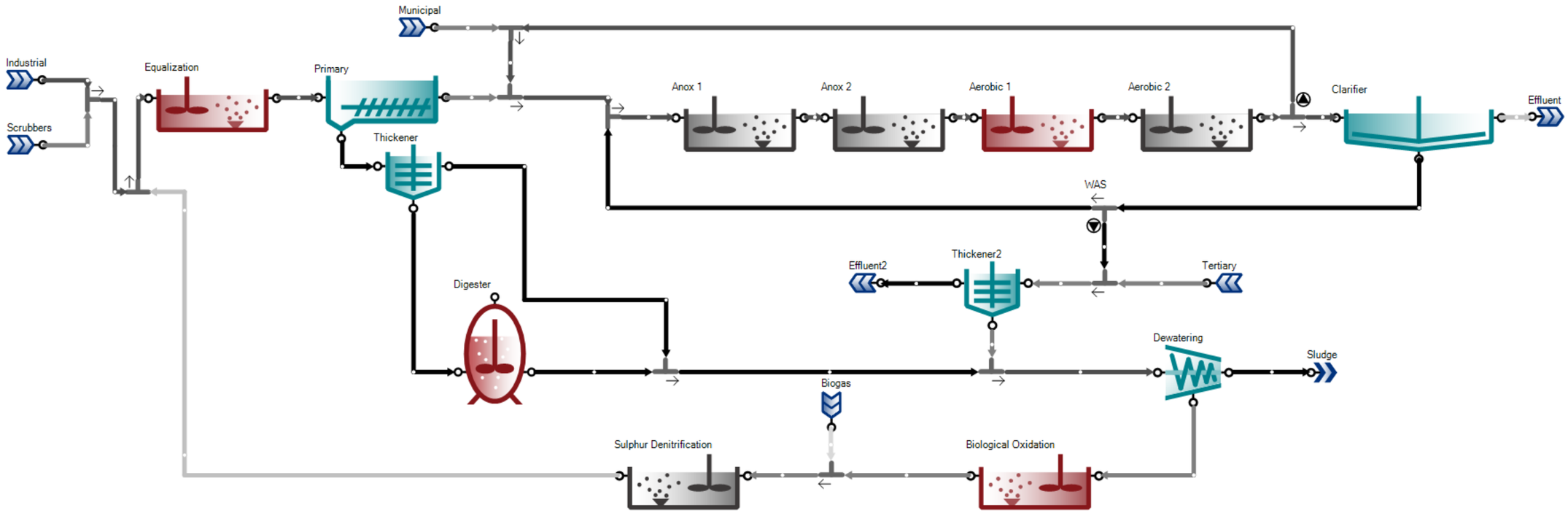

Figure 35: Model scheme Configuration III implemented in SUMO.

In the following table are reported the operational conditions of the reactors.

Table 27: Operational conditions of the reactors.

Symbol	Equalization	Anoxic reactors	Aerobic reactors	Unit
Total Volume	6000	11000	26000	m^3
Dissolved Oxygen	2	0	1.5	g $O_2.m^{-3}$
HRT	-	0.055	0.26	d
Qair	300	-	19991	$Nm^3\ hr^{-1}$
T water	298	298	298	K

The model developed by PetWin 4.1 incorporates the four biomass components acting on sulphur species: sulphide oxidising bacteria; acetotrophic sulphur reducing bacteria; propionate degrading sulphur reducing bacteria; hydrogenotrophic sulphur reducing bacteria.

PetWin only considers two oxidation states; that is sulphide and sulphate. Thus in PetWin the oxidation of reduced sulphur compounds refers to the oxidation of sulphides (H_2S) to sulphates (SO_4^{2-}). Moreover, no modification on the model matrix was done. While the several modifications done in the SUMO model matrix are described in the following paragraph.

Model modifications

In SUMO, starting from a Two-Step denitrification/nitrification model a sulphur metabolism is introduced. Moreover a three hydrolysis processes were added to simulate the hydrolysis of: inert particulate COD X_U, endogenous decay products X_E and inorganic compounds X_{INORG}.

Previous attempts to apply standard models and commercially available software to simulate tannery WWTP behavior did not succeed, due to the complexity of the influent matrix and the high solids retention time (SRT) at which these plants tend to operate (~100 days). Indeed, the models currently available fail when simulating activated sludge processes

operating at elevated SRT. Moreover, the high SRT in the biological reactor make difficult the calibration of the mixed-liquor suspended (MLSS) and volatile solids (MLVSS). In real conditions, at high SRT even the COD fraction usually referred to as non-biodegradable is partially degraded, although at a lower rate.

The original model had 65 processes and 58 components, 15 processes and 7 components were added. The new model includes 80 processes and 65 components.

The introduction of the three hydrolysis processes is required because of the high level of the solid retention time (SRT) of the wastewater treatment plant modeled (70-100 days).

Figure 36 shows the Two-Step denitrification/nitrification scheme and the main biomasses modeled.

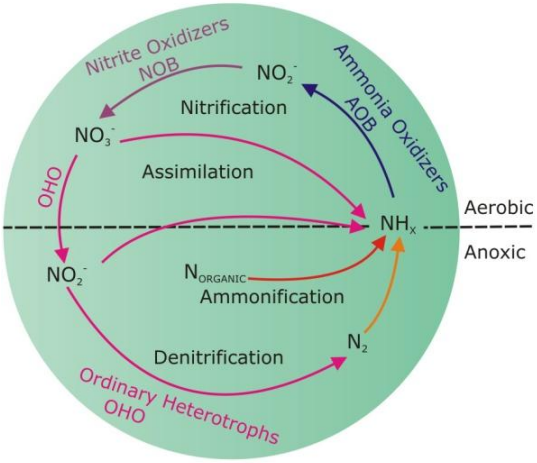

Figure 36: Two-step denitrification/nitrification model scheme.

The introduction of the sulphur compounds includes the calculation of the equilibrium matrix (charge balances and pH variations) for the dissociation of the sulphuric acid to sulphate ion in two steps and the dissociation of hydrogen sulphide to sulphide ion in two steps, following the reactions:

(1) $H_2SO_4\ (aq) + H_2O\ (l) \rightarrow H_3O^+\ (aq) + HSO_4{}^-(aq)$ First step of dissociation for sulphuric acid.

(2)$HSO_4{}^-(aq) + H_2O\ (l) \leftrightarrow H_3O^+\ (aq) + SO_4{}^{2-}(aq)$ Second step of dissociation.

(3)$H_2S\ (aq) + H_2O\ (l) \leftrightarrow H_3O^+\ (aq) + HS^-(aq)$ First step of dissociation for dissolved sulphide.

(4)$HS^-\ (aq) + H_2O\ (l) \leftrightarrow H_3O^+\ (aq) + S^{2-}(aq)$ Second step of dissociation.

Figure 37 shows sulphur metabolism.

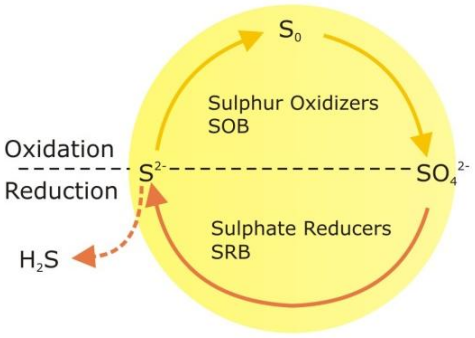

Figure 37: Sulphur metabolism scheme.

As shown in figure 37 the oxidation of the sulphide includes the intermediate step to elemental sulphur. One biomass was implemented for the sulphur oxidation, while two biomasses were considered for the sulphate reduction.

Modelling sulphur oxidizers biomass

For the sulphur oxidizers biomass (SOB) two steps are considered for the aerobic growth, while the anoxic growth includes four processes. The first step of the aerobic growth is the complete oxidation from S^{2-} to SO_4^{2-}, while the second step represent the half-oxidation from S^{2-} to S_0.

The anoxic growth considers four steps: SOB growth for nitrate reduction by H_2S, SOB growth for nitrite reduction by H_2S, SOB growth for nitrate reduction by S_0, SOB growth for nitrite reduction by S_0.

In anoxic conditions, autotrophic bacteria use sulphide as electron donor to reduce nitrate to nitrite and nitrogen gas. Two steps of nitrogen reductions were considered (from nitrate to nitrite and from nitrite to nitrogen gas), as far as two steps were considered for sulphide oxidation, while intermediate steps to thiosulphite or sulphite are neglected.

Figure 38 shows the Sulphur Oxidizers pathways.

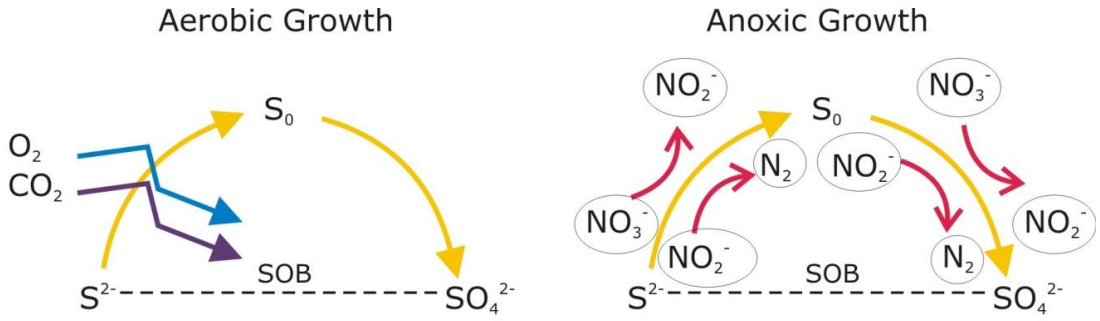

Figure 38: Sulphur oxidizers pathways scheme.

The sulphur denitrification process (anoxic growth) process was represented following the reactions:

(1) $40\ HS^- + 30\ NO_3^- + 5\ CO_2 + 1\ NH_4^+ + 39\ H^+ \rightarrow 40\ S_0 + 30\ NO_2^- + 1\ C_5H_7O_2N + 38\ H_2O$

(2) $40\ HS^- + 30\ NO_2^- + 5\ CO_2 + 1\ NH_4^+ + 69\ H^+ \rightarrow 40\ S_0 + 15\ N_2 + 1\ C_5H_7O_2N + 68\ H_2O$

(3) $13\ S_0 + 29\ NO_3^- + 5\ CO_2 + 1\ NH_4^+ + 16\ H_2O \rightarrow 13\ SO_4^{2-} + 29\ NO_2^- + 1\ C_5H_7O_2N + 30\ H^+$

(4) $13\ S_0 + 29\ NO_2^- + 5\ CO_2 + 1\ NH_4^+ + 86\ H^+ \rightarrow 13\ SO_4^{2-} + 14.5\ N_2 + 1\ C_5H_7O_2N + 42\ H_2O$

Modelling sulphate reducing biomasses

Sulphate reduction is performed by two major groups of SRB including incomplete oxidizers, which reduce compounds such as lactate to acetate and CO_2, and complete oxidizers, which completely convert acetate to CO_2 and HCO_3 (Chen et al., 2008). SRB may compete with methanogens, acetogens, or fermentative microorganisms for available acetate, H_2, propionate, and butyrate in anaerobic systems (McCartney and Oleszkiewicz, 1993; Colleran et al., 1995).

In the SUMO model of the anaerobic process there is no the differentiation of the volatile fatty acids and two biomasses performed the methanogenic step: the acetoclastic methanogens and the hydrogenotrophic methanogens. Similarly, two biomasses competes for the same substrates to produce H_2S. The sulphate reduction is carried out by: acetoclastic (VFA) and hydrogenotrophic Sulphate Reducers Biomasses (SRB).

Figure 39 shows the anaerobic digestion process with the inclusion of the sulphate reducing bacteria.

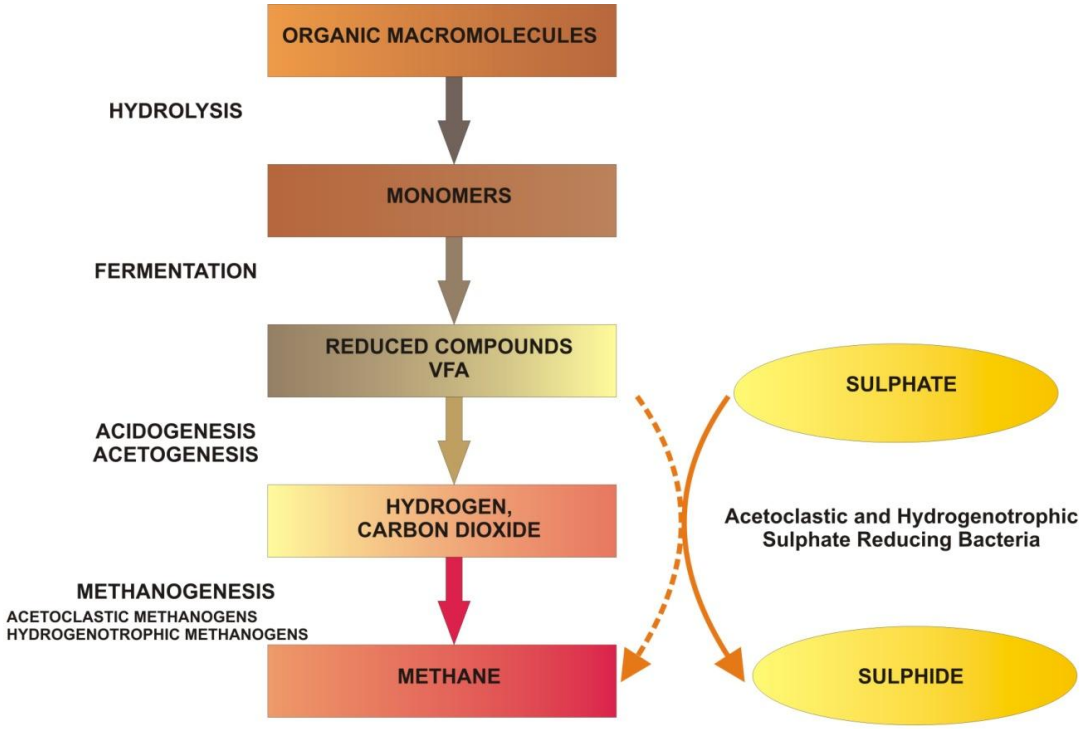

Figure 39: Anaerobic digestion process flow chart.

Particularly, figure 40 shows the Sulphate reduction pathways.

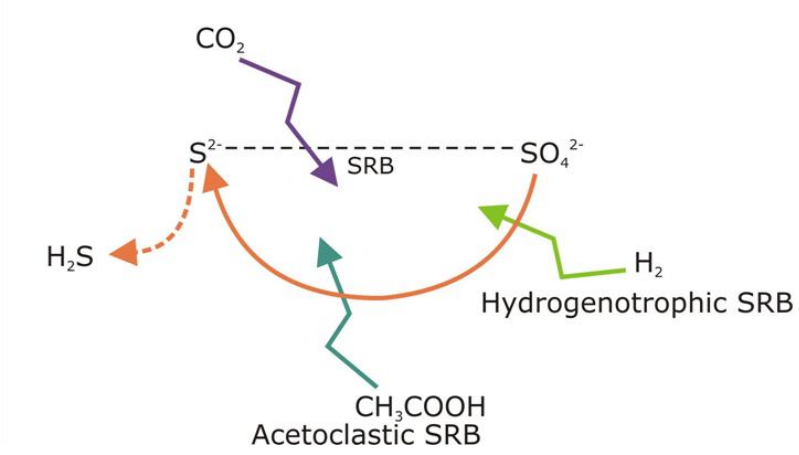

Figure 40: Sulphate reduction through Acetoclastic and Hydrogenotrophic SRB scheme.

Two stages of inhibition exist as a result of sulphate reduction. Primary inhibition is due to competition for common organic and inorganic substrates from SRB, which suppresses

methane production (Harada et al., 1994). Secondary inhibition results from the toxicity of sulphide to various bacteria groups (Anderson et al., 1982; Oude Elferink et al., 1994; Colleran et al., 1995; Colleran et al., 1998). Both of the processes were implemented in the model, particularly the second was implemented as a non-competitive inhibition of H_2S.

The gas transfer from dissolved sulphide to hydrogen sulphide gas is modeled as reported in figure 41.

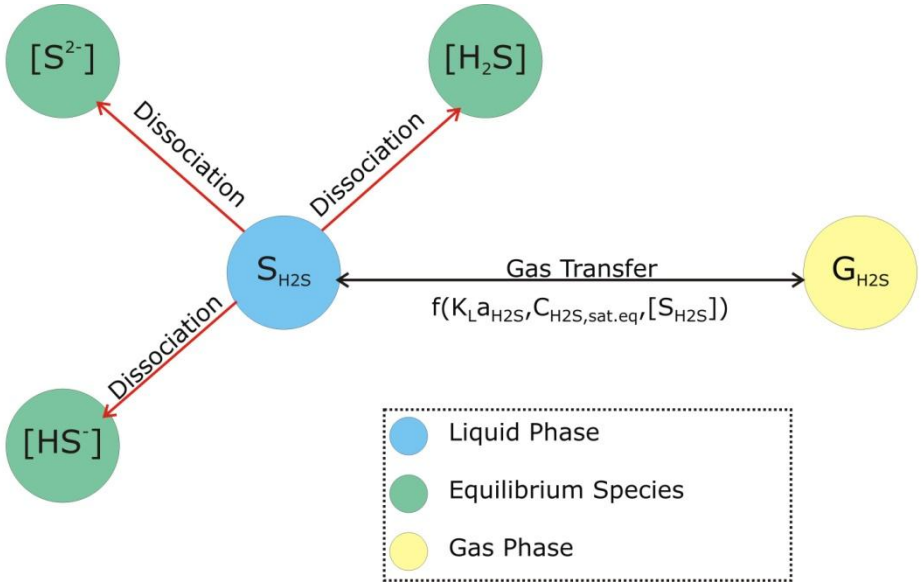

Figure 41: Hydrogen sulphide gas transfer in the model.

As shown in figure 41 the gas transfer equation is calculated as function of the K_La of H_2S (oxygen mass transfer coefficient of hydrogen sulphide), the value of the hydrogen sulphide saturation concentration ($C_{H2S,\ sat,\ eq}$) and the concentration of the dissolved sulphide.

The oxygen mass transfer coefficient of hydrogen sulphide is evaluated as a function of the mass transfer coefficient for oxygen at standard conditions for clean water (with the correction for the wastewater), the ratio between the diffusion coefficient of H_2S in water and the diffusion coefficient of O_2 in water and the correction factors for temperature and pressure at the field conditions.

The hydrogen sulphide saturation concentration is evaluated as a function of Henry constant value for H_2S, the molecular mass of H_2S and the correction factors for temperature and pressure at the field conditions.

Hydrogen sulphide-hydrogen sulphide ion-sulphide species dissociations were calculated with the following acid-base equations and chemistry principles:

$$[H_2S] = \frac{S_{H2S}}{MM_{H2S}[H^+]^2}([H^+]^2 + [H^+]K_{a1} + K_{a1}K_{a2})$$

$$[HS^-] = K_{a1}K_{a2}\frac{S_{H2S}}{MM_{H2S}[H^+]^2}([H^+]^2 + [H^+]K_{a1} + K_{a1}K_{a2})$$

$$[S^{2-}] = K_{a1}[H^+]\frac{S_{H2S}}{MM_{H2S}[H^+]^2}([H^+]^2 + [H^+]K_{a1} + K_{a1}K_{a2})$$

Where:

K_{a1} is the first step dissociation constant;

K_{a2} is the second step dissociation constant;

$[H^+]$ is the proton concentration;

S_{H2S} is the dissolved sulphide concentration.

Table 28 shows the model matrix of the sulphur metabolism and the integration of the hydrolysis steps.

Table 29 shows the rate equation added to the model matrix for the sulphate reduction, the sulphide oxidation and the hydrolysis processes.

Table 30 shows the parameters values.

Table 28: Rate coefficients and kinetic added to the model matrix for the sulphate reduction, the sulphide oxidation and the hydrolysis processes.

Component→ Process↓	S_{VFA}	S_B	X_B	X_U	X_E	X_{SOB}	$X_{SRB,A}$	$X_{SRB,H2}$	X_{INORG}
X_U Hydrolysis			1	-1					
X_E Hydrolysis		1			-1				
X_{INORG} Hydrolysis		1							-1
Ac_{SRB} Growth	-1						1		i_{IG}
Ac_{SRB} Decay							-1		$-i_{IG}$
$H2_{SRB}$ Growth								1	i_{IG}
$H2_{SRB}$ Decay								-1	$-i_{IG}$
SOB aerobic growth on H_2S						1			
SOB aerobic growth on S_0						1			
SOB growth for nitrate reduction by H_2S						1			
SOB growth for nitrite reduction by H_2S						1			
SOB growth for nitrate reduction by S_0						1			
SOB growth for nitrite reduction by S_0						1			
SOB dacay						-1			$-i_{IG}$
Hydrogen Sulphide gas transfer									

Component→ Process↓	**S_{NHx}**	**S_{NO2}**	**S_{NO3}**	**S_{N2}**	**$X_{N,B}$**	**S_{O2}**	**S_{H2}**	**S_{CO2}**	**S_{H2S}**	**S_{SO4}**	**S_{Se}**	**G_{H2S}**
X_U Hydrolysis	-1				$i_{N,Bio}$							
X_E Hydrolysis		-1			$i_{N,Bio}$							
X_{INORG} Hydrolysis			-1		$i_{N,Bio}$							
Ac_{SRB} Growth	$-i_{N,BIO}$							$-0.30 * \frac{(1-Y_{SRB,Ac})}{Y_{SRB,Ac}}$	$1 - Y_{SRB,Ac}$	$-(1 - Y_{SRB,Ac})$		
Ac_{SRB} Decay					$(1 - f_E) * i_{N,Bio}$							
$H2_{SRB}$ Growth	$-i_{N,BIO}$							$\frac{-0.30}{Y_{SRB,H2}}$	$1 - Y_{SRB,H2}$	$-(1 - Y_{SRB,H2})$		
$H2_{SRB}$ Decay					$(1 - f_E) * i_{N,Bio}$							
SOB aerobic growth on H_2S						$\frac{-(1 - Y_{SOB})}{Y_{SOB}}$		$-0.30 * \frac{(1 - Y_{SOB})}{Y_{SOB}}$	$\frac{-1}{Y_{SOB}}$		$\frac{1}{Y_{SOB}}$	
SOB aerobic growth on S_0						$\frac{-(1 - Y_{SOB})}{Y_{SOB}}$		$-0.30 * \frac{(1 - Y_{SOB})}{Y_{SOB}}$		$\frac{1}{Y_{SOB}}$	$\frac{-1}{Y_{SOB}}$	
SOB growth for nitrate reduction by H_2S		$\frac{1}{Y_{SOB}}$	$\frac{-1}{Y_{SOB}}$						$\frac{-C_{h2s,1} * (1 - Y_{SOB})}{Y_{SOB}}$		$\frac{C_{h2s,1} * (1 - Y_{SOB})}{Y_{SOB}}$	
SOB growth for nitrite reduction by H_2S		$\frac{1}{Y_{SOB}}$	$\frac{-1}{Y_{SOB}}$						$\frac{-C_{h2s,2} * (1 - Y_{SOB})}{Y_{SOB}}$		$\frac{C_{h2s,2} * (1 - Y_{SOB})}{Y_{SOB}}$	
SOB growth for nitrate reduction by S_0		$\frac{-1}{Y_{SOB}}$		$\frac{1}{Y_{SOB}}$						$\frac{C_{se,1} * (1 - Y_{SOB})}{Y_{SOB}}$	$\frac{-C_{se,1} * (1 - Y_{SOB})}{Y_{SOB}}$	
SOB growth for nitrite reduction by S_0		$\frac{-1}{Y_{SOB}}$		$\frac{1}{Y_{SOB}}$						$\frac{C_{se,2} * (1 - Y_{SOB})}{Y_{SOB}}$	$\frac{-C_{se,2} * (1 - Y_{SOB})}{Y_{SOB}}$	
SOB dacay					$(1 - f_E) * i_{N,Bio}$							
Hydrogen Sulphide gas transfer									1			$-1 * \frac{C_{ppm,Vconc}}{MM_{EQ,GH2S}} * R * Tnull/pSt * fvolume, L, G$

Table 29: Rate equation added to the model matrix for the sulphate reduction, the sulphide oxidation and the hydrolysis processes.

Component→ Process↓	Rate
X_U Hydrolysis	$k_{XU} * X_U$
X_E Hydrolysis	$k_{XE} * X_E$
X_{INORG} Hydrolysis	$k_{X,INORG} * X_{INORG}$
Ac_{SRB} Growth	$X_{SRB,A} * \mu_{SRB,A,T} * \frac{S_{SO4}}{K_{SO4}+S_{SO4}} * \frac{S_{VFA}}{K_{VFA}+S_{VFA}} * \frac{K_{O2}}{K_{O2}+S_{O2}} * NoncompinhS_{H2S} * Bellininh_{pH,SRB}$
Ac_{SRB} Decay	$X_{SRB,A} * b_{SRB,A,T}$
$H2_{SRB}$ Growth	$X_{SRB,H2} * \mu_{SRB,H2,T} * \frac{S_{SO4}}{K_{SO4}+S_{SO4}} * \frac{S_{H2}}{K_{H2}+S_{H2}} * \frac{K_{O2}}{K_{O2}+S_{O2}} * NoncompinhS_{H2S} * Bellininh_{pH,SRB}$
$H2_{SRB}$ Decay	$X_{SRB,H2} * b_{SRB,H2,T}$
SOB aerobic growth on H_2S	$X_{SOB} * \mu_{SOB,T} * \frac{S_{H2S}}{K_{S2}+S_{H2S}} * \frac{S_{NHx}}{K_{NHx,Bio}+S_{NHx}} * \frac{S_{O2}}{K_{O2}+S_{O2}} * \frac{S_{PO4}}{K_{PO4}+S_{PO4}} * \frac{S_{cat}}{K_{cat}+S_{cat}} * \frac{S_{an}}{K_{an}+S_{an}} * Bellininh_{pH,SOB}$
SOB aerobic growth on S_0	$X_{SOB} * \mu_{SOB,T} * \frac{S_{H2S}}{K_{S2}+S_{H2S}} * \frac{S_{NHx}}{K_{NHx,Bio}+S_{NHx}} * \frac{S_{O2}}{K_{O2}+S_{O2}} * \frac{S_{PO4}}{K_{PO4}+S_{PO4}} * \frac{S_{cat}}{K_{cat}+S_{cat}} * \frac{S_{an}}{K_{an}+S_{an}} * Bellininh_{pH,SOB}$
SOB growth for nitrate reduction by H_2S	$\mu_{SOB,T} * X_{SOB} * \eta_{SOB} * \frac{S_{H2S}}{K_{S2}+(S_{H2S} * \left(1+\frac{S_{H2S}}{K_{I,S2}}\right))} * \frac{S_{NO3}}{K_{NO3}+S_{NO3}} * \frac{K_{O2}}{K_{O2}+S_{O2}} * \frac{K_{NO2}}{K_{NO2}+S_{O2}} * \frac{S_{NHx}}{K_{NHx,Bio}+S_{NHx}}$
SOB growth for nitrite reduction by H_2S	$\mu_{SOB,T} * X_{SOB} * \eta_{SOB} * \frac{S_{H2S}}{K_{S2}+(S_{H2S} * \left(1+\frac{S_{H2S}}{K_{I,S2}}\right))} * \frac{S_{NO2}}{K_{NO2}+(S_{NO2} * \left(1+\frac{S_{NO2}}{K_{NO2}}\right))} * \frac{K_{O2}}{K_{O2}+S_{O2}} * \frac{S_{NHx}}{K_{NHx,Bio}+S_{NHx}}$
SOB growth for nitrate reduction by S_0	$\mu_{SOB,T} * X_{SOB} * \eta_{SOB} * \frac{S_{Se}}{K_{S0}+S_{Se}} * \frac{S_{NO3}}{K_{NO3}+S_{NO3}} * \frac{K_{O2}}{K_{O2}+S_{O2}} * \frac{K_{NO2}}{K_{NO2}+S_{O2}} * \frac{S_{NHx}}{K_{NHx,Bio}+S_{NHx}}$
SOB growth for nitrite reduction by S_0	$\mu_{SOB,T} * X_{SOB} * \eta_{SOB} * \frac{S_{Se}}{K_{S0}+S_{Se}} * \frac{S_{NO2}}{K_{NO2}+(S_{NO2} * \left(1+\frac{S_{NO2}}{K_{NO2}}\right))} * \frac{K_{O2}}{K_{O2}+S_{O2}} * \frac{S_{NHx}}{K_{NHx,Bio}+S_{NHx}}$
SOB dacay	$X_{SOB} * b_{SOB,T}$
Hydrogen Sulphide gas transfer	$k_{LaH2S} * (G_{H2S,sat,eq} - S_{H2S})$

Table 30: Model parameters.

Symbol	Name	Value	Unit	Symbol	Name	Value	Unit	Symbol	Name	Value	Unit
f_E	Endogenous fraction (death-regeneration)	0.08		K_S	Sulfide half-saturation coefficient for denitrifying autotrophic biomass	8	g $S.m^{-3}$	$b_{SRB,Ac}$	Decay rate for Ac SRB	0.02	d^{-1}
$f_{N,E}$	Ammonium nitrogen produced during XE hydrolysis	0.086	g COD / g VSS	η_{SOB}	Anoxic reduction factor for SOB	0.3	-	$b_{SRB,H2}$	Decay rate for H2 SRB	0.015	d^{-1}
$f_{N,U}$	Ammonium nitrogen produced during XU hydrolysis	0.02	g COD / g VSS	η_{Se}	Reduction factor for SOB elemental sulphur	0.2	-	b_{SOB}	Decay rate for SOB	0.5	d^{-1}
k_i	Hydrolisis rate of XE and XU	0.015	1/d	$Y_{SRB,Ac}$	Ac SRB yield	0.04		$K_{NO3,SOB}$	Half-saturation constant for nitrate SOB	109	g $N.m^{-3}$
$k_{i,INORG}$	Hydrolisis rate of XINORG	0.012	1/d	$Y_{SRB,H2}$	H2 SRB yield	0.03		K_{IH2S}	Inhibition factor for H2S	200	g $S.m^{-3}$
$i_{N,BIO}$	N content of biomasses	0.07	-	Y_{SOB}	SOB yield	0.15		K_{S0}	Sulfate half-saturation coefficient for denitrifying autotrophic biomass	8.5	g $S.m^{-3}$
$i_{P,BIO}$	P content of biomasses	0.02	-	$\mu_{SRB,Ac}$	Maximum specific growth rate of Ac SRB	8	d^{-1}	K_{SO4}	SO4 half saturation for SRB	250	g $COD.m^{-3}$
i_{IG}	Synthesis inorganics in active biomass	0.21	g TSS / g COD	$\mu_{SRB,H2}$	Maximum specific growth rate of H2 SRB	30	d^{-1}	$K_{NO2,SOB}$	Half-saturation constant for nitrite SOB	10	g $N.m^{-3}$
f_{Na}	Sodium mass fraction in NaCl	0.393	mg CAT/mg	μ_{SOB}	Maximum specific growth rate of SOB	9	d^{-1}	$K_{I,S2}$	Inhibition for S^{2-}	2000	g $S.m^{-3}$
$C_{Se,1}$	SOB growth for nitrate reduction by S0	0.76	-	$C_{se,2}$	SOB growth for nitrate reduction by S0		-	$G_{H2S,sat,eq}$	Sulphide saturation concentration	10	mol $L^{-1}.bar^{-1}$
k_{LaH2S}	Oxygen mass transfer coefficient of hydrogen sulphide	76.40	d^{-1}	$C_{h2s,1}$	SOB growth for nitrite reduction by H2S			$C_{h2s,2}$	SOB growth for nitrite reduction by H2S		
Formula values	**Description**	**Formula**				**Formula values**		**Description**	**Formula**		
$Bellininh_{pH,i}$	Bell-shaped inhibition with check for pH availability	If (Sumo__pHEffects; $(1+2*10^{0.5+(K_{lo}-K_{hi})})/(1+10^{(var-K_{hi})}+10^{(K_{lo}-var)})$; 1)				$NoncompinhS_{H2S}$		Non-competitive inhibition	$\frac{1}{(1+var/K_{inh})}$		

In the comparison of the configurations was evaluated the energy demand (ED) of the plant. For Configuration I it was considered the ED for aeration only because represents more than the 60% of the total ED of the plant (Gori et al., 2013) and it was calculated by PetWin 4.0. For the anaerobic digestion process was evaluated the ED for the heating and the ED for the sludge mixing, following the hypothesis of Metcalf & Eddy IV edition, equation 14-15. The energy recovery was evaluated by considering a methane specific energy of 35.8 MJ m^{-3}.

Chapter IV: Results and Discussion

The chapter includes the presentation and the discussion of the results. Starting from the mass balance of Cuoiodepur WWTP, it was evaluated the primary sludge anaerobic digestion process. The experimental tests showed two key points of the process:

1. high values of ammonia nitrogen after the digestion due to the rich protein-based substrate;
2. high value of H_2S in the biogas due to the presence of sulphate in the influent.

The simulations underline a close link between the AD process and the biological denitrification (sulphide denitrification in this case).

4.1 Cuoiodepur historical data analysis

As mentioned before, the WWTP treats almost exclusively tannery industrial wastewater, and, as a consequence, it is affected by the variability of industrial productions that change with weekly cycles and depend on market trends; moreover, every year during August, a low load is collected due to the reduction of the production.

Figure 42 shows the influents total COD: municipal and industrial wastewater. Figure 42 A shows the total COD concentrations in the year 2013, while Figure 42 B shows the total COD mass weekly variation January-June 2013.

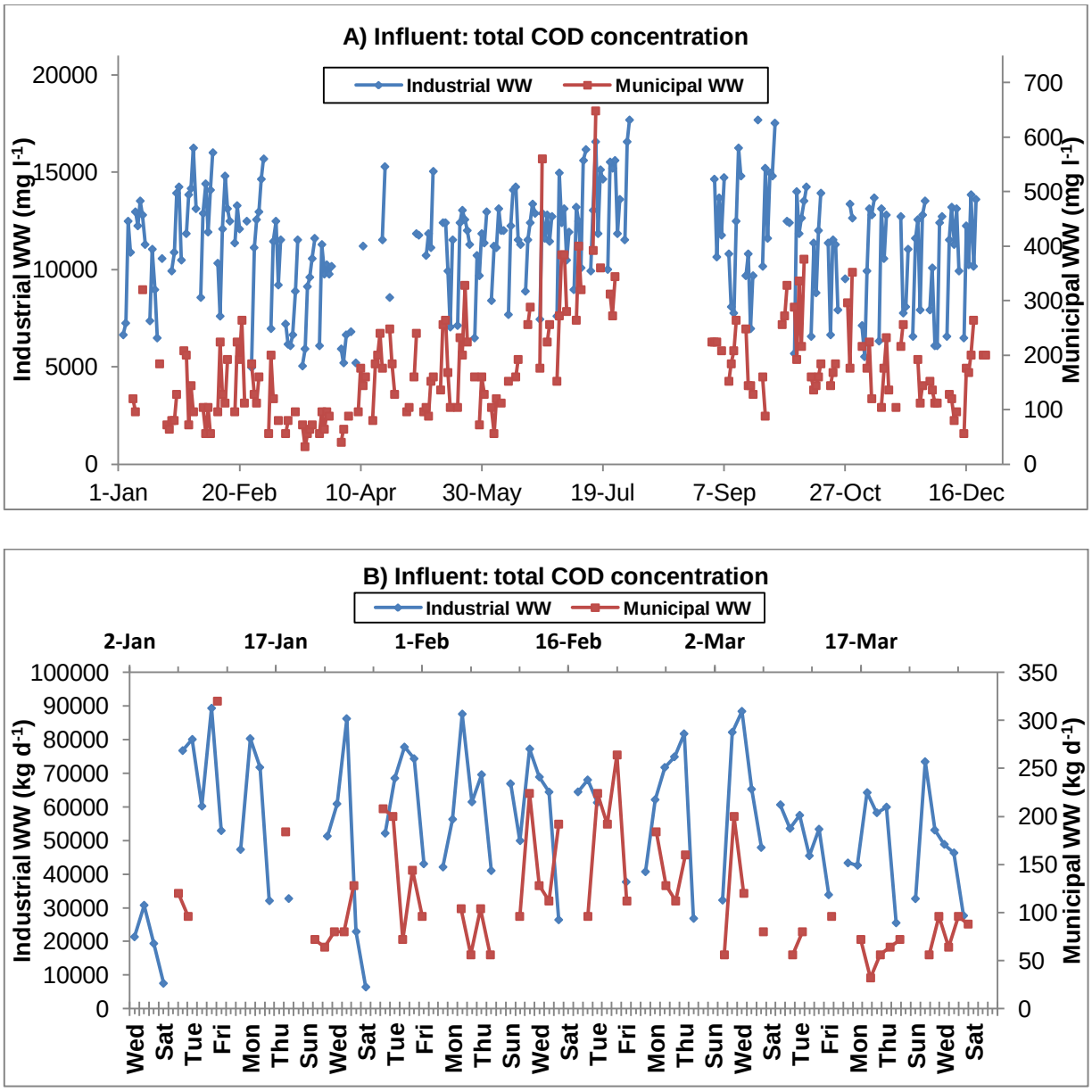

Figure 42: Total COD characterization of the municipal and industrial wastewater influents. A: total COD concentrations year 2013. B: total COD mass weekly variation Jan-March 2013.

The total COD concentration in the industrial wastewater during the year was almost constant at 11253±2821 mg COD l^{-1}, while the total COD concentration in the municipal wastewater was 175±95 mg COD l^{-1} and was higher during spring-summer and less during the cold months. No data available for August because as the less productive month, the WWTP is usually under maintenance.

As shown in figure 42 B, the industrial influent has a weekly trend, the total COD mass (and the concentration) is higher from Monday to Friday, while is lower during the weekend. Almost an opposite trend characterize the municipal influent, higher load during the weekend and lower load during the week.

Table 31 shows the average and the standard deviation of the parameters monitored in the influents during the year 2013.

Table 31: Influents concentrations, year 2013.

Influent	Parameter	Unit	Average	St. Dev.	Unit	Value
Industrial WW	pH	-	8.02	0.69	-	
	Total COD	mg l^{-1}	11253	2821	kg d^{-1}	51437
	Filtered COD	mg l^{-1}	5313	1218	kg d^{-1}	24286
	Suspended solids	mg l^{-1}	4735	1759	kg d^{-1}	21644
	Total N	mg N l^{-1}	749	150	kg N d^{-1}	3424
	Filtered N	mg N l^{-1}	548	129	kg N d^{-1}	2505
	Organic N	mg N l^{-1}	229	80	kg N d^{-1}	1047
	Ammonia N	mg $N\_NH_4^+$ l^{-1}	310	83	kg N d^{-1}	1417
	Chloride	mg l^{-1}	6204	1405	kg d^{-1}	28358
	Sulphate	mg S l^{-1}	806	193	kg S d^{-1}	3684
	Total P	mg l^{-1}	21	5	kg d^{-1}	96
	Q	m^3 d^{-1}	4571	1987		
Municipal WW	pH	-	7.74	0.28	-	
	Total COD	mg l^{-1}	174	95	kg d^{-1}	632
	Filtered N	mg N l^{-1}	32	10	kg N d^{-1}	116
	Ammonia N	mg $N\_NH_4^+$ l^{-1}	23	8	Kg N d^{-1}	83
	Total P	mg l^{-1}	2.71	1.00	kg d^{-1}	10
	Q	m^3 d^{-1}	3630	1248		

As shown in table 31 the industrial flow is characterized by high values of COD, SS, Nitrogen, Sulphate and Chloride; while the municipal wastewater is characterized by low values of the parameters. Moreover, the COD mass flow rate of the industrial is much higher than the municipal one, i.e. if COD is the key parameter, the industrial influent total COD represent 99% of the total influent in the plant.

Figure 43 shows the COD characterization of the industrial influent during the year (2013).

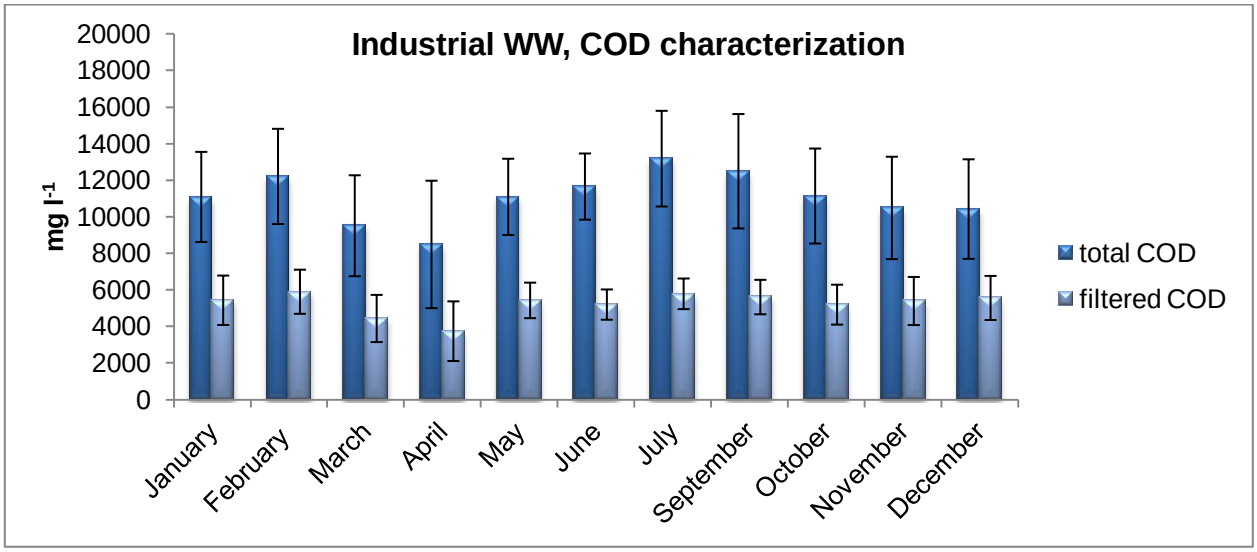

Figure 43: COD characterization of the industrial influent, 2013.

The dynamics of the COD concentration in the industrial influent is strongly influenced by two main factors: the intensity of industrial process and the mixing with the water runoff during the rainy months. There was not a clear reflection of first factor during this year, while the second reduced the COD (as a dilution) during the Fall (October-December). Moreover, in the area usually is raining in the early spring (March-April) and in the same period the Easter holidays causes a reduction of the production. The peak value was reached in July at 13170±2617 mg l^{-1}, while the filtered COD was 5778±383 mg l^{-1} and it is globally the 44-53% of the total COD.

The nitrogen compounds, figure 44, follows the same COD trend.

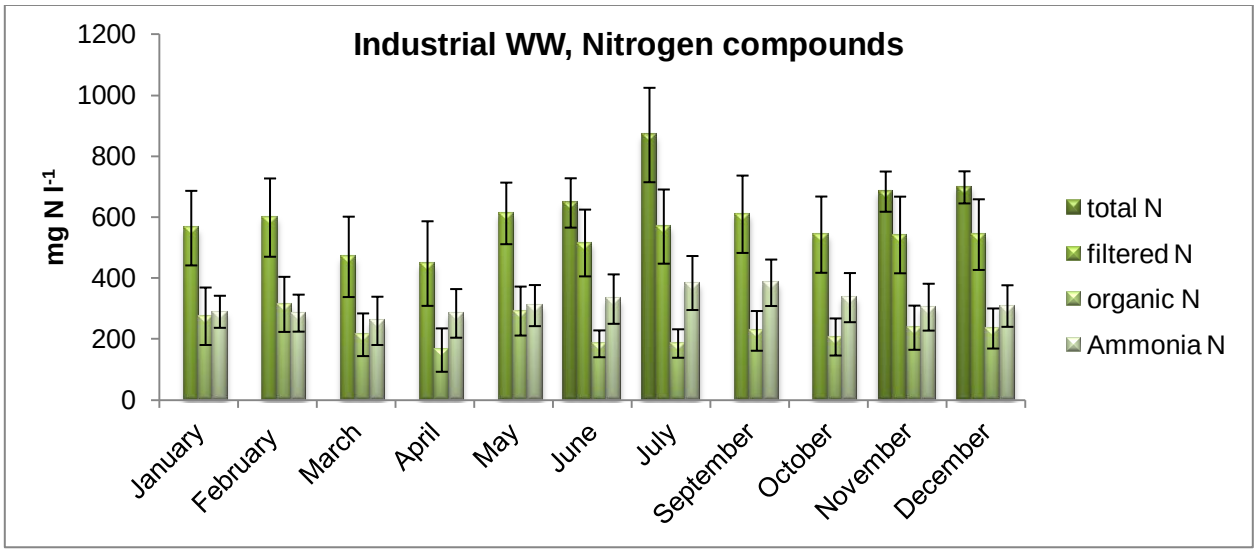

Figure 44: Nitrogen compounds characterization in the industrial influent.

The peak value of the organic nitrogen was reached in February at 314±30 mg N l^{-1} and it represented almost the 30% of the total nitrogen, while the ammonia nitrogen was in that month 285±61 mg N l^{-1} and it is the 46% of the total nitrogen. The great part of the total nitrogen is soluble nitrogen.

Figure 45 shows the concentration of sulphur compounds in the industrial influent.

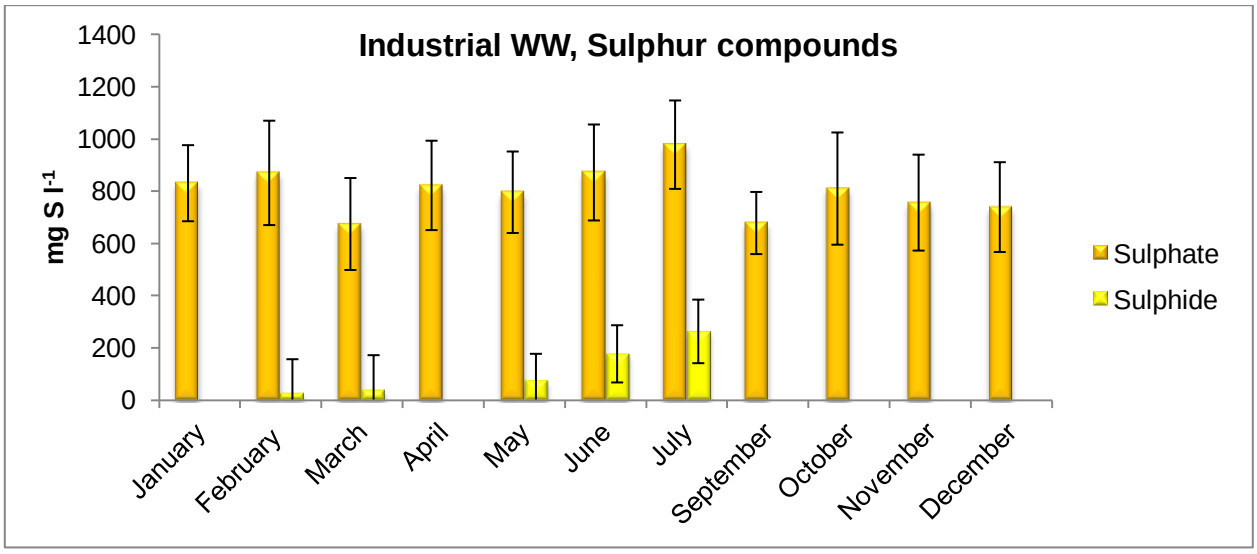

Figure 45: Sulphur compounds concentration in the industrial influent.

The sulphate follows the same trend of the other parameters. The sulphide characterization was hardly accurate because the samples were not stabilized, it was decided to concentrate in 7 days a 24 hours sampling investigation.

Figure 46 shows the trend of the influent sulphide concentration on 24 hours sampling. The sampling campaign was an intensive analysis on 7 days with stabilized samples (NaOH).

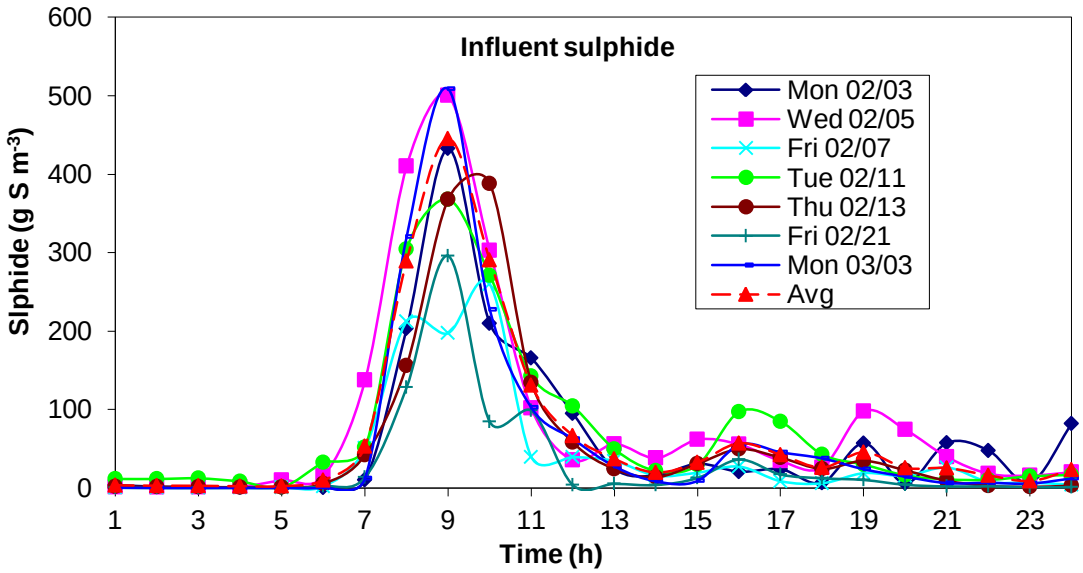

Figure 46: Influent sulphide concentration on 24 hours sampling.

The peak of sulphide influent is in the morning around 9 am, while in the afternoon other 2 mid-peak at 4 and 7 pm. Moreover, the intensive analysis confirmed the weekly dynamics, the load is more at the beginning of the week, while is less at the end. After the intensive campaign it is possible to assume that the peak of the influent concentration of sulphide was in the range of 50-450 mg l^{-1}.

All the information collected and shown previously were used to close the mass balance of the equalization tank in terms of COD and sulphur. Figure 47 shows the equalization tank mass balance. To complete the equalization mass balance a combination of the information based on routinely and intensive analysis was considered.

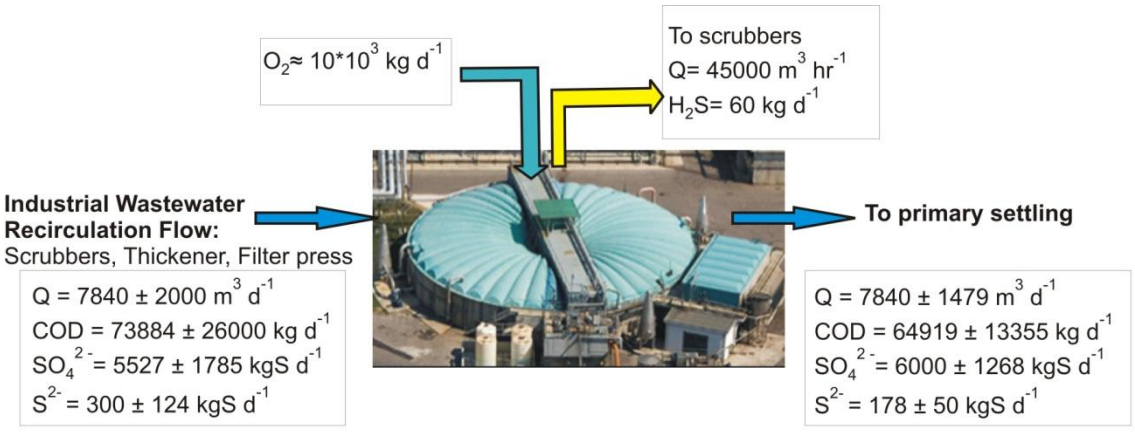

Figure 47: Mass balance for the equalization tank.

The equalization mass balance shows that almost 9% of the COD total influent was reduced and 60% of the sulphide was oxidized to sulphate. Moreover, the sulphur influent in the plant is characterized by the 5% of sulphide and the 95% of sulphate.

The analysis was extended to the all plant configuration. The temperature in the aerated tank during the year is in the range 30-20 °C, while the dissolved oxygen (DO) average in 2013 was in the range 1.5-2.5 mg l^{-1}. The solids concentration of the biological compartment is link to the SRT of the process itself, in the Cuoiodepur WWTP usually the mixed liquor suspended solids (MLSS) concentration is in the range 7500-9000 mg l^{-1} and the volatile fraction (MLVSS) is the 77-88 % of the total.

Figure 48 shows the COD and sulphur compounds mass balance of the plant for the year 2013.

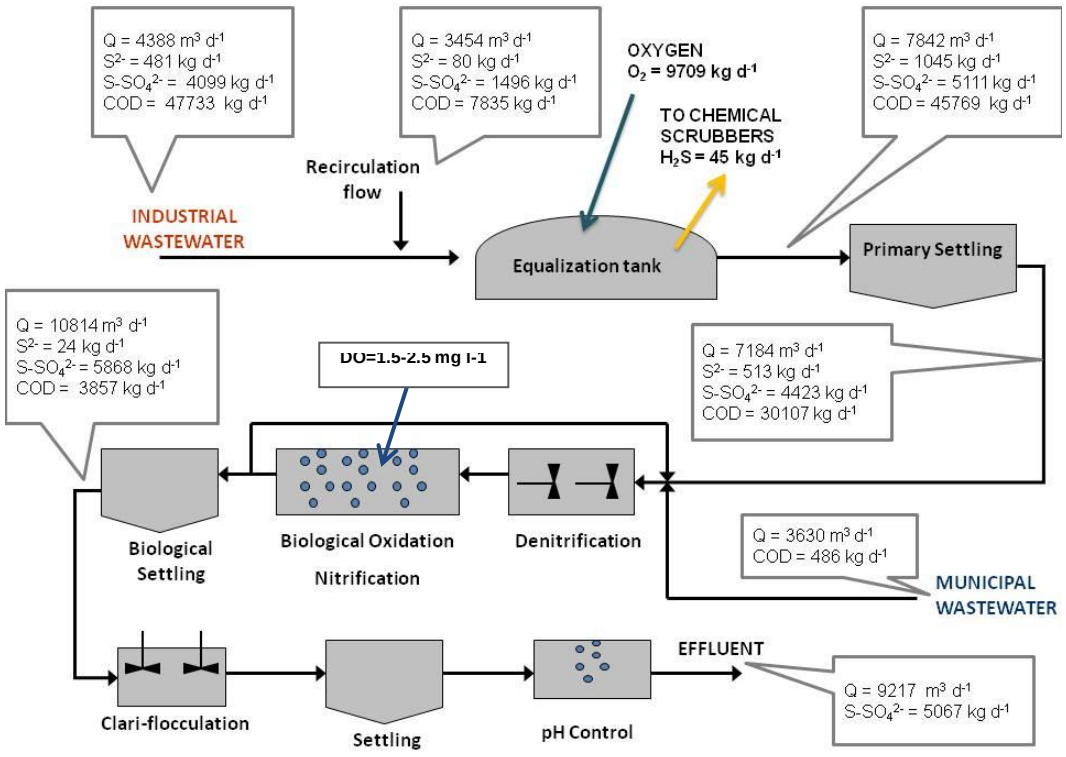

Figure 48: COD and sulphur compounds mass balance.

The mass balance shows that the sulphur compound is mostly sulphate and the sulphur in the recirculation flow is around 30% of the total influent. The removal efficiency of the activated sludge section is 87% in terms of total COD.

4.2 Anaerobic batch tests

As explained in the materials and methods (Chapter 3.2) two test sets were performed: the anaerobic digestion of VTPS-CDPS and the anaerobic co-digestion of sludge and solid waste. The first set includes 6 tests (T1 to T6) with different VTPS to CDPS volumetric ratios, while the second includes 3 tests (T7 to T9) with different VTPS to TIF mass ratios.

Figure 49 shows the headspace pressure trends of T1 to T6 tests.

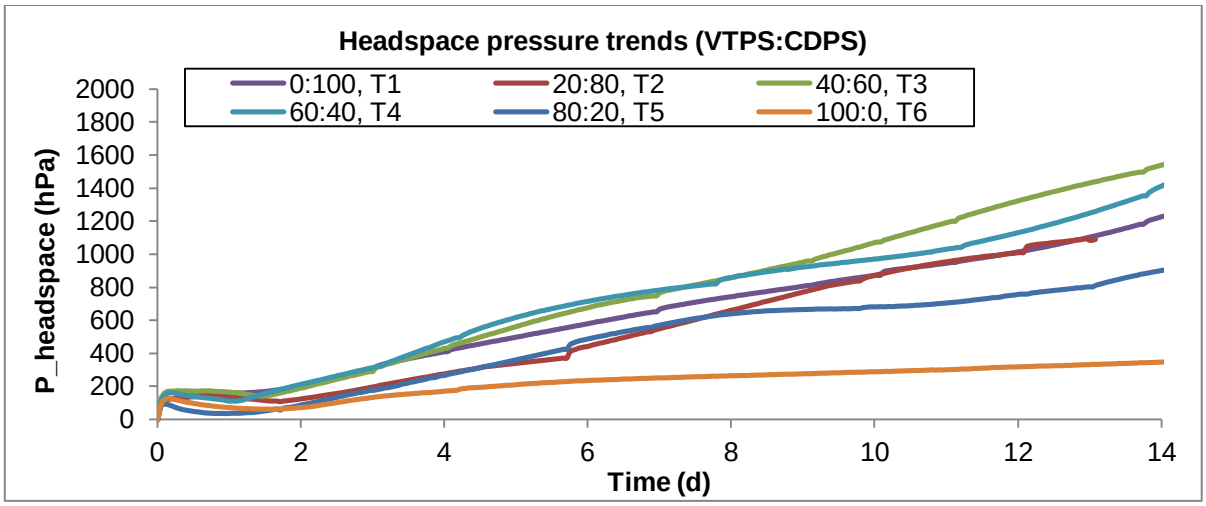

Figure 49: Headspace pressure trends in the batch tests.

As a qualitative analysis of Figure 49, it is possible to notice that in the first days (from 0 to 2 day) the tests with VTPS are characterized by lower slopes. This can be related to a slow hydrolysis process due to the complexity of the substrate. Furthermore, T3 showed the highest biogas production, but T4 reached the highest specific production.

Figure 50 shows the methane percentage in the biogas. The batch test was carried out by Laboratorio ARCHA (Pisa, Italy) for the digestion of VTPS only.

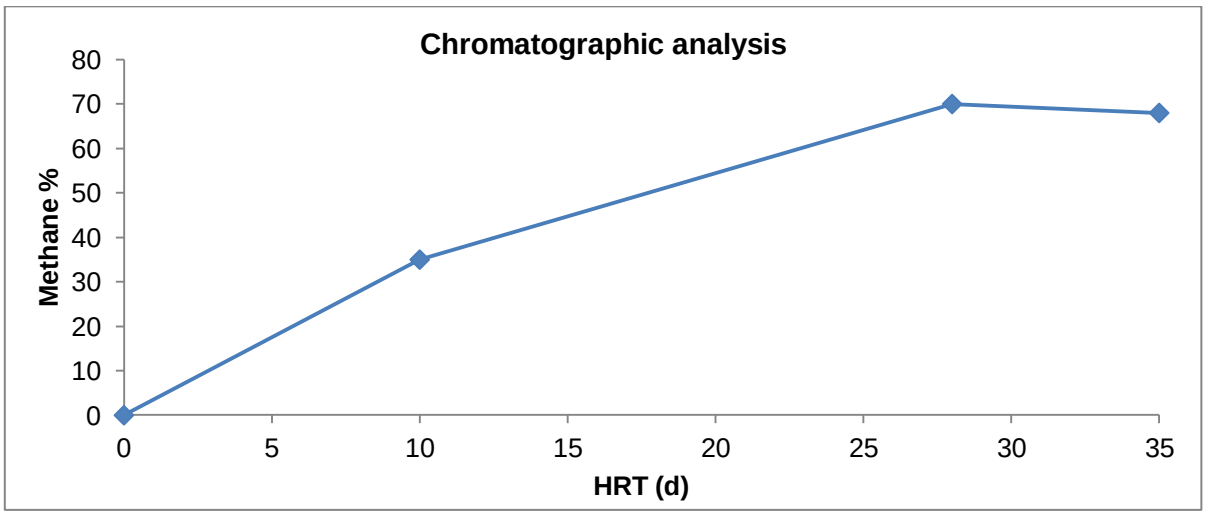

Figure 50: Chromatographic analysis, methane percentage in the biogas of VTPS digestion.

As shown in figure 50 it is possible to reach a methane percentage of 65% at 25 days of HRT, while at 10-15 days of HRT the CH_4 concentration is 30-45%.

Figure 51 shows the COD and VS removal during the tests (average and standard deviation).

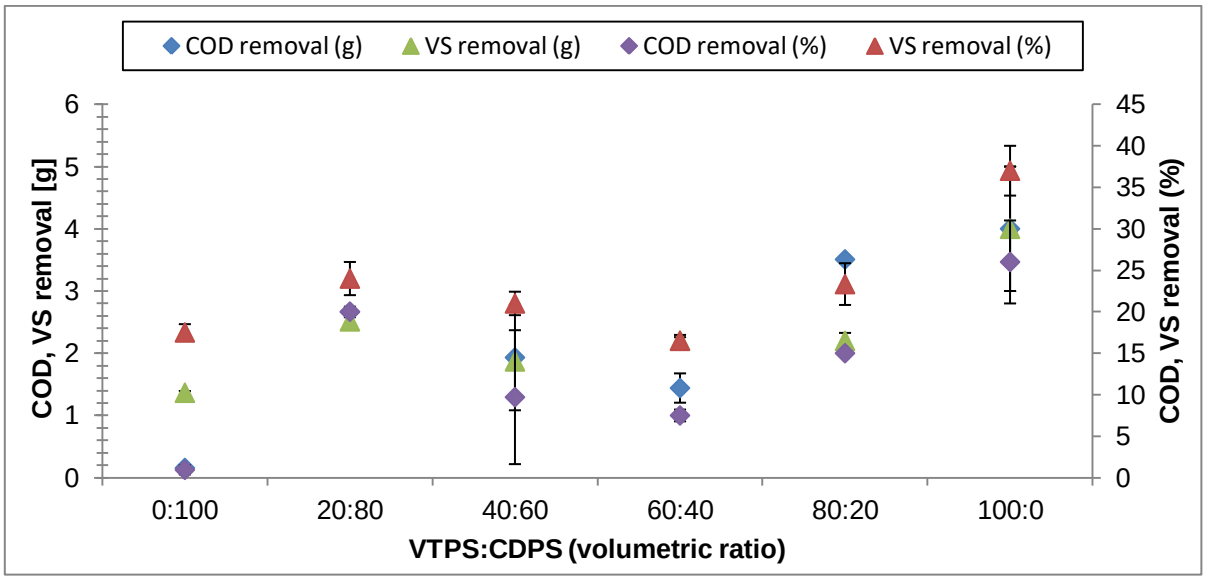

Figure 51: COD and VS removal in the anaerobic digestion batch tests with different VTPS:CDPS volumetric ratios.

The VS removal is almost stable in the range of 15-25% and with a 37% removal for the 100:0 test. The COD and VS removals follow almost the same trend; however, the COD values should be higher than VS values. Standardized methods are available for the measurements of COD for water and wastewater. However, COD measurements for solid substrates have been traditionally specifically adapted, where the samples have to be properly homogenized and diluted (Raposo et al., 2012). Because of the accuracy of the analysis, the VS was considered as the most reliable parameter and COD was considered for the trend but not as a key parameter. As shown in figure 51 there is no specific trend in the VS and COD removal adding VTPS to CDPS in the anaerobic digestion tests. The addition of the VTPS did not improve or worsen the anaerobic digestion.

Figure 52 shows the final value of the specific biogas produced during the tests, calculated from the headspace pressure as in Eq.1.

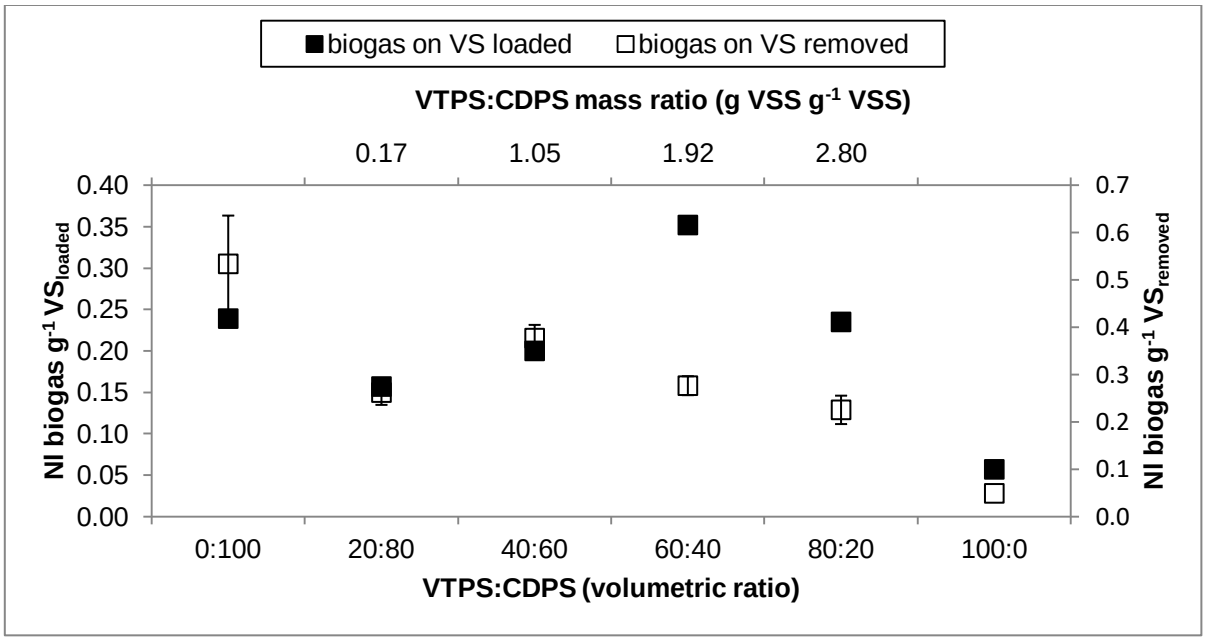

Figure 52: Specific biogas production in the batch tests.

The specific biogas production in terms of Nl of biogas on grams VS removed is all in the range 0.2-0.4 with the exception of the last test (100:0 test).

The biogas production is in the range 0.15-0.35 Nl g^{-1}VS loaded for all the tests, while in 0:100 test was 0.057 Nl g^{-1}VS. However, 60:40 and 0:100 test showed values in contrast between the biogas production and the VS removal. The T-student correlation were applied to evaluate the correlation between tests 60:40 and 0:100 to the other tests in terms of VS removal and the specific biogas production. The results showed that both the tests (60:40 and 0:100) for both the components analyzed are characterized by T test values below 0.05 meaning that they are significantly uncorrelated.

To evaluate the inhibitory effects due to sulphur compounds, figure 53 shows the sulphate removal and the COD to sulphate ratio in the tests.

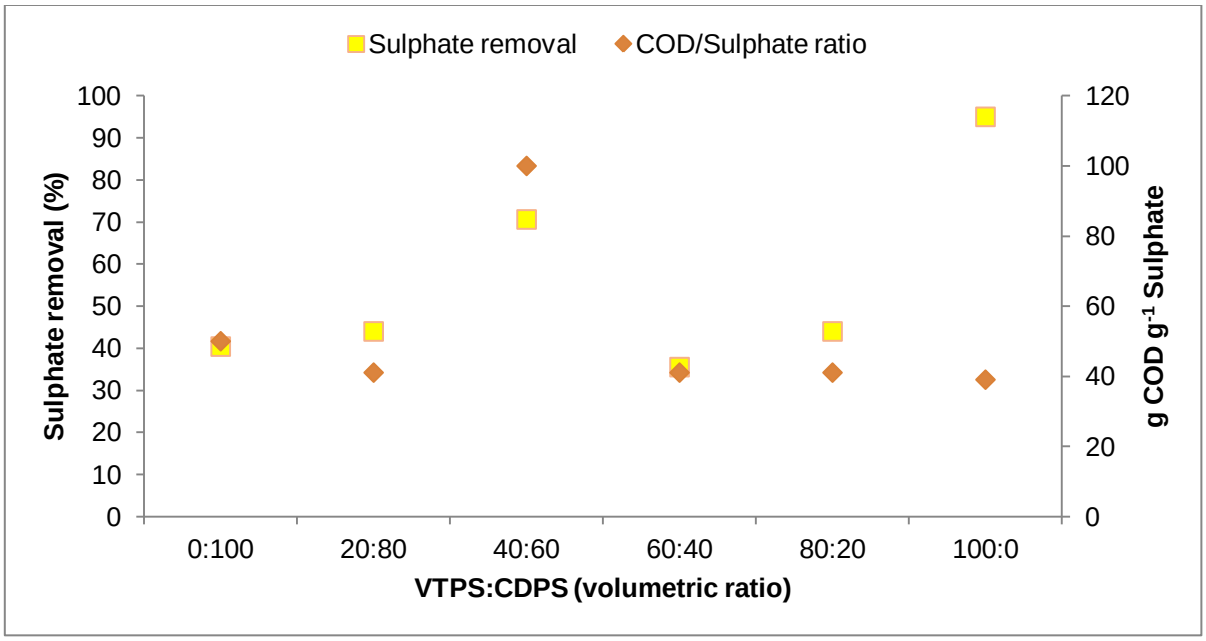

Figure 53: Sulphate removal and COD to sulphate ratio in the batch tests.

Factors such as COD/SO_4^{2-} ratio, the relative population of SRB and other anaerobes, and the sensitivity of SRB and other anaerobes to sulfide toxicity influence the competition between SRB and acetogens. As a result, the literature on anaerobic digestion of sulphate containing wastewaters is highly complex and often contradictory (Chen et al., 2008). However, Chen et al., 2008, reported values of COD/sulphate for the competition between SRB and other anaerobes, below 10.

The COD/sulphate ratio values in the tests were far from the inhibitory values, moreover it is possible to notice that a little ehigh sulphate removal is related to low COD/sulphate values that means more was the presence of sulphate higher was the removal and vice versa. However, the sulphate removal was in the range 0f 40-50% and the COD to sulphate ratio was in the range of 40-60 gCOD g^{-1} sulphate for all the experiments except for T3 and T6 (40:60 and 100:0, VTPS:CDPS, respectively).

Figure 54 shows the headspace pressure trend of the co-digestion's tests VTPS: TIF at different mass ratio (1:2, 1:1, 2:1 in tests T7, T8 and T9, respectively).

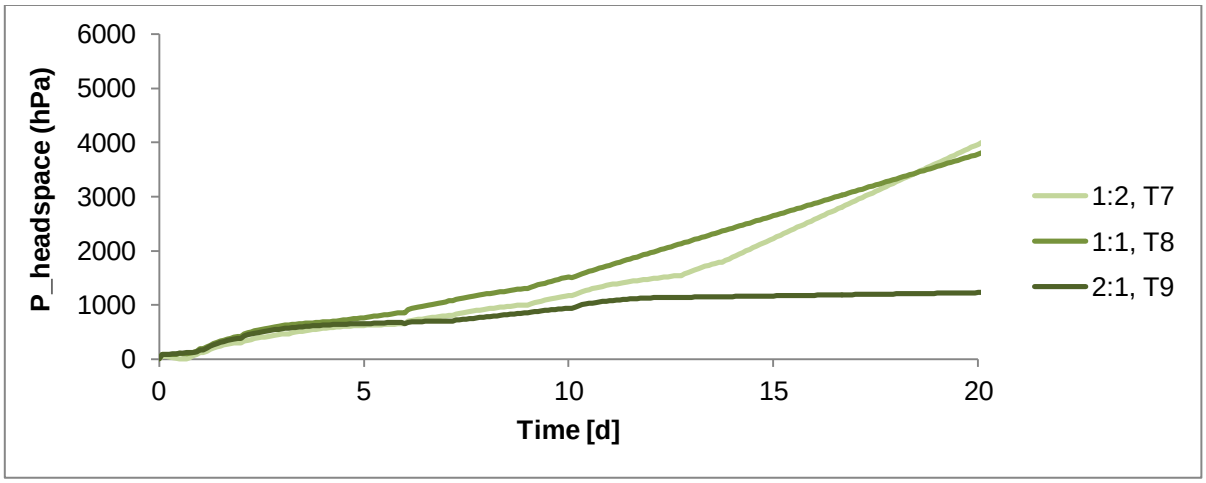

Figure 54: Headspace pressure trends in the batch co-digestion tests.

The curves show comparable behavior until day 14. Test T9 had almost a constant biogas production rate throughout the test (constant linear trend), suggesting that the low presence of fleshing resulted in a more homogenized mixture and no phase stratification limited the process from the beginning. Conversely, a sharp increase in biogas production rate was registered after day 14 for the most fleshing-rich test, T7 and T8, reaching a final overpressure value almost double than T9. This result remarks that anaerobic digestion of fleshing requires a long hydrolysis step and, at that same time, that lipid-rich mediums, as fleshing is, are valuable substrates due to their high methane yield (Cirne et al., 2007). Some studies already addressed the problem of hydrolysis as limiting phase for fleshing anaerobic digestion as well as the operational clogging problem in the reactor due to not-liquefied fats in the feeding. Besides size reduction through mechanical grinding, some authors reported positive effects of enzyme addition (Zerdani et al., 2004; Vasudevan et al., 2007; Berardino and Martinho, 2009) and of thermal pre-treatment at termophilic temperatures (Zupančič and Jemec, 2010).

Moreover, the ammonium value at the end of the tests were 985±35 mg N_NH_4 l^{-1}, 755±14 mg N_NH_4 l^{-1} for T7 and T9, respectively and the sulphate reduction in all cases was around 94%.

The specific biogas production in the co-digestion's tests VTPS: TIF at different mass ratio (1:2, 1:1, 2:1 in tests T7, T8 and T9, respectively) is reported in Figure 55.

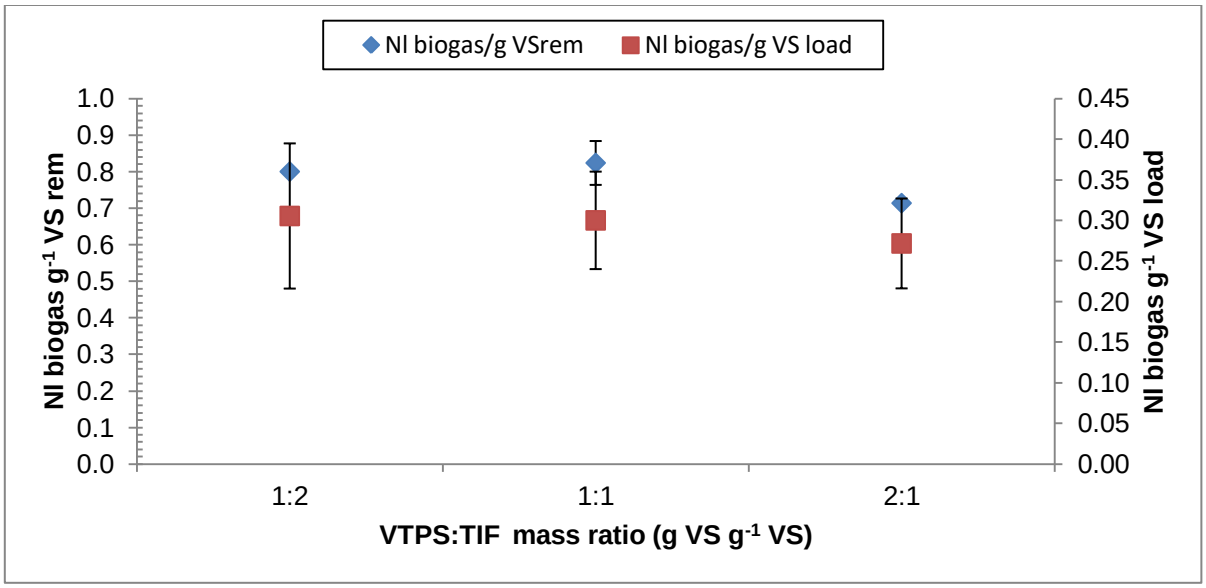

Figure 55: Specific biogas production for the co-digestion batch tests.

The co-digestion of VTPS and TIF lead to a significant increase in SBP in comparison with blank test T6 (VTPS only) and, specifically, the higher amount of fleshing in the mixture is related to the higher observed SBP. The VS removal was 22.3, 23.33 and 25.5 % for test 1:2, 1:1, 2:1.

4.3 Continuous tests

As mentioned previously in chapter 3.3 the AD continuous tests includes two scales: laboratory and pilot scale. Moreover, different SRT and substrates were tested. Starting from the smallest scale to the biggest all the results obtained will be discussed in the following paragraphs.

4.3.1. Laboratory scale tests

The laboratory scale tests were conducted with the aim of the adaptation of the biomass on the VTPS sludge, increasing the percentage of VTPS in a CDPS anaerobic digestion. Moreover, it was evaluated the potential increase of the performances, increasing the VTPS in the mixture.

Figure 56 shows the variable width notched box plots data distribution for the following parameters: the influent organic loading rate (OLR); sulphate loading rate (SLR),

ammonium of the effluent, VS, sulphate removal and the VFA (as acetate) in the sludge effluent for each reactor.

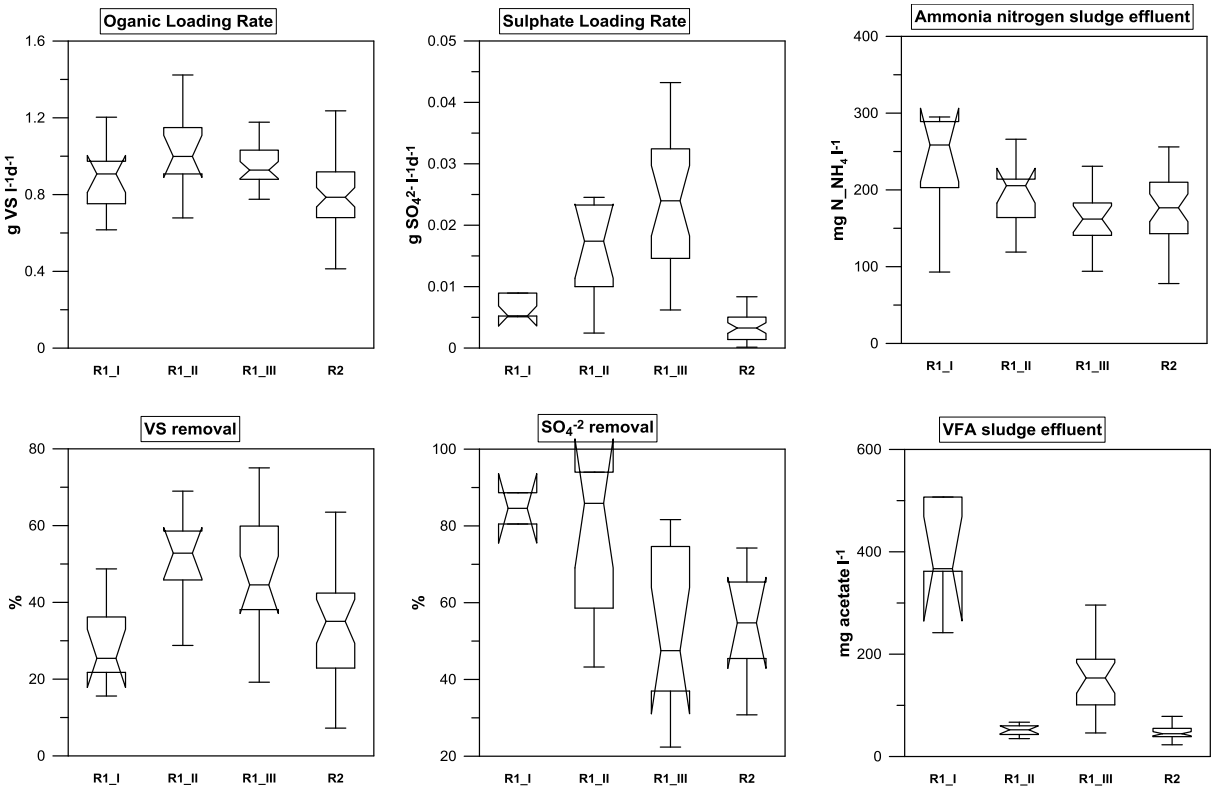

Figure 56: Variable width notched box plots data distribution of the laboratory scale reactors.

As shown in figure 56, increasing the OLR (consequently the SLR) by the increase of VTPS, there was an increase of the VS removal from 30% to 45-41 %, R2, R1_II R1_III, respectively. During the first period, R1_I has been characterized by almost the same OLR (lower SLR) as R1_II and R1_III but less VS removal, probably due to the slow adaptation of the biomass to the new substrate and the slow start-up of the reactor. This hypothesis can be confirmed by the highest value of VFA reached in the period, compared to the other reactors. The ammonia nitrogen in the effluent was almost in the same range 100-300 mg N_NH_4 l^{-1} for the reactors. Data on sulphate were characterized by the highest values of dispersion due to the variation of the concentration in the influent sludge during the year. Figures 57 and 58 show the cumulative biogas production recorded in R1 and R2 compared to the cumulative VS mass of the sludge influent and effluent. As mentioned in the materials and methods paragraph, the start-up phase is excluded, day 0 refers at the first day after the start-up.

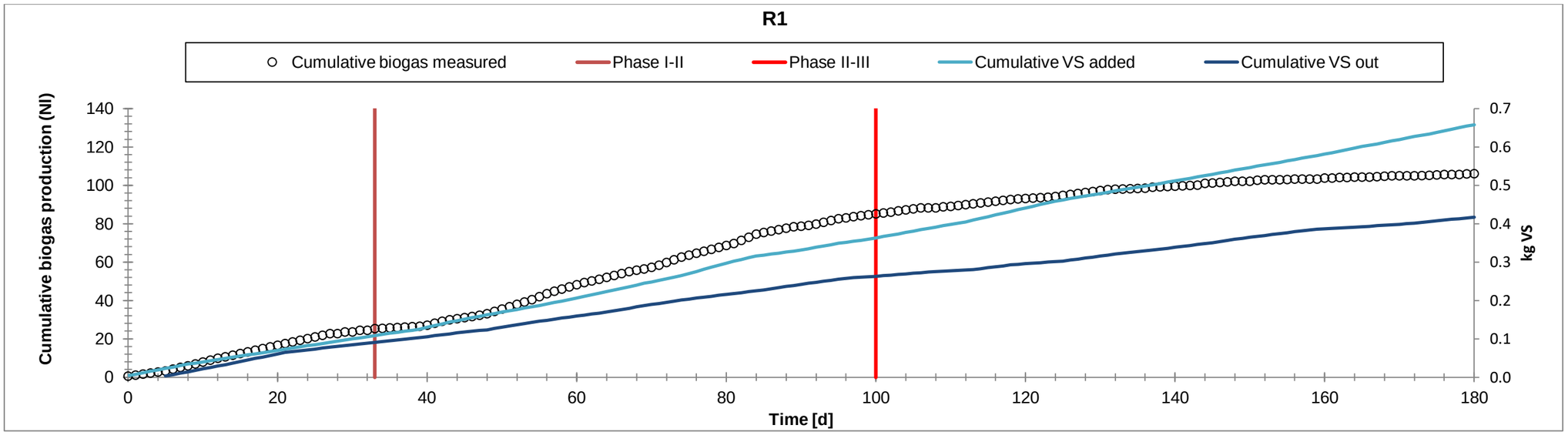

Figure 57: Cumulative biogas production and cumulative VS influent and effluent mass in R1 (laboratory scale test).

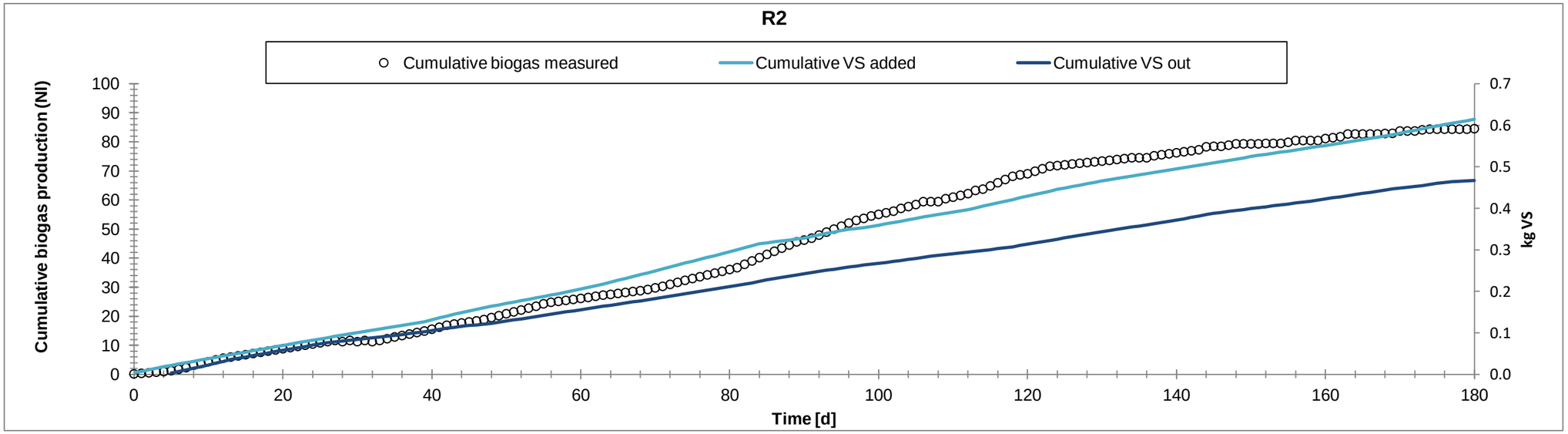

Figure 58: Cumulative biogas production and cumulative VS influent and effluent mass in R2 (laboratory scale test).

Figure 57 shows a correlation between the biogas production and the VS removal trends (represented by the differences between the two cumulative curves: VS added and out) in phase I and II. While, in phase III the higher VS removal (represented by an increasing of the distances between the two blue curves) is associated with a lower biogas production (represented by a decrease in the cumulative biogas production curve slope). This is probably due to leaks from the reactor, so the biogas production was not recorded properly.

Figure 59 shows a correlation between the biogas production and the VS removal trends. The specific biogas production of R2 (control reactor) was 0.19±0.08 Nl biogas g^{-1}VS load, while the specific biogas production was for R1 phase I and II, 0.18±0.05 Nl biogas g^{-1}VS load and 0.21±0.09 Nl biogas g^{-1}VS load, respectively.

Table 32 shows the results of the mass balance of the reactors for the estimation of the methane percentage. The methane production was estimated through the mass balance equations Eq. 2 and Eq. 3, while the CH_4 percentage was calculated through the combination of the mass balance and the measured biogas.

Table 32: Mass balances results (laboratory scale test).

Reactor	Phase	CH_4	Biogas	CH_4
		Nl $d^{-1}_{estimated}$	Nl $d^{-1}_{measured}$	% $_{estimated}$
R1	I	0.42	0.64±0.10	66
	II	0.53	0.80±0.27	66
	III	0.31	0.47±0.18	66
R2		0.33	0.50±0.2	66

The digestion of municipal and vegetal tannery primary sludge up to 70:30 volumetric ratio allows the possibility to improves the anaerobic sludge digestion performances compared to municipal only or tannery digestion only. Moreover, no significant inhibitory effects on anaerobic digestion were evident.

4.3.2. Pilot scale tests

Figure 59 shows the OLR in kg of VS per m^3d^{-1} and the SLR in kg of sulphate per m^3d^{-1} for all reactors during the time (after the start-up phase).

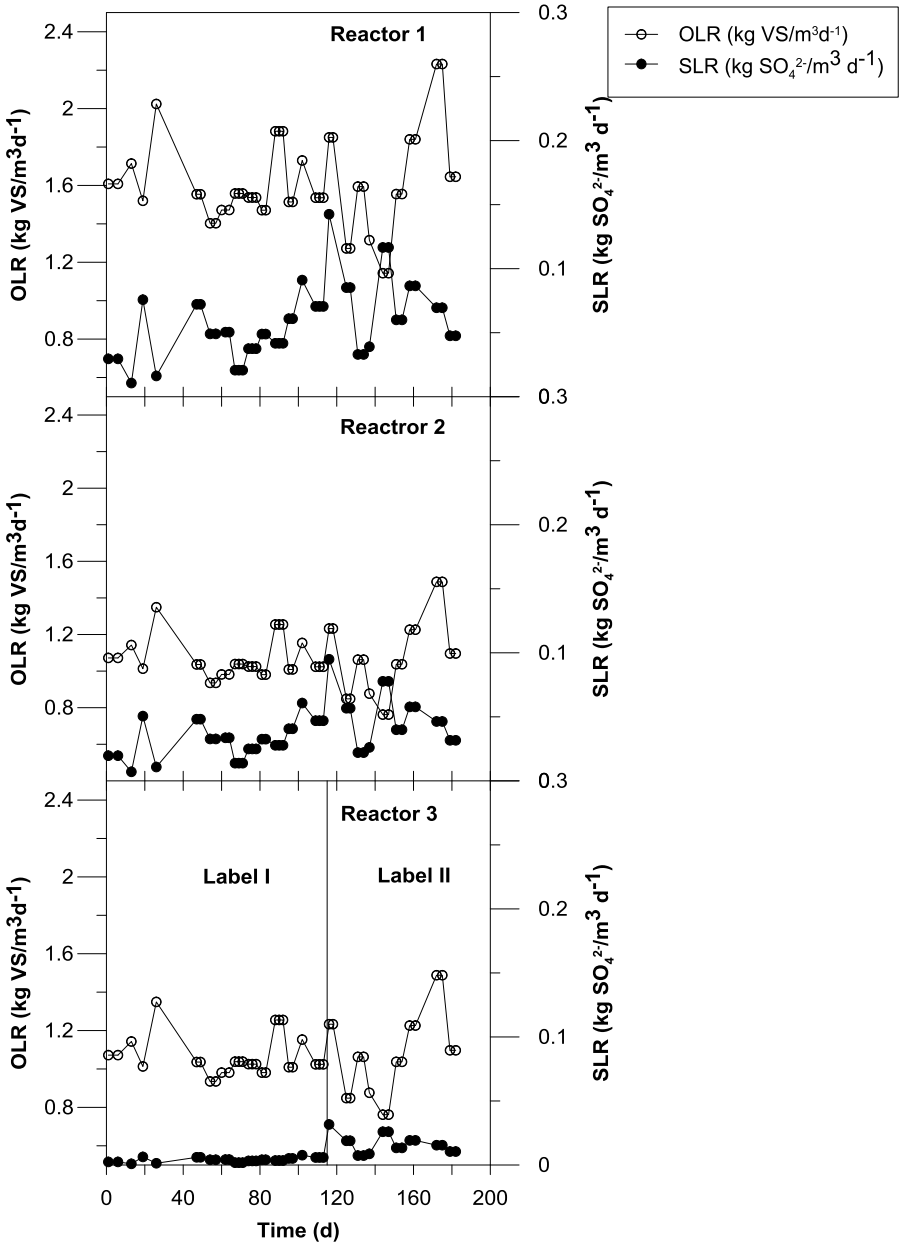

Figure 59: The OLR and the SLR for all reactors during the time (after the start-up phase, pilot scale tests, Volume = 130 l).

The OLR of the feeding was in the average of 1.60±0.23 and 1.07±0.16 kg VS/m^3 d^{-1}, R1 and R2 respectively, while 1.07±0.15 and 1.2±0.22 kg VS/m^3 d^{-1} for R3, label I and II.

Consequently, the SLR for R1 and R2 was in the average of 0.057±0.028 and 0.038±0.019 kg S/m^3 d^{-1}, while 0.009±0.004 and 0.012±0.005 kg S/m^3 d^{-1} for R3, label I and II, respectively.

Figure 60 shows the variable width notched box plots data distribution for the following parameters: the influent organic loading rate (OLR); sulphate loading rate (SLR), ammonium of the effluent, VS, sulphate removal and the theoretical methane production for each reactor.

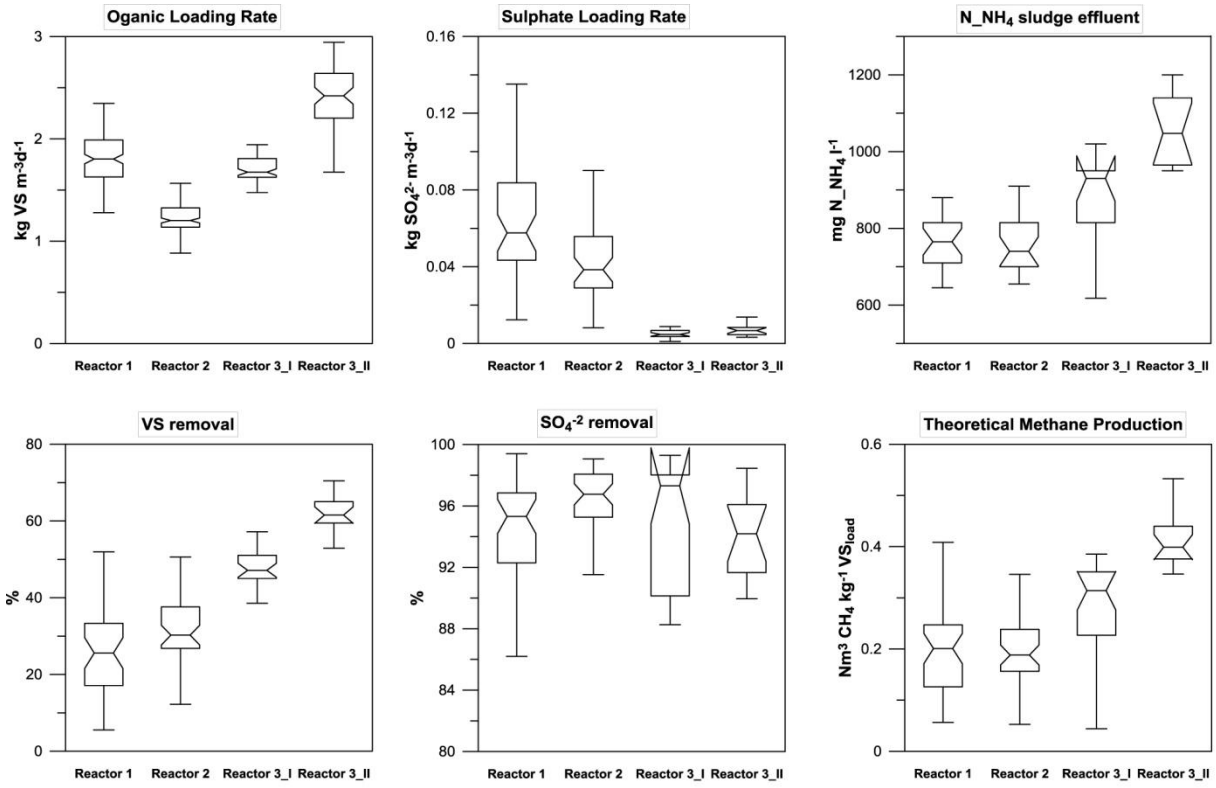

Figure 60: Variable width notched box plots data distribution of the pilot scale reactors (pilot scale tests, Volume = 130 l).

The variable width notched box plot analysis showed a quite high standard deviations of the data, reflecting the load variability real of an industrial wastewater treatment plant.

The co-digestion with fleshing (Reactor 3) resulted in higher ammonium concentration in the digested sludge (857±139 and 1052±86 mg N_NH_4 l^{-1} in Reactor 3 Label I and II, respectively, compared to 755±61 mg N_NH_4 l^{-1}, 760±69 mg N_NH_4 l^{-1} in Reactor 1 and 2), reasonably due to the biodegradation of proteins in the organic substrate. Literature reports

for ammonia inhibition values of 4.2-10 g l^{-1} (Chen et al., 2008), in the reactors were recorded values much lower than this. According to the results, the biodegradable fraction of fleshing was evaluated around 82%, for the conditions tested.

The sulphide concentration in the effluent was recorded for both reactors approximately the same, 43±19 mg S^{2-} l^{-1} and at 40±27 mg S^{2-} l^{-1} for Reactor 2 and 3 label I, respectively, while in label II, the sulphide concentration in the effluent was recorded at 121±40 mg S^{2-} l^{-1}. Moreover, in Reactor 1 the sulphide concentration in the effluent was recorded at 77±26 mg S^{2-} l^{-1}. The inhibitory sulphide levels reported in the literature were in the range of 100–800 mg l^{-1} dissolved sulphide or approximately 50–400 mg l^{-1} undissociated H_2S (Parkin et al., 1990).

Despite data dispersion, the increase of OLR from Reactor 2 to Reactor 3 label I and II can be clearly related to the observed increase in VS removal and, consequently, in the theoretical methane production, represented by a linear correlation. Referring to the same reactors, the decrease in sulphate loads is also considered responsible for the higher methane production, although in a much lower extent due to the modest loading values in all reactors.

However, the increasing the OLR and the SLR from Reactor 2 to Reactor 1, caused a decreases of the VS and sulphate removal of 20% and 2%, respectively. Even though, the theoretical methane productions were approximately the same in the two reactors for the two values of HRT.

Figure 61 shows the trend of the inhibition factors of free ammonia and sulphide compared to the methane theoretical production. The inhibition factors were combined following in Eq. 6.

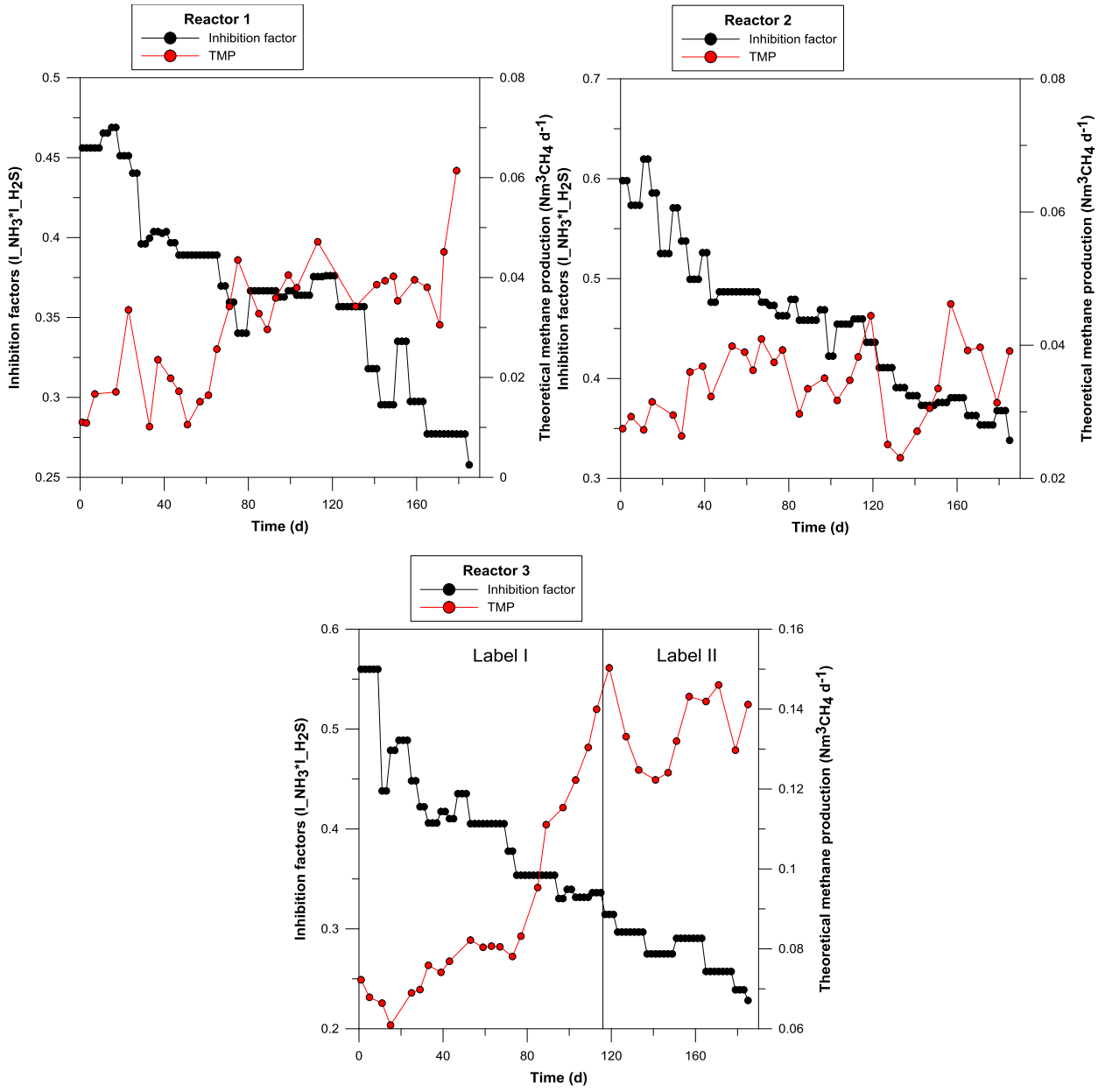

Figure 61: Inhibition factors trends and theoretical methane production trends (pilot scale tests, Volume = 130 l).

The inhibition factor must be intended as a reduction factor of the production, i.e. when the value is close to 1 the inhibition is low, on the contrary values close to 0 means high inhibition.

For all reactors, the theoretical methane production follows an opposite trend compared to the inhibition factor, moreover with an increase of TIF as a substrate (Reactor 3_II), there was an increasing of the theoretical methane production more than the inhibitory effects due

to NH_3 and sulphide. This exclude the inhibitory effects of the two components for the concentrations tested. If the inhibitory effects are excluded, the rather low VS removal efficiency is possible due to an ineffective mixing in the reactor that can generate dead zones and the stratification of the sludge. Moreover, if the compound is not well mixed, the collection of the outlet from the bottom may negatively affect the quality of the sample.

Table 33 shows the mass balance of the reactors. For the estimation a 45% and 65% of methane in the biogas was hypothesized for HRT 15 and 25 days (Reactor 1 and 2, 3) respectively, as a result of the batch test (Figure 53). The GC analysis on 3 samples of Reactor 2 confirmed the biogas characterization: 66±6% of methane and 32±7 of carbon dioxide.

Reactor 2 shows a lower specific biogas production compared to Reactor 1. The increase of the OLR can be the bottleneck of the process, from Reactor 1 to Reactor 2. However, Reactor 3 showed different results, increasing the OLR by the addition of fleshing, the specific biogas production increase. Reactor 2 could be affected by a not efficient mixing more than the other reactors.

Figure 62 shows the cumulative theoretical methane production based on the mass balances estimations.

The cumulative curve of theoretical methane production show a very good performance for Reactor 3. The addition of fleshing helped to reach more than the double of the theoretical methane production at the end of the test. There is an agreement in the comparison of the results in literature, Basak et al., 2014 showed a specific biogas production of 0.3-0.5 liters of biogas per grams of VS added in the reactor with a VS removal of 40-52 % for the co-digestion of sludge and fleshing.

Table 33: Mass balance of the reactors (pilot scale tests, Volume = 130 l).

Reactor	VS (kg d^{-1})			COD (kg d^{-1})			Sulphate (kg S d^{-1})			Theoretical methane production (Nl d^{-1})	Specific biogas production (Nl g^{-1} VS load)	H_2S in the biogas (%)
	in	out	VS removed	in	out	COD removed	in	out	Sulphate removed	estimated		
1	0.26±0.04	0.19±0.02	0.07	0.50±0.10	0.36±0.03	0.14	$4\ 10^{-3}$±$2\ 10^{-3}$	$1\ 10^{-4}$±$8\ 10^{-5}$	$3.90\ 10^{-3}$	48	0.44	3
2	0.15±0.03	0.11±0.01	0.04	0.30±0.06	0.19±0.02	0.11	$2\ 10^{-3}$±$1\ 10^{-3}$	$7\ 10^{-5}$±$5\ 10^{-5}$	$1.93\ 10^{-3}$	40	0.32	3
3_I	0.22±0.01	0.11±0.01	0.11	0.43±0.02	0.20±0.01	0.23	$2\ 10^{-3}$±$6\ 10^{-4}$	$4\ 10^{-5}$±$1\ 10^{-5}$	$1.96\ 10^{-3}$	76	0.46	1
3_II	0.30±0.03	0.12±0.01	0.18	0.63±0.07	0.21±0.03	0.42	$2\ 10^{-3}$±$1\ 10^{-3}$	$1\ 10^{-4}$±$6\ 10^{-5}$	$1.90\ 10^{-3}$	143	0.62	1

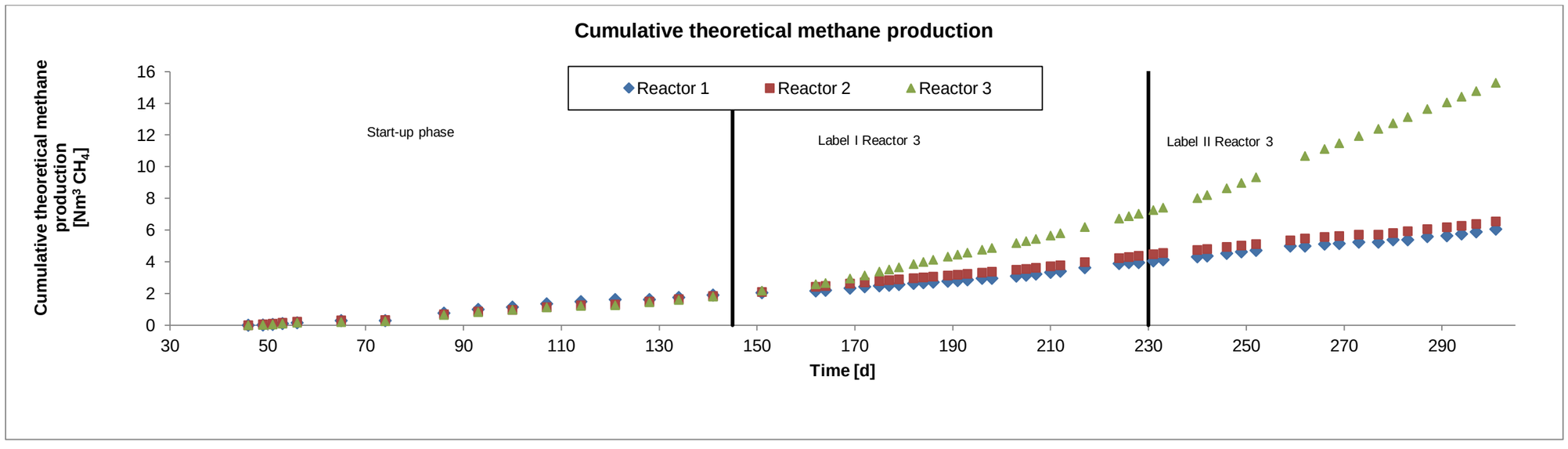

Figure 62: Cumulative theoretical methane production in the reactors (pilot scale tests, Volume = 130 l).

Figure 63 shows the variable width notched box plots data distribution for the following parameters in the influent organic loading rate (OLR); sulphate loading rate (SLR), while ammonium of the effluent, VS, sulphate removal and the theoretical methane production for the reactor in label I and II.

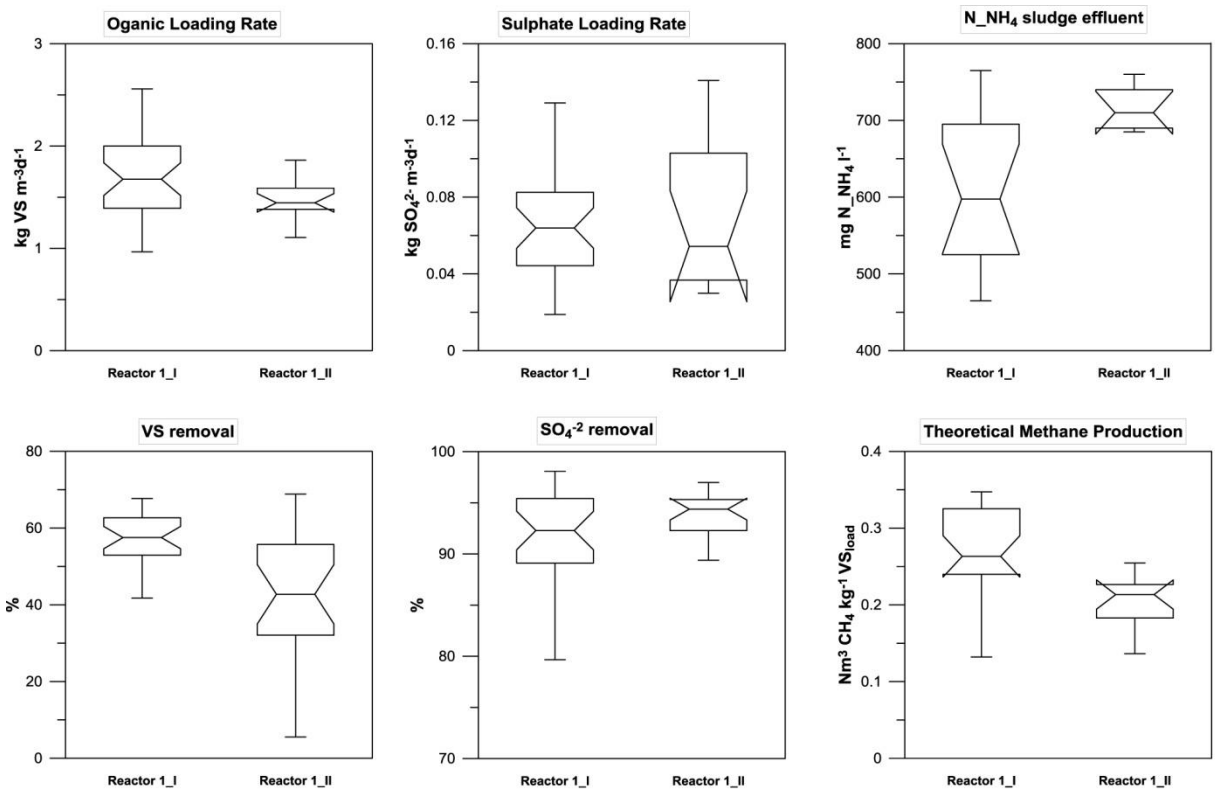

Figure 63: Variable width notched box plots data distribution of the pilot scale reactor (pilot scale tests, Volume = 5 m^3).

The variable width notched box plot analysis showed again a quite high standard deviation of the data, reflecting the load variability real of an industrial wastewater treatment plant.

In the comparison between this results and the previous results (pilot scale reactors 130 l of volume, HRT 15 and 25 days) almost the same results are obtained. It is possible to assume that in the anaerobic digestion process, in mesophilic conditions, at an HRT in a range of 20-30 days:

- VS removal is in the range 40-60%;
- The TMP is in the range 0.2-0.3 $Nm^{-3}CH_4$ kg^{-1} VS load;

- The ammonia nitrogen in the sludge effluent is in the range 600-800 mg N_NH_4 l^{-1};
- The sulphate reduction is in the range 90-100 %.

Table 34 shows the mass balance of the reactor.

The mass balance confirmed the characterization of the biogas with 70-71% of the methane and at least 1% of H_2S. Moreover, the biogas production was estimated at more than 3 Nm^3 per day.

Table 35 shows the characterization of the digested sludge in terms of acetic, propionic, butyric and valeric acids.

The decreasing values of VFAs, from sample 1 to 3, showed the increasing in the reactor performances. Moreover, the decrease of butyric acid and the increase of propionic and acetic acids confirmed the normal anaerobic fermentation (Cenni et al., 1982). No-accumulation and consequently no-inhibition factors were evaluated.

Table 34: Mass balance of the reactor (pilot scale tests, Volume = 5 m^3).

HRT (d)	VS ($kg\ d^{-1}$)		COD ($kg\ d^{-1}$)		Sulphate ($kg\ S\ d^{-1}$)		Sulphide ($kg\ S\ d^{-1}$)	CH_4 (%)	CO_2 (%)	N_2 (%)	Biogas ($Nm^{-3}\ d^{-1}$)	H_2S in the biogas (%)	N_2 in the biogas (%)
	in	out	in	out	in	out	out	measured			estimated		
20	7±1	3±1	13±2	6±1	0.09±0.05	0.02±0.01	0.04±0.01	71±1	26±1	3±1	3.45	1	2
30	6±1	2.8±0.3	12±3	6±1	0.10±0.01	0.01±0.002	0.04±0.01	70±1	29±1	1±1	3.15	1	2

Table 35: VFAs characterization of the digested sludge, wet-based analysis (pilot scale tests, Volume = 5 m^3).

	Sample 1 (start-up)		Sample 2 (20 d HRT)		Sample 3 (20 d HRT)		Average	St. Dev.	
	$mg\ kg^{-1}$	%	$mg\ kg^{-1}$	%	$mg\ kg^{-1}$	%	$mg\ kg^{-1}$		%
Acetic acid	1094	74	618	42	327	22	680	387	53
Propionic acid	229	15	573	39	506	34	436	182	34
Butyric acid	110	7	35	2	22	1	55	47	4
Valeric acid	15	1	24	2	5	0	14	10	1
VFAs	1479		1353		984		1272	257	

4.4 Sulphide denitrification laboratory scale tests

The sulphide denitrification was evaluated in two reactors where the denitrification process took place from nitrate to nitrogen gas and from nitrite to N_2 for reactor 1 and 2, respectively.

Figure 64 shows nitrate and nitrite concentrations in influent and outlet during the test in reactor 1 (after the start-up phase). Moreover, the graph shows the temperature trend.

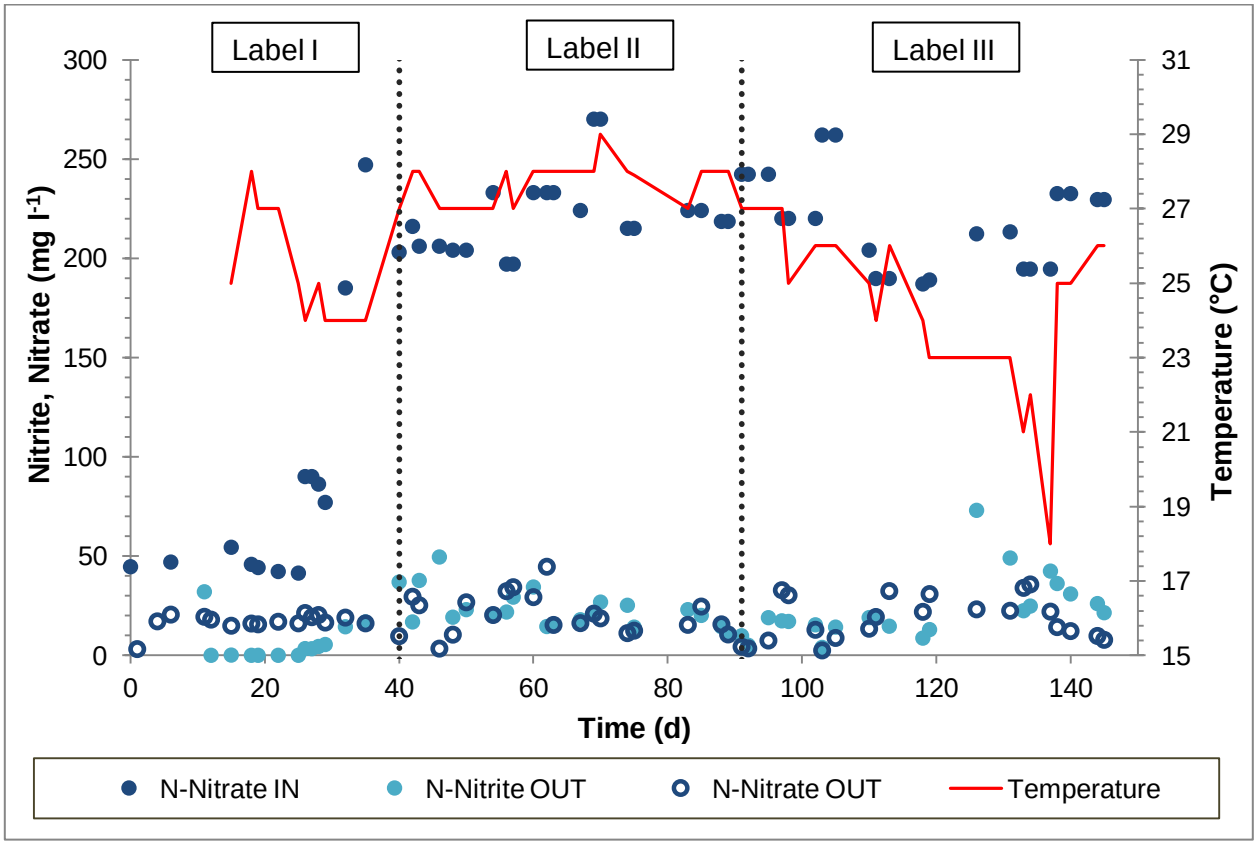

Figure 64: Sulphide denitrification test, reactor 1, nitrate and nitrite concentrations, temperature trend.

Changing the SRT from 20 to 5 days (Label I to II), did not improve the denitrification process. Despite a drop down in the temperature trend (from 23 to 18 °C) it was not highlighted a repercussion in the process. The denitrification process was evaluated as(?) incomplete because a concentration of approximately 25 mg $N\text{-}NO_2^-$ l^{-1} remains in the effluent.

Figure 65 shows the sulphur compounds mass in reactor 1 and the temperature trend during the test (after the start-up phase).

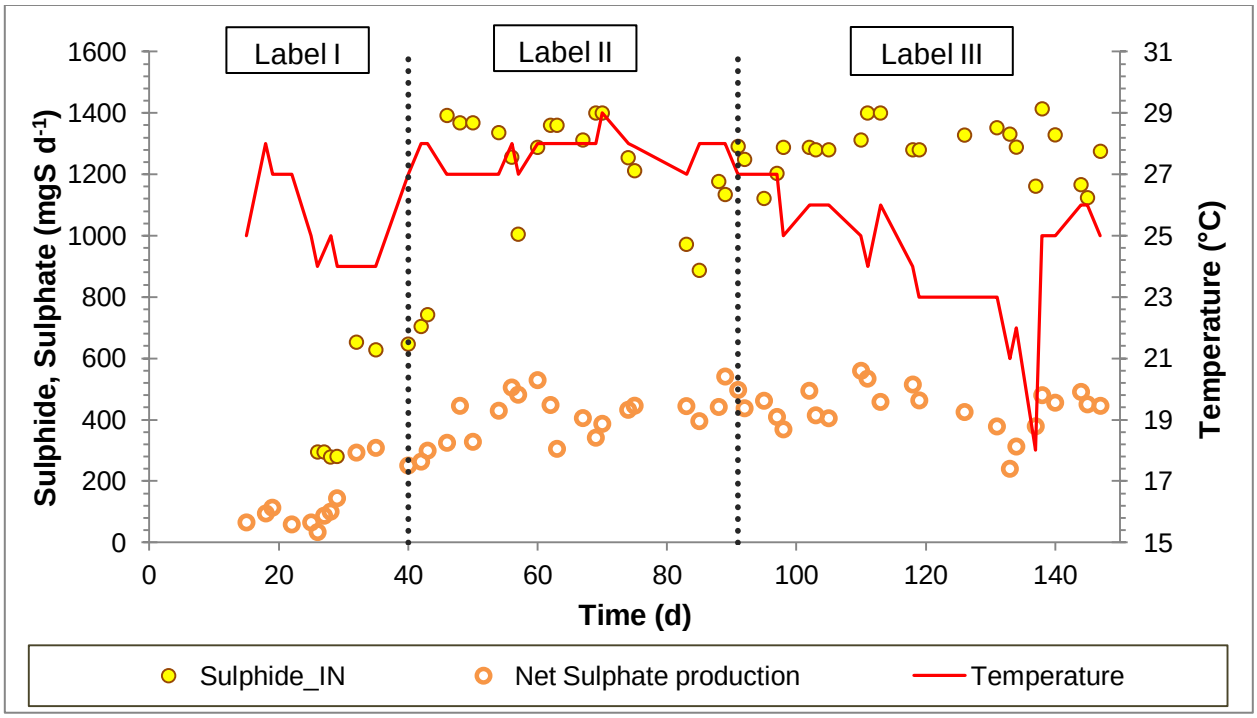

Figure 65: Sulphur compounds concentration and temperature trend during the test, reactor 1.

In figure 65 the net sulphate production was evaluated as a difference between the mass of the sulphate inlet and the outlet. The temperature trend in the range evaluated does not influence the process. With the hypothesis of no stripping gas and no intermediate products, the sulphide oxidation was evaluated at 69%.

The sulphur mass balance was not closed if not considering intermediate products. The second hypothesis comprises an elemental sulphur and thiosulphate intermediate products calculated through equation 7 and 8.

Table 36 shows the sulphur mass balance in reactor 1 during the test.

Table 36: Sulphur mass balance in reactor 1, sulphide denitrification lab scale test.

Label	Compound	In (mgS d^{-1})	Out (mg d^{-1})	In-Out (%)
II	$S\text{-}SO_4^{2-}$ measured	92 ± 10	526 ± 107	6.5
	$S\text{-}S^{2-}$ measured	1320 ± 109	0	
	$S\text{-}S_2O_3^{2-}$ estimated	-	793	
	$S\text{-}S_0$ estimated	-	0	
	Total S	1412	1319	
III	$S\text{-}SO_4^{2-}$ measured	105 ± 18	676 ± 80	7.7
	$S\text{-}S^{2-}$ measured	1384 ± 104	0	
	$S\text{-}S_2O_3^{2-}$ estimated	-	508	
	$S\text{-}S_0$ estimated	-	190	
	Total S	1489	1374	

According to the estimation shown in table 36, in label II the mass balance was closed with an error of 6.5%, while an error of 7.7% was found for label III.

Figure 66 shows nitrite concentrations influent and outlet during the test in reactor 2 (after the start-up phase). Moreover, the graph shows the temperature trend.

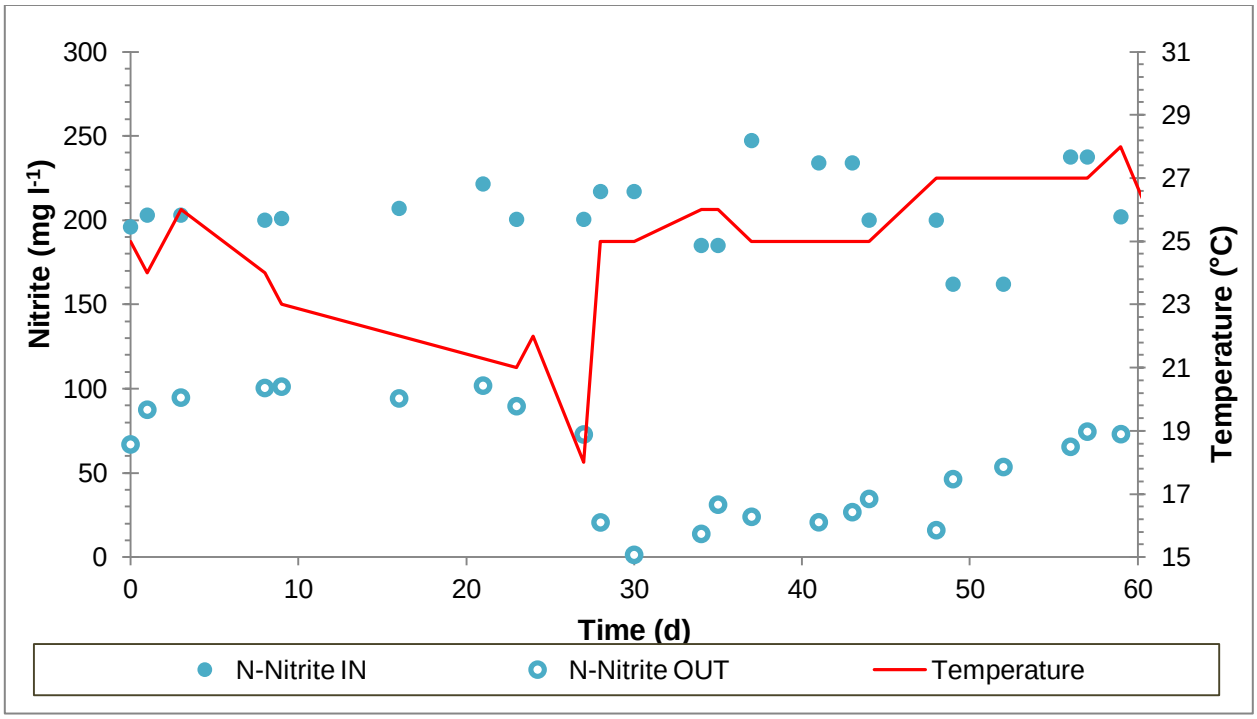

Figure 66: Sulphide denitritation test, reactor 2, nitrite concentration and temperature trend.

As shown in Figure 66, a drop down in the temperature trend (from 25 to 19 °C) not highlighted a repercussion in the process. The denitritation process was evaluated with a removal efficiency of 87.5%.

Figure 67 shows the sulphur compounds mass in reactor 2 and the temperature trend during the test (after the start-up phase).

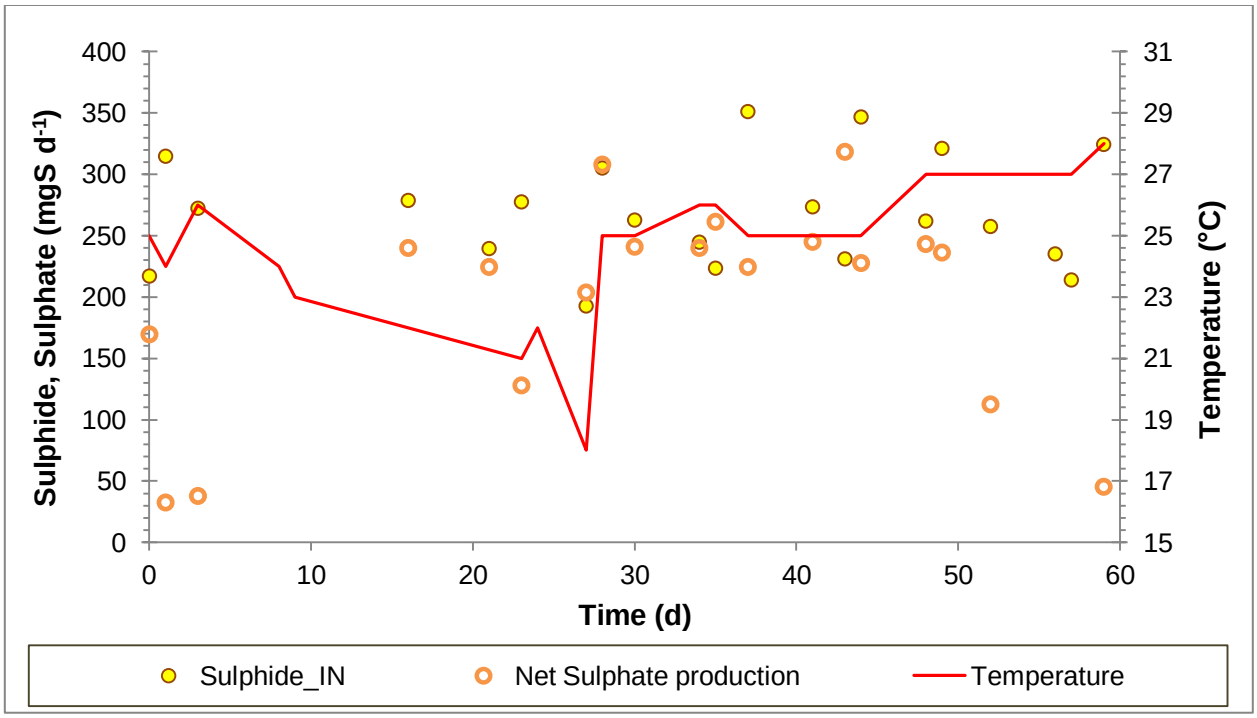

Figure 67: Sulphur compounds concentration and temperature trend during the test, reactor 2.

As shown in figure 67, when temperature was stable approximately at 25 °C and the nitrite was removed (from day 30 to 50), sulphide was oxidized to sulphate. However, more uncertainties was highlighted until day 30 and after day 50.

4.5 Anaerobic digestion modelling (ADM1)

The anaerobic digestion batch tests were modelled through the application of the modified ADM1 with the inclusion of sulphur metabolism, as reported in chapter 3.5.1. In this paragraph is reported the calibration and the validation of the modified model.

Calibration and validation

Two batch tests were chosen to calibrate and validate the model with the modifications of the ADM1: T1 and T6, VTPS:CDPS 0:100 and 100:0, respectively, because T1 and T6 were the control tests.

The disintegration-hydrolysis step is well recognized as the bottleneck of the AD process and can be crucial its implementation and parameters estimation in the model (Batstone et al., 2002; Batstone & Keller, 2003; Angelidaki & Sanders, 2004; Lauwers et al., 2013). Moreover, few informations are available regarding the SRB biomasses introduced.

Sensitivity analysis has been widely applied to reduce model complexity, to determine the significance of model parameters and to identify dominant parameters (Barrera et al., 2015).

For the following parameters was applied the linear sensitivity analysis:

- complex particulate disintegration first order constant (k_{dis});
- carbohydrate hydrolysis first order constant ($k_{hyd, ch}$);
- lipid hydrolysis first order constant ($k_{hyd, li}$);
- protein hydrolysis first order constant ($k_{hyd, pr}$);
- sulphide inhibitory constant ($k_{I, h2s}$);
- maximum uptake rate for acetate degrading organisms SRB ($k_{m, ac, SRB}$);
- maximum uptake rate for hydrogen degrading organisms SRB ($k_{m, h2, SRB}$);
- maximum uptake rate for propionate degrading organisms SRB ($k_{m, pro, SRB}$).

The estimation of the sensitivity functions is done in AQUASIM 2.0 as following: Chosing an arbitrary variable (y) calculated by AQUASIM and a model parameter (p) represented by a constant variable or by a real list variable, the absolute sensitivity function measures the absolute-absolute, relative-absolute, absolute-relative or relative-relative changes in y per unit of changes in p. All the changes are calculated in linear approximation only. This makes possible a quantitative comparisons of the effect of different parameters p on a common variable y. Bigger is the shape of the sensitivity functions (within the range of available data), the more is the accuracy of the parameters identifiable.

Figures 68 and 69 show the results of the sensitivity analysis, the sensitivity functions of the parameters of COD and sulfate concentration in the reactor.

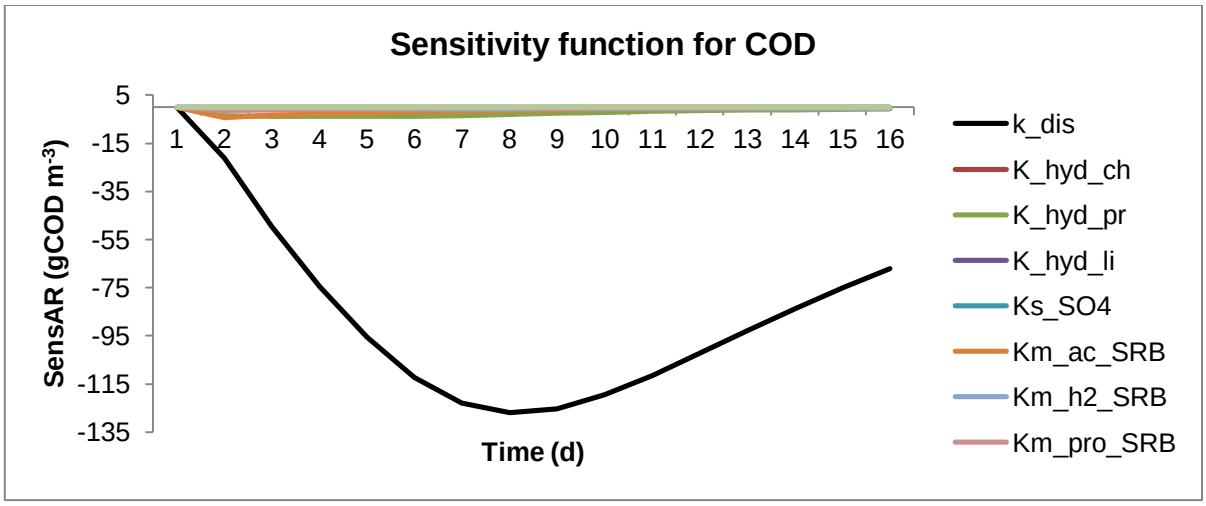

Figure 68: Sensitivity function for COD.

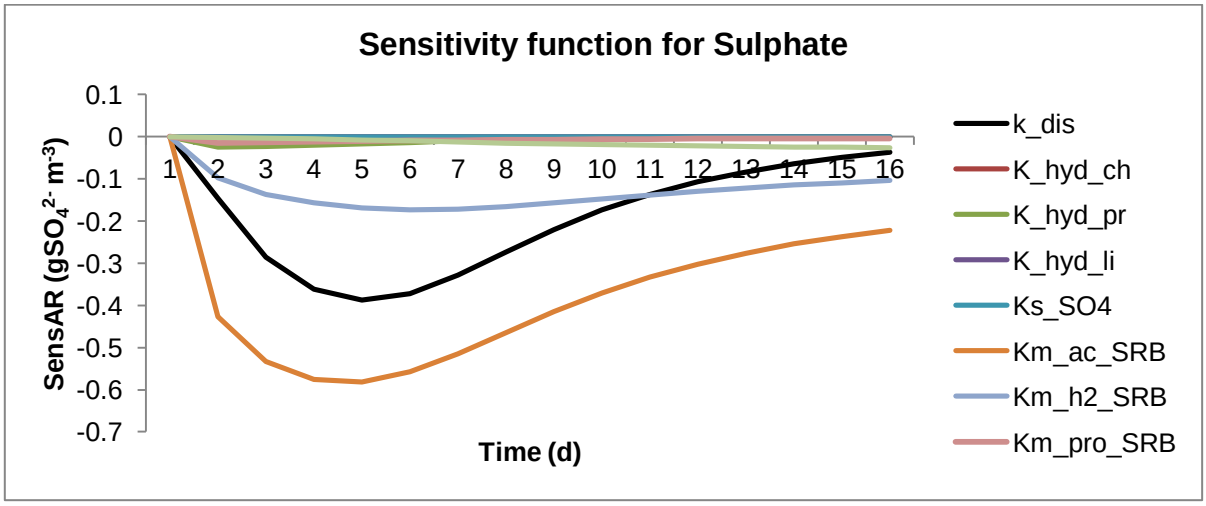

Figure 69: Sensitivity function for sulphate.

The sensitivity analysis shows the importance of the calibrations of the parameters: k_{dis}; $k_{m,h2,\ SRB}$; $k_{m,\ ac,\ SRB}$ for the evaluated variables (COD and sulphate).

The calibration of the more sensitive model parameters was done through the application of the algorithm of the secant method in AQUASIM 2.0. After choosing the parameters that must be estimated, the target for the estimation is defined by choosing a variable. In this case, the constants were estimated using as a target variable the biogas recorded in the batch tests.

Table 37 shows the results of the parameters estimation.

Table 37: Parameter estimation values.

Parameter	Unit	Fedorovich et al., 2003	Barrera et al., 2015	Our calibration
k_{dis}	d^{-1}	-	-	0.15
$k_{m,\ h2,\ SRB}$	kg COD/kg X d^{-1}	26.7	63	30
$k_{m,\ ac,\ SRB}$	kg COD/kg X d^{-1}	7.1	18.5	3

After the sensitive analysis and the calibration, the results of the experimental tests T1 and T6 were compared to the ADM1 simulation results of the same tests. Figures 70 and 71 show the model simulation results after the calibration, test T1 and T6 respectively. The obtained values were compared to the average results of the batch tests.

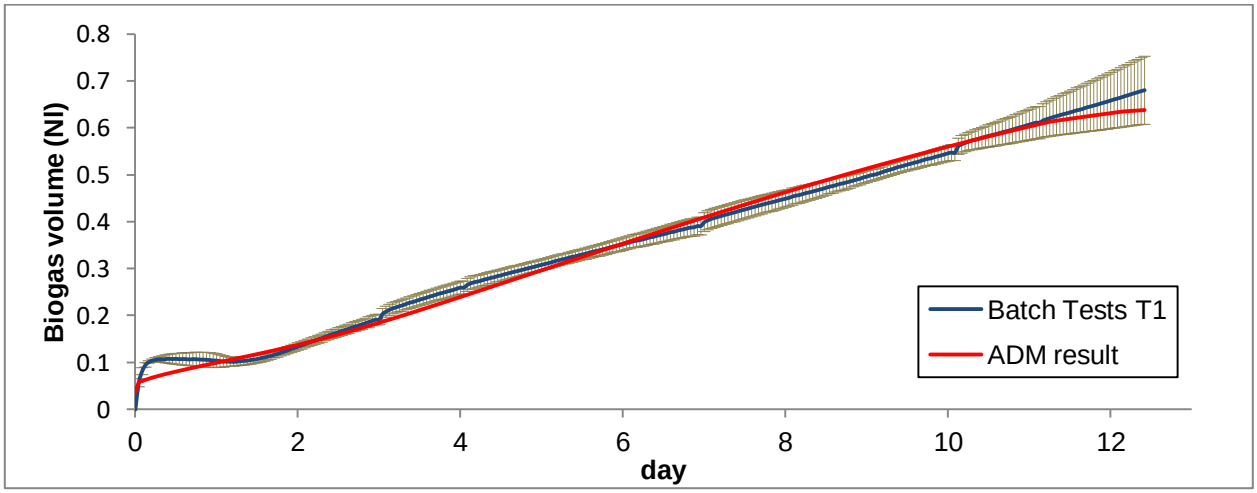

Figure 70: Batch tests (with deviation standard) and simulation results, test T1.

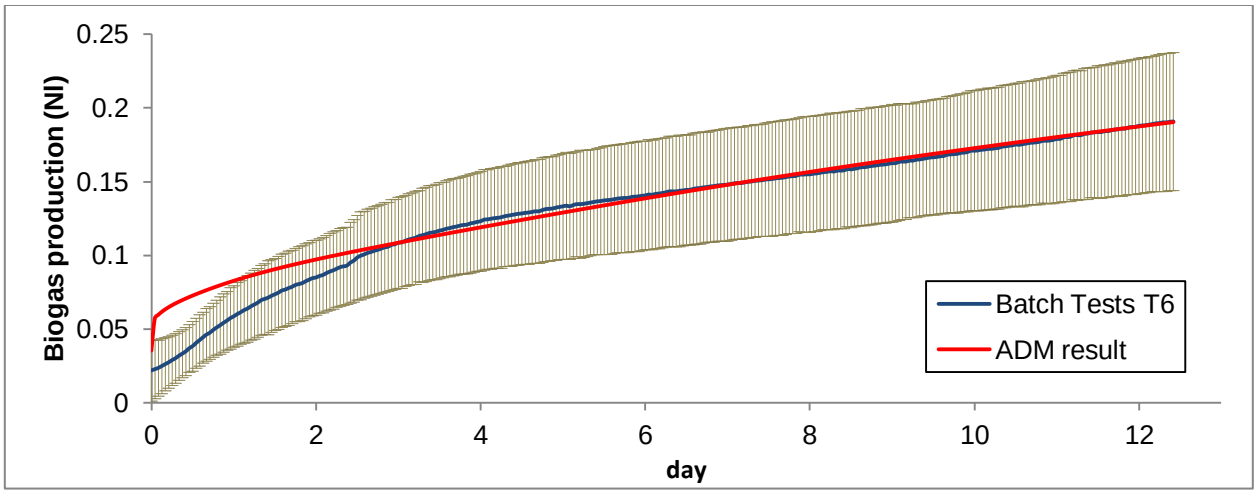

Figure 71: Batch tests (with deviation standard) and simulation results, test T6.

As shown in figure 70 the model represented properly the batch tests, the simulation fits the data. Figure 71 shows a good data fitting (model-batch tests data) after day 2, on the contrary the first part of the tests (from 0 to day 2) was not perfectly represented by the model. However, the model result was in the high deviation standard of the data.

4.6 Full plant modelling

The current configuration (Configuration I) was used to calibrate and validate the models. Particularly, for this purpose the calibration was done with the data of the first part of the year (average of 5 months, from January to May) and then the model was run with the same calibrated values with the data of the second part of the year (average of 4 months, from September to December) by changing the influent load, the DO and temperature values.

With PetWin 4.0 software were done steady state and dynamic state simulations, while with SUMO, steady state simulations only.

4.6.1. Calibration and validation, steady state simulations

For the simulation of the full plant the calibration was based on the information available from literature and previous studies.

The data used in the simulations was the average of a daily samples in 5 months. Table 38 shows the error percentage in the main parameters between the model and the plant data for

the industrial and municipal wastewater influents to verify the assumptions made in the characterizations.

Table 38: Error percentage in the characterization, model-plant data.

	PetWin 4.0		**SUMO**	
	Industrial influent Error (%)	**Municipal influent Error (%)**	**Industrial influent Error (%)**	**Municipal influent Error (%)**
Total COD	0.0	0.0	0.2	2.4
TSS	0.1	-	0.1	-
pH	0.0	0.0	0.0	0.0
Total N	1	0.0	0.7	2.3
NH_X	0.5	0.0	0.0	2.9
Total P	0.0	-	4.0	-
Sulphate	0.0	-	0.1	-
Filtered COD	2	-	4.4	-
Chloride	0.0	-	0.0	-

With both softwares, the percentage errors in the influent characterizations for the parameters monitored are all below the 5%.

Based on the literature review of modelling vegetable tannery wastewater (Lubello et al., 2009), the key parameters are the hydrolysis rate and the kinetic parameters for the ammonia oxidizing (AOB) and the ordinary heterotrophic bacteria (OHO). Specifically, the rate of hydrolysis is considered the most important parameter in the process of matching experimental data with simulator predictions (Dhar et al., 2011). Hence, the calibration focused on these parameters tuning on the basis of historical data on influent and effluent concentrations.

Table 39 shows the calibration of the main kinetic values, in comparison with software default and literature values.

Table 39: Kinetic parameters calibration.

	Name	PetWin 4.0 default values	SUMO default values	Lubello et al. (2009)	Kaelin et al. (2009)	Our calibration
AOB (T=20°C)	Max. spec. growth rate [d^{-1}]	0.9	0.85	0.38	0.12	0.45
	Yield [mg_{COD} mg^{-1}_{N}]	0.15	0.15	0.24	0.18	0.13
NOB (T=20°C)	Max. spec. growth rate [d^{-1}]	0.7	0.65	N/A	0.08	0.45
	Yield [mg_{COD} mg^{-1}_{N}]	0.09	0.09	N/A	0.06	0.09
OHO (T=20°C)	Max. spec. growth rate [d^{-1}]	3.2	4.0	5.1	3.0	5.0
	Yield [mg_{COD} mg^{-1}_{N}]	0.66	0.6	N/A	0.04	0.6

As shown in table 39, the kinetics of nitrification, denitrification resulted slower compared to standard models.

Table 40 shows the results of the model prediction after the calibration compared to plant data for the steady state simulations with PetWin 4.0.

Table 40: Comparison of effluents values, steady state simulations with PetWin 4.0 and SUMO.

	Parameter	Units	Plant Data	Configuration I PetWin 4.0 results	Configuration I SUMO results
WWTP Effluent	Filtered COD	mg l^{-1}	356±51	374	344
	Nitrate	mg_N l^{-1}	10±3.89	9.41	11
	Nitrite	mg_N l^{-1}	1±0.5	0.70	0.78
	Ammonia	mg_N l^{-1}	4±2	4.34	4
	Total Sulphates	mg_S l^{-1}	567±102	570	568
	Total Sulphides	mg_S l^{-1}	N/A	0.01	0.01
Biological reactor	MLSS	mg l^{-1}	9800±806	10918	9992
	MLVSS	mg l^{-1}	7843±508	8707	7743
Primary sludge	Total COD	mg l^{-1}	46710±8527	43328	39223
	VS	mg l^{-1}	24128±3712	25448	23649
	Total N	mg_N l^{-1}	1537±61	1005	1068
	Total Sulphates	mg_S l^{-1}	334±166	350	394

As shown in table 40, the calibration for the parameters allowed a satisfactory representation of the real data. However, the high SRT in the biological reactor (approximately 60 days) made difficult the calibration of the mixed-liquor suspended (MLSS) and volatile solids (MLVSS). In real conditions, at high SRT even the COD fraction usually referred to as non-biodegradable is partially degraded, although at a lower rate. This can explain the lower MLVSS:MLSS predicted by the PetWin 4.0 model, which does not account for such a retardation. The models developed represents with a good agreement the real data. The modifications made in SUMO allows to represents the data value inside the deviation standard error, moreover the percentage error between the model and data is 2% and 1% for MLSS and MLVSS, respectively.

The validation and calibration of the model for the Configuration I at the steady state was used for the steady state of the following 4 months of the year and for the dynamic simulations.

Figure 72 shows the comparison between the model simulation and the plant data in the two phases of the year, for the MLSS and MLVSS.

Figures 73 and 74 show the nitrogen compounds, filtered COD (sCOD) and sulphates in the effluent in the comparison between model simulation and plant data.

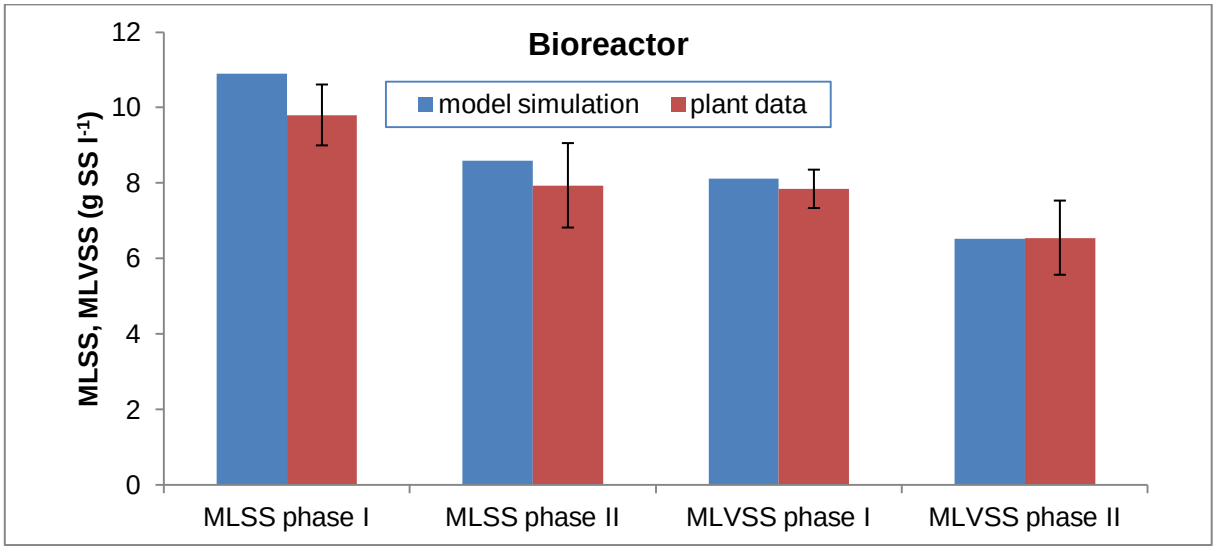

Figure 72: MLSS, MLVSS in the bioreactors, plant data and model simulations.

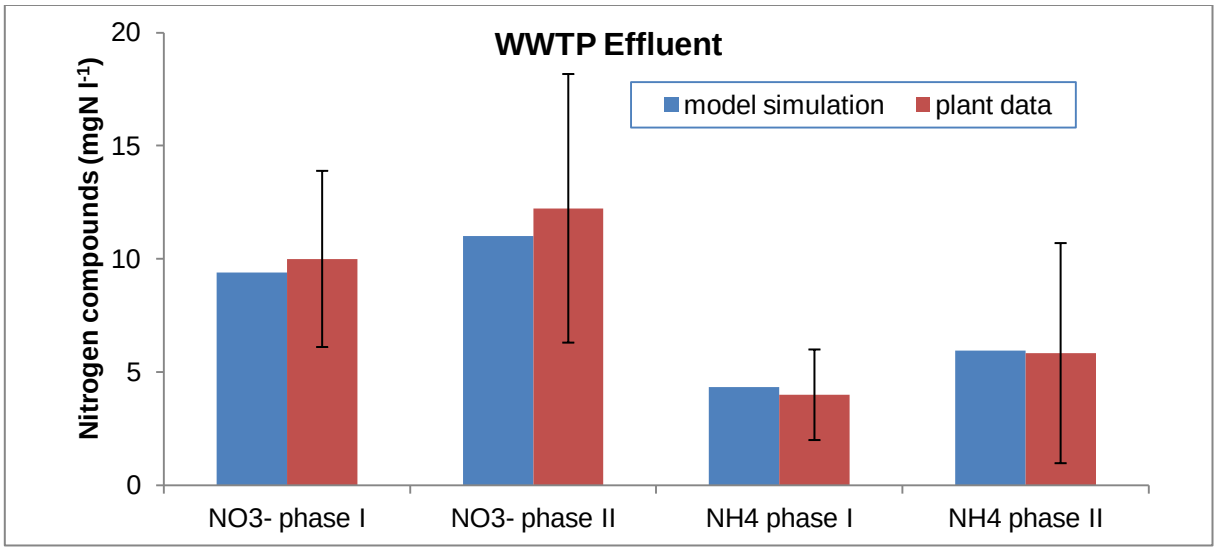

Figure 73: Nitrogen compounds in the effluent, plant data and simulation results.

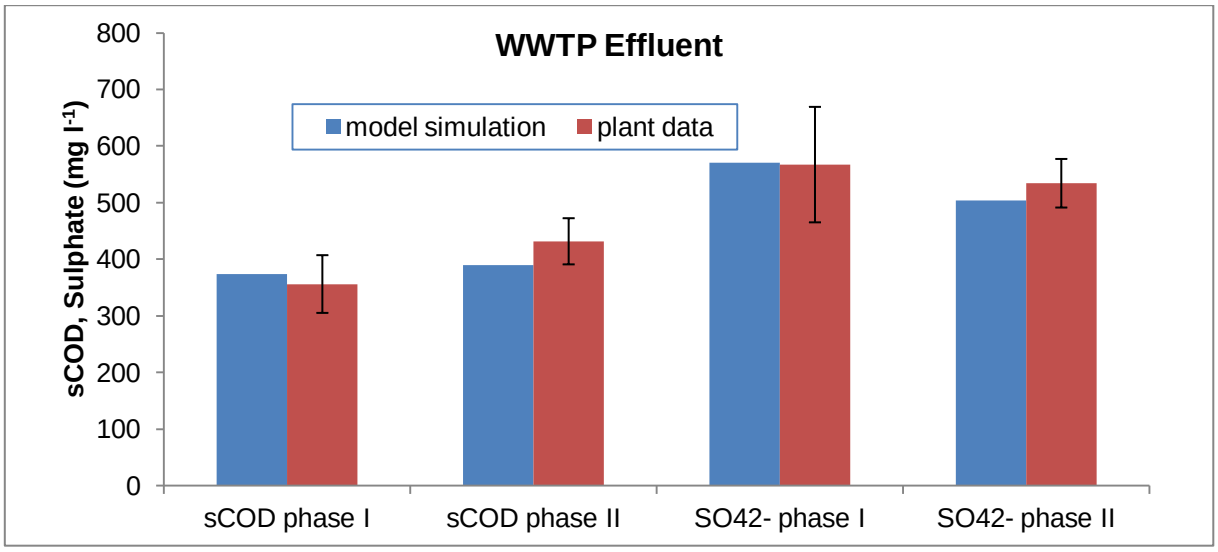

Figure 74: Filtered COD and sulphate in the effluent, plant data and simulation results.

As shown in figures 72, 73 and 74 the model was able to match the plant data for the two periods of the year.

4.6.2. Dynamic state simulations

Figure 75 shows the results of the MLSS and MLVSS concentrations in the bioreactor for the dynamic state simulation.

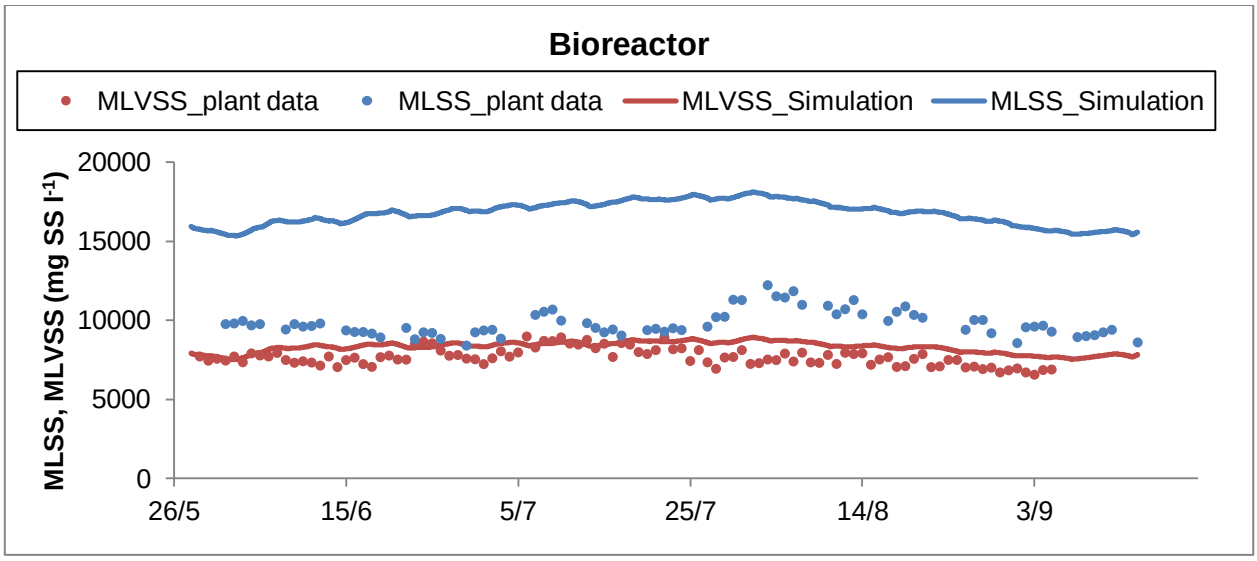

Figure 75: MLSS and MLVSS concentrations in the bioreactor for the dynamic state simulation.

As mentioned previously for the steady state simulations, the high SRT in the biological reactor (approximately 60 days) made difficult the calibration of the mixed-liquor suspended (MLSS) and volatile solids (MLVSS). In real conditions, at high SRT even the COD fraction usually referred to as non-biodegradable is partially degraded, although at a lower rate. This can explain the lower MLVSS:MLSS predicted by the PetWin 4.0 model, which does not account for such a retardation. Based on this experience, the dynamic simulation was selected to find a good agreement between plant data and model results only for the MLVSS. The data trend of MLVSS was well represented by the model.

Figure 76 shows the simulation results of the effluent in terms of filtered COD and sulphate.

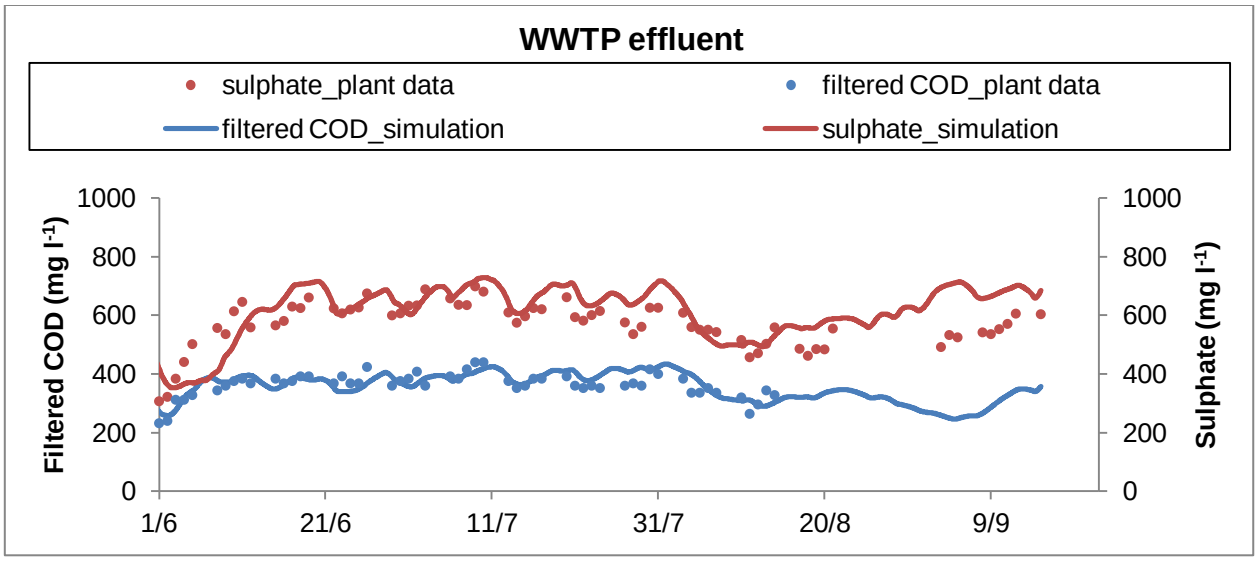

Figure 76: Simulation results of the effluent in terms of filtered COD and sulphate.

As shown in figure 76, there was a good match of plant data and simulation results of the effluent characterizations in terms of filtered COD and sulphate effluent. Both trends were predicted by the model.

Figure 77 shows the simulation results of the effluent in terms of nitrogen compounds.

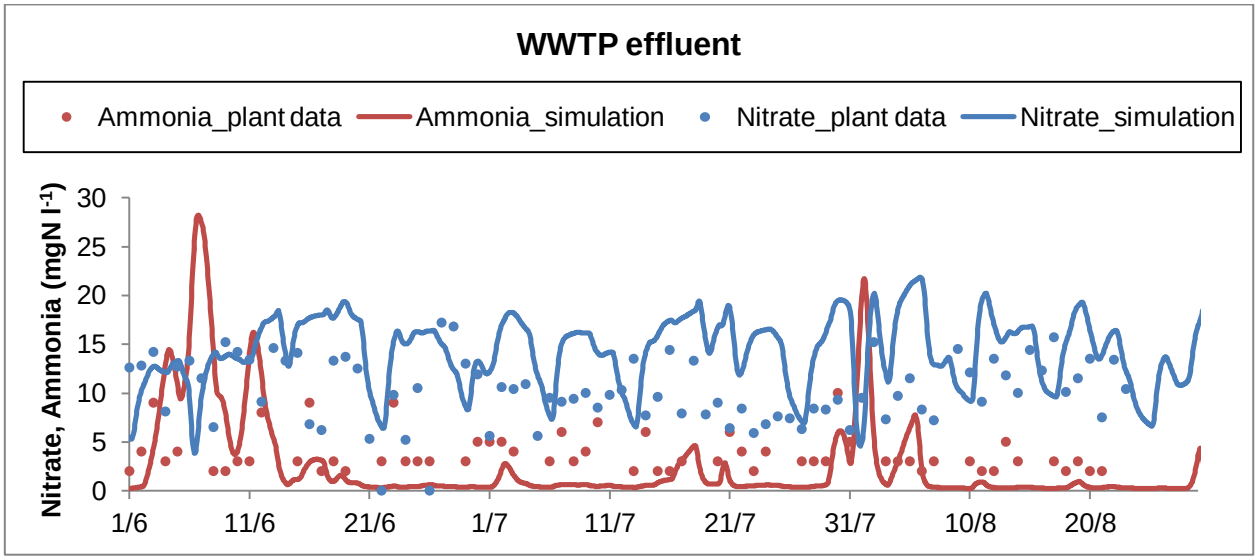

Figure 77: Simulation results of the effluent in terms of nitrogen compounds, nitrate and ammonia nitrogen.

A quite good agreement was found between the data and the model results for the nitrogen compounds. However, the ammonia nitrogen was underestimated while the nitrate was over

estimated. This can be related to anoxic zone that could be present in the biological reactor not represented by the model.

4.6.3. Comparison of the configurations

Table 41 shows the results of the steady state simulations for Configuration I and II with PetWin.

Table 41: Steady state simulations with PetWin, comparisons between Configuration I and II.

	Parameter	Units	Configuration I (existing process)	Configuration II (process with primary sludge AD)
WWTP Effluent	Filtered COD	$mg\ l^{-1}$	374	382
	Nitrate	$mg_N\ l^{-1}$	9.41	10.05
	Nitrite	$mg_N\ l^{-1}$	0.70	0.74
	Ammonia	$mg_N\ l^{-1}$	4.34	4.17
	Total Sulphates	$mg_S\ l^{-1}$	570	519
	Total Sulphides	$mg_S\ l^{-1}$	0.01	0.01
Biogas (HRT_{AD} 20 d)	Q	m^3d^{-1}	-	8304
	Methane	%	-	60
	Hydrogen sulphide	%	-	3
Sludge (HRT_{AD} 20 d)	VS removal	%	-	50

The AD simulation confirmed the results obtained with the pilot scale reactor at 20d of HRT in terms of VS and COD removal, gas flow. The model underestimated a bit the methane production, while the H_2S as over estimated, $70_{pilot\ scale}$ to $60_{model\ prediction}$ for methane percentage and $1_{pilot\ scale}$ to $3_{model\ prediction}$ for H_2S percentage.

Table 42 shows the energy evaluations for the two configurations.

Table 42: Energy evaluations, comparison between Configuration I and II.

Parameter		Units	Configuration I (existing process)	Configuration II (process with primary sludge AD)
Energy demand for Aeration		kWh d^{-1}	6579	8064
Energy demand for Anaerobic digestion	**$ED_{heating}$**	kWh d^{-1}	-	24792
	ED_{mixing}		-	163
Energy recovery		kWh d^{-1}	-	28903

In the Configuration II the recirculation of the supernatant after AD process produced an increase of the aeration ED. Moreover, the huge amount of energy required for the AD process suggests the evaluation of a different configuration, such as the inclusion of a thickener to reduce the digestor volume. However, that increase was compensated by the recovery for the biogas utilization.

In the energy recovery the biogas treatment was neglected, it is possible to suppose a reducing factor of at least 5% of the total value.

Table 43 shows the results of the sulphur denitrification at the steady state simulation with SUMO.

Table 43: Steady state simulations with SUMO, sulphur denitrification results.

	Sulphide Denitrification		
Parameter	**Unit**	**Influent**	**Effluent**
Sulphate	mg S-SO_4^{2-} L^{-1}	149	352
Elemental sulphur	mg S L^{-1}	0.008	7.9
Nitrite	mg N-NO_2^- L^{-1}	0.82	0.20
Nitrate	mg N-NO_3^- L^{-1}	103	43
Ammonium	mg N-NH_4 L^{-1}	0.09	1.9
Nitrogen (gas stream)	g N m^{-3}	-	438
H_2S (gas stream)	g S m^{-3}	111	3.7
S/N	g S g^{-1} N	2.3	-

According to Chung et al., 2014, Xu et al., 2016 and our experimental results with a S/N ratio of 5.65 more than 60% of nitrate reduction and the 90% of H_2S oxidation must be performed. The model shows a sulphide oxidation of 97%, while only the 58% of the nitrate removal. The higher sulphide oxidation and the lower nitrate reduction suggested a correction of the stoichiometric coefficients in the matrix. However, the error can be considered irrelevant for the following evaluations.

For the complete oxidation of the supernatant it was evaluated an air flow rate of 2934 Nm^3hr^{-1}, so it is required approximately 437 kWh d^{-1} to oxide ammonia nitrogen to nitrate. The value is worthless in comparison with the air flow rate required to oxidize the ammonia nitrogen recirculated in the main stream which was evaluated approximately at 65326 Nm^3 hr^{-1}. After the sulphide denitrification process the biogas can be directly treated and the supernatant is already denitrified.

Conclusions

In this study an alternative treatment train along with the existing one were evaluated to assess the technical feasibility of anaerobic digestion of vegetable tannery sludge and the co-digestion of sludge plus fleshing. Moreover, the sulphide denitrification was tested to treat both the supernatant from after the digestion process (with high ammonia concentration) and the biogas (with high sulphide concentration). The process was investigated through both experimental activity and modelling.

The batch tests on anaerobic digestion of tannery sludge as co-substrate with conventional domestic sludge confirmed the feasibility of the process, but no significant improvements in process efficiency were observed. Conversely, co-digestion of tannery sludge with fleshing exhibited better process performance in comparison with blank test on sole vegetable tannery sludge, indicating that fleshing can exert a positive impact to the process, but requiring long hydrolysis step. Although none of the results showed inhibition phenomena, particular attention should be paid when facing substrate mixture with fleshing, due to its high inhibiting compounds content such as lipids, proteins and the low COD:N ratio.

Batch tests results were confirmed by laboratory scale results. The digestion of municipal and vegetable tannery primary sludge with up to 70:30 volumetric ratio improved the digestion performance. Moreover, no evident inhibitory effects on anaerobic digestion were evident.

Pilot scale tests showed almost the same results for the anaerobic digestion of vegetable tannery sludge with an HRT of 20 and 30 days. The anaerobic digestion process of vegetable tannery primary sludge, in mesophilic conditions, with an HRT in a range 20-30 days: the VS removal is in the range 40-60%; the theoretical methane production is in the range 0.2-0.3 $Nm^{-3}CH_4$ kg^{-1} VS load; the ammonia nitrogen in the sludge effluent is in the range 600-800 mg $N\text{-}NH_4$ l^{-1} and the sulphate reduction is in the range 90-100 %.

Moreover, our results suggested that the anaerobic co-digestion of vegetable tannery industry primary sludge and tanning industry fleshing may be a promising solution to avoid

the inhibitory effects of digesting two single substrates separately while increasing the process efficiency. The addition of fleshing helped to reach more than the double of the theoretical methane production at the end of the test, in the comparison with the control test (at the same HRT and vegetable tannery sludge digestion only). Higher VS removal was shown in co-digestion with fleshing, and no inhibitory effects were recorded in all reactors. Complete sulphate reduction was observed in all reactors, however its competing influence with biogas production was considered and found to be negligible.

The addition of sulphate reducing biomasses in the ADM1 and the parameters estimations allows the representations of the control batch tests (T1 and T6) in the deviation standard of the experimental results.

The goal of the full plant model modifications was to properly simulate a wastewater treatment plant with high values of sludge retention time (60-100 days) and the integration in the model of sulphur cycle (both sulphate reduction and sulphide oxidation).

The proposed model is the first that includes all these processes and can be useful for the simulation of industrial wastewater plants operating with water containing sulphur and recalcitrant compounds, such as paper mill, petrochemical wastewater, etc. The good agreement between plant data and model results validated the proposed model.

Model simulations are a good tool to evaluate alternative configurations. The comparisons of the configurations showed that with the inclusion of the anaerobic digestion in the plant it is required to consider also the biological denitrification process because a recirculation of 600-1000 mg $N\text{-}NH_4$ l^{-1} was evaluated. The proposed model further confirmed that the sulphide denitrification process is a promising novel treatment.

Future research

Future research should attempt to further investigate suitable and cost-effective pre-treatment solutions for full-scale applications of the anaerobic co-digestion of fleshing and sludge. Moreover, in order to simulate the co-digestion process in a full scale plant, several processes must be added to the AD model, such as a two-step hydrolysis, different phases inside the reactor to represent the interactions between the solid particles and the sludge, furthermore, a differentiation of the complex particulates into a slowly and readily complex particulates might be required.

References

All the citations will be listed here alphabetically.

An, S., Tang, K., Nemati, M., 2010. Simultaneous biodesulphurization and denitrifi- cation using an oil reservoir microbial culture: effects of sulphide loading rate and sulphide to nitrate loading ratio. Water Res. 44 (5), 1531e1541.

Andrews J, Pearson EA. Kinetics and characteristics of volatile fatty acid production in anaerobic fermentation processes. Int J Air Water Pollut 1965;9:439e61.

Anderson, G.K., Donnelly, T., Mckeown, K.J., 1982. Identification and control of inhibition in the anaerobic treatment of industrial waste- water. Process Biochem. 17, 28–32.

Angelidaki, I., & Sanders, W. (2004). Assessment of the anaerobic biodegradability of macropollutants. *Reviews in Environmental Science and Biotechnology*, *3*(2), 117–129. http://doi.org/10.1007/s11157-004-2502-3

Anthonisen, A. C., Loher, R. C., Prakasam, T. B. S., Srinath, E. G. (1976). Inhibition of nitrification by ammonia and nitrous acid. *J Water Pollut Control Fed 48:* 835-849.

Arpat, Agenzia regionale protezione ambiente Toscana: http://www.arpat.toscana.it/

Avcioğlu, E., Karahan-Gül, O.¨, & Orhon, D. (2003). Estimation of stoichiometric and kinetic coefficients of ASM3 under aerobic and anoxic conditions via respirometry. *Water Science and Technology*, *48*(8), 185–194.

Banu, J. R., Kaliappan, S., & Yeom, I. T. (2007). Treatment of domestic wastewater using upflow anaerobic sludge blanket reactor. *International Journal of Environmental Science and Technology*, *4*(3), 363–370. http://doi.org/10.1007/s00449-009-0321-1

Barrera, E. L., Spanjers, H., Solon, K., Amerlinck, Y., Nopens, I., & Dewulf, J. (2015). Modeling the anaerobic digestion of cane-molasses vinasse: Extension of the Anaerobic Digestion Model No. 1 (ADM1) with sulfate reduction for a very high strength and sulfate rich wastewater. *Water Research*, *71*, 42–54. http://doi.org/10.1016/j.watres.2014.12.026

Basak, S. R., Rouf, M. A., Hossain, M. D., Islam, M. S., & Rabeya, T. (2014). Anaerobic digestion of tannery solid waste by mixing with different substrates, *49*(2), 119–124.

Batstone, D. J., & Keller, J. (2003). Industrial applications of the IWA anaerobic digestion model No.1 (ADM1). *Water Science and Technology*, *47*(12), 199–206.

Batstone, D. J., Keller, J., Angelidaki, I., Kalyuzhnyi, S. V., Pavlostathis, S. G., Rozzi, a., … Vavilin, V. a. (2002). The IWA Anaerobic Digestion Model No 1 (ADM1). *Water Science and Technology*, *45*(10), 65–73. http://doi.org/10.2166/wst.2008.678

Bautista, M. E., Pérez, L., García, M. T., Cuadros, S., & Marsal, A. (2015). Valorization of tannery wastes: Lipoamino acid surfactant mixtures from the protein fraction of process wastewater. *Chemical Engineering Journal*, *262*, 399–408. http://doi.org/10.1016/j.cej.2014.10.004

Berardino, S. Di, & Martinho, A. (2009). Co-digestion of tanning residues and sludge. Retrieved from http://repositorio.lneg.pt/handle/10400.9/596

Beristain, C.R., Sierra-Alvarez, R., Rowlette, P., Razo Flores, E., Gomez, J., Field, J.A., 2006. Sulfide oxidation under chemolithoautotrophic denitrifying conditions. Biotechnol. Bioeng. 95 (6), 1148e1157.

Cenni, F., Dondo, G., & Tombetti, F. (1982). Anaerobic digestion of tannery wastes. *Agricultural Wastes*, *4*(3), 241–243. http://doi.org/10.1016/0141-4607(82)90016-6

Chen, K.-W., Lin, L.-C., & Lee, W.-S. (2014). Analyzing the Carbon Footprint of the Finished Bovine Leather: A Case Study of Aniline Leather. *Energy Procedia*, *61*, 1063–1066. http://doi.org/10.1016/j.egypro.2014.11.1023

Chen, Y., Cheng, J. J., & Creamer, K. S. (2008). Inhibition of anaerobic digestion process: A review. *Bioresource Technology*, *99*(10), 4044–4064. http://doi.org/10.1016/j.biortech.2007.01.057

Chung, J., Amin, K., Kim, S., Yoon, S., Kwon, K., & Bae, W. (2014). Autotrophic denitrification of nitrate and nitrite using thiosulfate as an electron donor. *Water Research*, *58C*, 169–178. http://doi.org/10.1016/j.watres.2014.03.071

Cirne DG, Paloumet X, Björnsson L, Alves MM and Mattiasson B (2007), Anaerobic digestion of lipid-rich waste – effects of lipid concentration, Renewable Energy, 32: 965–975.

Colleran, E., Finnegan, S., Lens, P., 1995. Anaerobic treatment of sulphate-containing waste streams. Anton. van Leeuw. 67, 29–46.

Colleran, E., Pender, S., Phipott, U., O'Flaherty, V., Leahy, B., 1998. Full-scale and laboratory-scale anaerobic treatment of citric acid production wastewater. Biodegradation 9, 233–245.

Daryapurkar, R. a., Nandy, T., Kaul, S. N., Deshpande, C. V., & Szpyrkowicz, L. (2001). Evaluation of kinetic constants for anaerobic fixed film fixed bed reactors treating tannery wastewater. *International Journal of Environmental Studies*, *58*(6), 835–860. http://doi.org/10.1080/00207230108711371

Dhar, B.R.; Elbeshbishy, E.; Hafez, H.; Nakhla, G.; Madhumita, B.R. Thermo-oxidative pretreatment of municipal waste activated sludge for volatile sulfur compounds removal and enhanced anaerobic digestion. Chem. Eng. J. 2011, 174, 166–174.

Dhayalan, K., Fathima, N. N., Gnanamani, a., Rao, J. R., Nair, B. U., & Ramasami, T. (2007). Biodegradability of leathers through anaerobic pathway. *Waste Management*, *27*(6), 760–767. http://doi.org/10.1016/j.wasman.2006.03.019

Euro Chlor. (2010). The European Chlor-Alkali industry : an electricity intensive sector exposed to carbon leakage. *Production*, (May), 2–6.

Eastman, J. A. & Ferguson, J. F., Solubilization of particulate organic carbon during the acid-phase of anaerobic digestion. J. Wat. Pollut. Contr. Fed., 53 (1981) 352-66.

Epa, Environmental Protection Agency: https://www3.epa.gov/

Fajardo, C., Mosquera-Corral, A., Campos, J. L.&Méndez, R. 2012 Autotrophic denitrification with sulphide in a sequencing batch reactor. Journal of Environmental Management 113, 552–556.

Fedorovich, V., Lens, P., & Kalyuzhnyi, S. (2003). Extension of Anaerobic Digestion Model No. 1 with processes of sulfate reduction. *Applied Biochemistry and Biotechnology*, *109*(1-3), 33–45. http://doi.org/10.1385/ABAB:109:1-3:33

Ganesh R, Balaji G, Ramanujam RA. Biodegradation of tannery wastewater using sequencing batch reactor—respirometric assessment. Bioresour Technol 2006;97: 1815–21.

Gernaey, K. V., Van Loosdrecht, M. C. M., Henze, M., Lind, M., & Jørgensen, S. B. (2004). Activated sludge wastewater treatment plant modelling and simulation: State of the art. *Environmental Modelling and Software*, *19*(9), 763–783. http://doi.org/10.1016/j.envsoft.2003.03.005

Gori, R., Giaccherini, F., Jiang, L. M., Sobhani, R., & Rosso, D. (2013). Role of primary sedimentation on plant-wide energy recovery and carbon footprint. *Water Science and Technology*, *68*(4), 870–878. http://doi.org/10.2166/wst.2013.270

Gori, R., Jiang, L. M., Sobhani, R., & Rosso, D. (2011). Effects of soluble and particulate substrate on the carbon and energy footprint of wastewater treatment processes. *Water Research*, *45*(18), 5858–5872. http://doi.org/10.1016/j.watres.2011.08.036

Gujer, W., Henze, M., Mino, T., van Loosdrecht, M., 1999. Activated sludge model No. 3. Water Science and Technology 39 (1), 183–193.

Harada, H., Uemura, S., Monomoi, K., 1994. Interactions between sulphate-reducing bacteria and methane-producing bacteria in UASB reactors fed with low strength wastes containing different levels of sulphate. Water Res., 355–367.

Henze, M., Grady Jr., C.P.L., Gujer, W., Marais, G.V.R., Matsuo, T., 1987. Activated Sludge Model No.1. IAWPRC Scientific and Technical Report No. 1. IAWPRC, London.

Henze, M., Gujer, W., Mino, T., van Loosdrecht, M.C.M., 2000. Activated Sludge Models ASM1, ASM2, ASM2d and ASM3. Scientific and Technical Report No.9. IWA Publishing.

ISTAT: http://www.istat.it/it/censimento-popolazione/censimento-popolazione-2011

Insel GH, Görgün E, Artan N, Orhon D. Model based optimization of nitrogen removal in a full scale activated sludge plant. Environ Eng Sci 2009;26:471–80.

Jeppsson, U., & Olsson, G. (1996). Modelling aspects of wastewater treatment processes. *Department of Industrial Electrical Engineering and Automation*, (1), 444.

Kaelin, D., Manser, R., Rieger, L., Eugster, J., Rottermann, K., & Siegrist, H. (2009). Extension of ASM3 for two-step nitrification and denitrification and its calibration and validation with batch tests and pilot scale data. *Water Research*, *43*(6), 1680–1692. http://doi.org/10.1016/j.watres.2008.12.039

Karahan O, Dogruel S, Dulekgurgen E, Orhon D. COD fractionation of tannery wastewater particle size distribution, biodegradability and modelling. Water Res 2008;42: 1083–92.

Kim, H.-R., Lee, I.-S., Bae, J.-H., 2004. Performance of a sulphur-utilizing fluidized bed reactor for post-denitrification. Process Biochem. 39 (11), 1591e1597.

Kleerebezem, R.&Mendez, R. 2002 Autotrophic denitrification for combined hydrogen sulphide removal from biogas and post- denitrification. Water Science and Technology 45,349–356.

Kral., J. B. and I., & G. Clonfero, M. B. and F. S. (2011). Introduction To Treatment of Tannery Effluents. *What Every Tanner Should Know about Effluent Treatment*, 1–69. Retrieved from http://www.unido.org/fileadmin/user_media/Publications/Pub_free/Introduction_to_treatment_of_tannery_effluents.pdf\npapers2://publication/uuid/15072894-9C6C-41E1-8B8F-7287B6278FA9

Lauwers, J., Appels, L., Thompson, I. P., Degrève, J., Van Impe, J. F., & Dewil, R. (2013). Mathematical modelling of anaerobic digestion of biomass and waste: Power and limitations. *Progress in Energy and Combustion Science*, *39*(4), 383–402. http://doi.org/10.1016/j.pecs.2013.03.003

Lefebvre, O., Vasudevan, N., Torrijos, M., Thanasekaran, K., & Moletta, R. (2006). Anaerobic digestion of tannery soak liquor with an aerobic post-treatment. *Water Research*, *40*(7), 1492–1500. http://doi.org/10.1016/j.watres.2006.02.004

Lofrano, G., Meriç, S., Zengin, G. E., & Orhon, D. (2013). Chemical and biological treatment technologies for leather tannery chemicals and wastewaters: A review. *Science of the Total Environment*, *461-462*, 265–281. http://doi.org/10.1016/j.scitotenv.2013.05.004

Lu, H., Wang, J., Li, S., Chen, G. H., van Loosdrecht, M. C. M. & Ekama, G. A. 2009 Steady-state model-based evaluation of sulfate reduction, autotrophic denitrification and nitrification integrated (SANI) process. Water Research 43 (14), 3613–3621.

Mannucci, A., Munz, G., Mori, G., & Lubello, C. (2010). Anaerobic treatment of vegetable tannery wastewaters : A review. *DES*, *264*(1-2), 1–8. http://doi.org/10.1016/j.desal.2010.07.021

Mata-Alvarez, J., Dosta, J., Romero-Güiza, M. S., Fonoll, X., Peces, M., & Astals, S. (2014). A critical review on anaerobic co-digestion achievements between 2010 and 2013. *Renewable and Sustainable Energy Reviews*, *36*, 412–427. http://doi.org/10.1016/j.rser.2014.04.039

McCartney, D. M., & Oleszkiewicz, J. a. (1991). Sulfide inhibition of anaerobic degradation of lactate and acetate. *Water Research*, *25*(2), 203–209. http://doi.org/10.1016/0043-1354(91)90030-T

Mora, M., Guisasola, A., Gamisans, X., & Gabriel, D. (2014). Examining thiosulfate-driven autotrophic denitrification through respirometry. *Chemosphere*, *113*, 1–8. http://doi.org/10.1016/j.chemosphere.2014.03.083

Mora, M., López, L. R., Gamisans, X., & Gabriel, D. (2014). Coupling respirometry and titrimetry for the characterization of the biological activity of a SO-NR consortium. *Chemical Engineering Journal*, *251*, 111–115. http://doi.org/10.1016/j.cej.2014.04.024

Munz, G., Gori, R., Cammilli, L., & Lubello, C. (2008). Characterization of tannery wastewater and biomass in a membrane bioreactor using respirometric analysis. *Bioresource Technology*, *99*(18), 8612–8618. http://doi.org/10.1016/j.biortech.2008.04.004

Munz, G., Gori, R., Mori, G., & Lubello, C. (2007). Powdered activated carbon and membrane bioreactors (MBRPAC) for tannery wastewater treatment: long term effect on biological and filtration process performances. *Desalination*, *207*(1-3), 349–360. http://doi.org/10.1016/j.desal.2006.08.010

Munz, G., Mannucci, A., Arreola-Vargas, J., Alatriste-Mondragon, F., Giaccherini, F., & Mori, G. (2015). Nitrite and nitrate as electron acceptors for biological sulphide oxidation. *Water Science and Technology*, *72*(4), 593–599. http://doi.org/10.2166/wst.2015.252

Mwinyihija, M. (2010). Ecotoxicological diagnosis in the tanning industry. *Ecotoxicological Diagnosis in the Tanning Industry*, 1–140. http://doi.org/10.1007/978-1-4419-6266-9

Namini, M. T., Heydarian, S. M., Bonakdarpour, B. & Farjah, A. 2008 Removal ofH2S from synthetic waste gas stream using a biotrickling filter. Iranian Journal Chemical Engineering 5, 40–51.

Organization, U. N. I. D. (2000). Regional programme for pollution control in the tanning industry in South-East Asia, (August), 27.

Orhon D, Ubay Cokgör E. COD fractionation in wastewater characterisation—the state of the art. J Chem Technol Biotechnol 1997;68:283–93.

Orhon D, Sozen S, Ubay-Cokgor E, Ates E. The effect of chemical settling on the kinetics and design of activated sludge for tannery wastewater. Water Sci Technol 1998;38: 355–62.

Orhon D, Ates Genceli E, Ubay Cokgor E. Characterization and modeling of activated sludge for tannery wastewater. Water Environ Res 1999;71:50–63

Oude Elferink, S.J.W.H., Visser, A., Hulshoff Pol, L.W., Stams, A.J.M., 1994. Sulphate reduction in methanogenic bioreactors. FEMS Micro- biol. Rev. 15, 119–136.

Pan, Y., Ni, B.-J., Yuan, Z., 2013. Modeling electron competition among nitrogen oxides reduction and N2O accumulation in denitrification. Environ. Sci. Technol. 47 (19), 11083e11091.

Parkin GF, Speece RE, Yang CHY, Kocher WM. Response of methane fermen- tation systems to industrial toxicants. J Water Control Fed 1983;55:44–53.

Portavella, M., Contribution of skins to the residual COD of beamhouse process, Bull. AQEIC 45 (1994) 15–18.

Pitk, P., Kaparaju, P., & Vilu, R. (2012). Methane potential of sterilized solid slaughterhouse wastes. *Bioresource Technology*, *116*, 42–46. http://doi.org/10.1016/j.biortech.2012.04.038

Qian, J., Liu, R., Wei, L., Lu, H., Chen, G.-H., 2015a. System evaluation and microbial analysis of a sulfur cycle-based wastewater treatment process for co-treatment of simple wet flue gas desulfurization wastes with freshwater sewage. Water Res.

Qian, J., Lu, H., Cui, Y., Wei, L., Liu, R., Chen, G.-H., 2015b. Investigation on thiosulfate-involved organics and nitrogen removal by a sulfur cycle-based biological wastewater treatment process. Water Res. 691, 295e306.

Raju, A., Rose, C., Muralidhara Rao, N., 1997. Enzymatic hydrolysis of tannery fleshings using chicken intestine proteases. Animal Feed Science and Technology 66 (1–4), 139–147.

Raposo, F., De La Rubia, M. A., Fern??ndez-Cegr??, V., & Borja, R. (2012). Anaerobic digestion of solid organic substrates in batch mode: An overview relating to methane yields and experimental procedures. *Renewable and Sustainable Energy Reviews*, *16*(1), 861–877. http://doi.org/10.1016/j.rser.2011.09.008

Rosso, D., & Bolzonella, D. (2009). Carbon footprint of aerobic biological treatment of winery wastewater. *Water Science and Technology*, *60*(5), 1185–1189. http://doi.org/10.2166/wst.2009.556

Shanmugam, P., & Horan, N. J. (2009). Optimising the biogas production from leather fleshing waste by co-digestion with MSW. *Bioresource Technology*, *100*(18), 4117–4120. http://doi.org/10.1016/j.biortech.2009.03.052

Sahinkaya, E., Kilic, A., Duygulu, B., 2014. Pilot and full scale applications of sulfur- based autotrophic denitrification process for nitrate removal from activated sludge process effluent. Water Res. 601, 210-217.

Sierra-Alvarez, R., Beristain-Cardoso, R., Salazar, M., G omez, J., Razo-Flores, E., Field, J.A., 2007. Chemolithotrophic denitrification with elemental sulfur for groundwater treatment. Water Res. 41 (6), 1253e1262.

Soares, M.I.M., 2002. Denitrification of groundwater with elemental sulfur. Water Res. 36 (5), 1392e1395.

Sri Bala Kameswari, K., Kalyanaraman, C., Porselvam, S., & Thanasekaran, K. (2012). Optimization of inoculum to substrate ratio for bio-energy generation in co-digestion of tannery solid wastes. *Clean Technologies and Environmental Policy*, *14*(2), 241–250. http://doi.org/10.1007/s10098-011-0391-z

Sundar VJ, Gnanamani A, Muralidharan C, Chandrababu NK, Mandal, AB (2010) Recovery and utilization of proteinous wastes of leather making: a review. Rev Environ Sci Biotechnol 10(2):151–163.

Sun, Y., Nemati, M., 2012. Evaluation of sulfur-based autotrophic denitrification and denitritation for biological removal of nitrate and nitrite from contaminated waters. Bioresour. Technol. 1141, 207e216.

Thangamani, a., Rajakumar, S., & Ramanujam, R. a. (2010). Anaerobic co-digestion of hazardous tannery solid waste and primary sludge: Biodegradation kinetics and metabolite analysis. *Clean Technologies and Environmental Policy*, *12*(5), 517–524. http://doi.org/10.1007/s10098-009-0256-x

Un-Fao. (2013). World statistical compendium for raw hides and skins, leather and leather footwear 1993-2012. *Trade and*, 193.

Vaiopoulou, E., Melidis, P., Aivasidis, A., 2005. Sulfide removal in wastewater from petrochemical industries by autotrophic denitrification. Water Res. 39 (17), 4101e4109.

van Hulle, S.W.H., Vandeweyer, H.J.P., Meesschaert, B.D., Vanrolleghem, P.A., Dejans, P., Dumoulin, A., 2010. Engineering aspects and practical application of autotrophic nitrogen removal from nitrogen rich streams. Chem. Eng. J 162 (1), 1e20.

van Langerak, E.P.A., Hamelers, H.V.M. and Lettinga, G. (1997). Influent calcium removal by crystallization reusing anaerobic effluent alkalinity. Wat. Sci. Tech., 36(6–7), 341–348.

Vasudevan, N., D. R. (2007). Biotechnological process for the treatment of fleshing from tannery industries for methane generation. *Current*, *93*(11), 10–12.

Vijayaraghavan, K., & Murthy, D. V. S. (1997). Effect of toxic substances in anaerobic treatment of tannery wastewaters. *Bioprocess Engineering*, *16*(3), 151–155. http://doi.org/10.1007/s004490050302

Wu, L., Loo, Y. Y. & Koe, L. C. C. 2001 A pilot study of a biotrickling filter for the treatment of

odorous sewage air. Water Science and Technology 44 (9), 295–299.

Xu, G., Yin, F., Chen, S., Xu, Y., & Yu, H.-Q. (2016). Mathematical modeling of autotrophic denitrification (AD) process with sulphide as electron donor. *Water Research*, *91*, 225–234. http://doi.org/10.1016/j.watres.2016.01.011

Zerdani, L. M. Faid and Malke, A., Int. J. Agric. Biol., 2004, 6, 758–761.

Zupančič, G. D., & Jemec, a. (2010). Anaerobic digestion of tannery waste: Semi-continuous and anaerobic sequencing batch reactor processes. *Bioresource Technology*, *101*(1), 26–33. http://doi.org/10.1016/j.biortech.2009.07.028

Appendix

Munz, G., Mannucci, A., Arreola-Vargas, J., Alatriste-Mondragon, F., Giaccherini, F., Mori, G. (2015). Nitrite and nitrate as electron acceptors for biological sulphide oxidation. Water Science and Technology.

- IWA-NRR2016 Denver, Colorado July 10th-13th Integration of Denitrification with Sulphide in Tannery Wastewater Treatment train operating Anaerobic Digestion of Primary Sludge;
- SIDISA 2016, Rome, Italy 19th-23rd June: A modified version of the adm1 hydrolysis formulation for simulating anaerobic digestion of tannery sludge and waste. Polizzi, Giaccherini, Alatriste-Mondragon, Lubello, Rosso, Munz;
- Ecomondo 2015 (Rimini, Italy): Anaerobic co-digestion of fleshing and tannery sludge: laboratory scale tests;
- Ecomondo 2014 (Rimini, Italy): “Potenzialita’ della co-digestione anaerobica di fanghi conciari e civili”;
- IWA XI Simposio Latinoamericano de Digestiòn Anaerobia (Havana, Cuba): “Anaerobic Digestion of vegetable tannery and municipal sludge”;
- IWA XI Simposio Latinoamericano de Digestiòn Anaerobia (Havana, Cuba): “Nitrite and nitrate as electron acceptors for biological sulphide oxidation”;
- WEF/IWA Residuals and Biosolids Conference 2015 (Washington, USA): “Anaerobic co-digestion of fleshing and primary sludge of vegetable tanning industry”;
- IWA-NRR2015, May 18-21, 2015 (Gdansk, Poland): “Stoichiometry of sulphide oxidation with nitrate as electron acceptor”;
- Ecomondo 2015 (Rimini, Italy): “Anaerobic co-digestion of fleshing and tannery sludge: laboratory scale tests”;
- IWA 14th World congress on anaerobic digestion 2015, Viña del Mar, Chile: “Pilot scale tests on anaerobic co-digestion of vegetable tannery sludge and fleshing”.

Notation

- AD: anaerobic digestion;
- AOB: aerobic ammonia oxidizers;
- bCOD: biodegradable COD;
- CDPS: common domestic primary sludge;
- pCOD: particulate COD;
- sCOD: soluble COD;
- DO: dissolved oxygen;
- HRT: hydraulic retention time;
- IRSA-CNR: Italian Institute of Water Research-National Research Council;
- MLSS: mixed-liquor suspended solids;
- MLVSS: mixed-liquor volatile suspended solids;
- NOB: nitrite oxidizers;
- OHO: ordinary heterotrophs;
- OLR: organic loading rate;
- SBP: specific biogas production;
- SOB: sulphide oxidizing biomass;
- SRB: sulphate reducing biomass;
- SRT: solid retention time;
- SS: suspended solids;
- TDS: total dissolved solids;
- TIF: tannery industrial fleshing;
- TMP: theoretical methane potential;
- TS: total solids;
- VS: volatile solids;
- VTPS: vegetable tannery primary sludge;
- WW: wastewater;
- WWTP: wastewater treatment plant.

...I ended up with a broken fiddle--

And a broken laugh, and a thousand memories,

And not a single regret.

Fiddler Jones, "Spoon River Anthology" Edgar Lee Masters

I met a bunch of great people, more than expected...I'll never forget anyone of them, my fellas.

Thanks to my family and my old friends, I love the way we are "sgangherati"...I am only a branch of the tree.

Thanks to my tutors Prof. Lubello and Prof. Dockhorn, to all the experts and professors that taught me something. Thanks to Daniel who inspired me the art of being meticulous and kind.

Thanks to Giulio and Diego, I tried my best to assimilate your knowledge. You trusted me more than I trust myself. I am glad that I worked with both of you because you are good professors, but above all, you are great people.

Thanks to Angela and Bob, you embraced me as part of the family, you have such a big heart full of love and you know how to share it!

...clear eyes, full hearts, can't lose!